THE ENGINEERING PROPERTIES AND DURABILITY PERFORMANCE OF ALKALI-ACTIVATED (POFA-GGBS-PFA) TERNARY HYBRID GEOPOLYMER COMPOSITE

WONG WENG SHEN

A project report submitted in partial fulfilment of the requirements for the award of the degree of Bachelor of Science (Hons) Construction Management

Faculty of Engineering and Green Technology
Universiti Tunku Abdul Rahman

May 2017

DECLARATION

I hereby declare that this project report is based on my original work except for citations and quotations which have been duly acknowledged. I also declare that it has not been previously and concurrently submitted for any other degree or award at UTAR or other institutions.

Signature : _____

Name : WONG WENG SHEN

ID No. : 13AGB03193

Date : 1st May 2017

APPROVAL FOR SUBMISSION

I certify that this project report entitled **"THE ENGINEERING PROPERTIES AND DURABILITY PERFORMANCE OF ALKALO-ACTIVATED (POFA-GGBS-PFA) TERNARY HYBRID GEOPOLYMER COMPOSITE"** was prepared by **WONG WENG SHEN** has met the required standard for submission in partial fulfilment of the requirements for the award of Bachelor of Science (Hons) Construction Management at Universiti Tunku Abdul Rahman.

Approved by,

Signature : _____

Supervisor : Dr. Kwan Wai Hoe

Date : 1st May 2017

Specially dedicated to my supervisor, Dr. Kwan Wai Hoe for his inspiration, enthusiasm, and supervision. Besides, dedicated to my parents and caretakers for nursing me with knowledge and love. Finally, thanks to all who supporting throughout this journey of making this thesis report

ACKNOWLEDGEMENTS

I would like to thank everyone who had contributed to the successful completion of this project. I would like to express my gratitude to my research supervisor, Dr. Kwan Wai Hoe for this invaluable advice, guidance and his enormous patience throughout the development of this research.

In addition, I would like to express my gratitude to my loving parents and friends who had helped and given me encouragement, support, and motivation, as well as their advice and financial support throughout the course of my study in UTAR.

Apart from that, there are several individuals with whom I am truly grateful for their advice and contributions to this research and dissertation of this thesis such as my beloved friends.

THE ENGINEERING PROPERTIES AND DURABILITY PERFORMANCE OF ALKALI-ACTIVATED (POFA-GGBS-PFA) TERNARY HYBRID GEOPOLYMER COMPOSITE

ABSTRACT

Geopolymer technology involves production of cementless, environmental-friendly concrete which synthesizes from manufacture waste products including Ground Granulated Blast-furnace Slag (GGBS), Pulverized Fly Ash (PFA) and Palm Oil Fuel Ash (POFA) with merits to dwindle the enormous amount of industrial waste ash as well as the contribution in carbon footprint annually. High pH alkali activation facilitates dissociation of pozzolanic compound. After all, studies had proven elevated temperature curing is still required for conventional geopolymer product. This research presents the development of alkali-activated POFA-GGBS-PFA ternary hybrid geopolymer mortar under ambient-temperature curing condition. It also analyses to what extend the GGBS in ternary blended geopolymer improves the engineering properties and durability performance. A series of engineering properties tests of compressive strength, density ultrasonic pulse velocity and flow ability were carried out. Moreover, durability performance of ambient-cured ternary blended geopolymer mortar was examined via water absorption test, porosity test and capillary absorption test. Results showed that the setting time prolonged as the replacement level of PFA and POFA increased. Further, the compressive strength of examined specimens was found to be in the range of 30.71 to 55.02 MPa at 56 days. Inclusion of GGBS showed positive correlation with the engineering properties as well as better durable geopolymer product at ambient temperature.

Keywords: Geopolymer, Ground granulated blast-furnace slag (GGBS), Pulverized fly ash (PFA), Palm oil fuel ash (POFA), Compressive strength, Microstructure, SiO_2/Al_2O_3 ratio.

TABLE OF CONTENTS

DECLARATION **ii**
APPROVAL FOR SUBMISSION **iii**
ACKNOWLEDGEMENTS **vi**
ABSTRACT **vii**
TABLE OF CONTENTS **viii**
LIST OF TABLES **xii**
LIST OF FIGURES **xiv**
LIST OF ABBREVIATIONS **xviii**
LIST OF SYMBOLS **xix**

CHAPTER

1 INTRODUCTION **1**
1.1 Research Background 1
1.2 Aim and Objectives 3
1.3 Problem Statement 3
1.4 Scope of Study and Limitation 7
1.5 Significant of Study 8
1.6 Research Framework 10

2 LITERATURE REVIEW **11**
2.1 Introduction 11
2.2 Geopolymer Concrete and Geopolymerization Process 12
2.3 Factors Affecting Geopolymer Strength Development 17

	2.3.1	Alkali Activator	17
	2.3.2	Water Content	21
2.4	Effects of GGBS, POFA and PFA on Engineering Properties of Geopolymer Concrete		22
	2.4.1	Compressive Strength	23
	2.4.2	Density	26
	2.4.3	Ultrasonic Pulse Velocity (UPV)	28
	2.4.4	Microstructure	29
	2.4.5	Workability	33
2.5	Effects of GGBS, POFA and PFA on Durability Performance of Geopolymer Concrete		35
	2.5.1	Porosity	35
	2.5.2	Water Absorption	36
	2.5.3	Capillary Absorption Coefficient	37
2.6	Summary and Conclusion of Literature Review		38
3	**RESEARCH METHODOLOGY**		**40**
3.1	Introduction		40
3.2	Materials		40
	3.2.1	GGBS	41
	3.2.2	PFA	41
	3.2.3	POFA	41
	3.2.4	Mining Sand	43
	3.2.5	Alkali Activator	44
3.3	Experimental Program		45
	3.3.1	Preparation of Specimens	47
3.4	Experimental Testing Method		54
	3.4.1	Compressive Test	55
	3.4.2	Density Test	56
	3.4.3	Ultrasonic Pulse Velocity (UPV) Test	57

	3.4.4	Scanning Electron Microscopy (SEM) Examination	58
	3.4.5	Water Absorption Test	59
	3.4.6	Porosity Test	60
	3.4.7	Capillary Absorption Test	61
	3.4.8	Flow Table Test	62
4	**RESULT AND DISCUSSION**		**63**
4.1	Introduction		63
4.2	Workability		64
4.3	Compressive Strength		69
4.4	Density		75
4.5	Ultrasonic Pulse Velocity (UPV)		80
4.6	Water Absorption		86
4.7	Porosity		91
4.8	Capillary Absorption Coefficient		98
4.9	Scanning Electron Microscopy (SEM) Examination		106
	4.9.1	SEM images of G10F60P30	107
	4.9.2	SEM images of G30F47P23	109
	4.9.3	SEM images of G50F33P17	111
	4.9.4	SEM images of G70F20P10	113
	4.9.5	SEM images of G90F7P3	116
4.10	Summary and Discussion on Experimental Result		118
5	**CONCLUSION AND RECOMMENDATION**		**119**
5.1	General Conclusion		119
5.2	Engineering Properties of Alkali-activated Ternary Hybrid Geopolymer Mortar		120
5.3	Durability Performance of Alkali-activated Ternary Hybrid Geopolymer Mortar		121
5.4	Recommendations for Future Researc		122

REFERENCES **123**

LIST OF STANDARDS **130**

LIST OF TABLES

TABLE	TITLE	PAGE
1.1	Generation of oil palm kernel shell, oil palm kernel and POFA in Year 2011 from Malaysian Palm Oil Board (MPOB)	4
1.2	Pollution index by country 2016 mid-year in Asia	6
2.1	Chemical composition of GGBS, POFA and PFA	13
2.2	Compressive strength at 28 days with ambient curing sources	20
3.1	Physical properties of GGBS, PFA and POFA	42
3.2	Sieve analysis for mining sand	43
3.3	Mix proportion of geopolymer mortar for optimum GGBS content	45
3.4	Mix proportion of geopolymer mortar for optimum PFA:POFA ratio	45
3.5	Control and constant variable	46
3.6	Test program schedule	51
4.1	Flow table test of geopolymer mortar	64
4.2	Compressive strength with varying replacement of GGBS, PFA and POFA	69
4.3	Density with varying replacement of GGBS, PFA and POFA	75

4.4	Quality assessment on UPV value	80
4.5	UPV value with varying replacement GGBS, PFA and POFA	80
4.6	Water absorption with varying replacement of GGBS, PFA and POFA	86
4.7	Porosity values with varying replacement of GGBS, PFA and POFA	91
4.8	Capillary absorption coefficient with varying replacement of GGBS	99
4.9	Gradient of capillary action graph with varying replacement of GGBS	100
4.10	Capillary absorption coefficient with varying PFA:POFA ratio	103
4.11	Gradient of capillary action graph with varying PFA:POFA ratio	104

LIST OF FIGURES

FIGURE	TITLE	PAGE
1.1	Compressive strength of various FA-sources geopolymer at 28 days	5
1.2	University of Queensland's Global Change Institute	9
1.3	Research framework	10
2.1	Composition of PS, PSS and PSDS	12
2.2	Chain diagram of Poly-sialate Oligomer	13
2.3	SEM image of 100 % GGBS geopolymer paste	29
2.4	SEM image of 100 % FA geopolymer paste	29
2.5	SEM images of 50 % GGBS & 50 % FA geopolymer paste	30
2.6	SEM image of Pulverized fly ash (PFA)	31
2.7	SEM image of GGBS	31
2.8	SEM image of POFA	32
2.9	SEM image of fly ash	32
3.1	GGBS, PFA and POFA binders	42
3.2	Particle size distribution chart	43
3.3	Alkali activator	44
3.4	Preparation of geopolymer mortar	47
3.5	Application of demoulding oil prior to specimen casting	48

3.6	Experimental specimens with varying replacement level of GGBS	49
3.7	Experimental specimens with varying PFA:POFA ratio	49
3.8	Ternary blended GGBS-PFA-POFA geopolymer mortar specimens	50
3.9	Experimental program flow chart for optimum replacement level of GGBS	52
3.10	Experimental program flow chart for optimum PFA:POFA ratio	53
3.11	Kenco compressor testing machine	55
3.12	Measurement of mass in air as well as mass submersed in water	56
3.13	Ultrasonic pulse velocity testing machine	57
3.14	Scanning electron microscopy machine	58
3.15	Vacuum-pressure vessel for obtaining saturated mass	60
3.16	Prism specimens for capillary absorption test	61
3.17	Flow table testing apparatus	62
4.1	Flow ability of geopolymer specimens	65
4.2	Flow table of G10F60P30	66
4.3	Flow table of G30F47P33	66
4.4	Flow table of G50F33P17	66
4.5	Flow table of G70F20P10	67
4.6	Flow table of G90F7P3 at first phase	67
4.7	Flow table of G90F7P3 at second phase	67
4.8	Flow table of PFA2.5:POFA0.5 with inclusion of superplasticizer	68

4.9	Flow table of PFA1:POFA2 with inclusion of superplasticizer	68
4.10	Effect of GGBS on compressive strength of geopolymer mortar	69
4.11	One-way ANOVA for replacement level of GGBS in synthesis of geopolymer binder versus compressive strength	72
4.12	Effect of PFA:POFA on compressive strength of geopolymer mortar	73
4.13	One-way ANOVA for varying PFA-to-POFA ratio in synthesis of geopolymer binder versus compressive strength	74
4.14	Effect of GGBS on density of geopolymer mortar	76
4.15	One-way ANOVA for replacement level of GGBS in synthesis of geopolymer binder versus density (kg/m3)	77
4.16	Effect of PFA-to-POFA ratio on density of geopolymer mortar	78
4.17	Linear correlation between compressive strength and density	79
4.18	Effect of GGBS on UPV value of geopolymer mortar	81
4.19	One-way ANOVA for replacement level of GGBS in synthesis of geopolymer binder versus UPV value	82
4.20	Effect of PFA-to-POFA ratio on UPV value of geopolymer mortar	83
4.21	Positive correlation between compressive strength with UPV values	84
4.22	Surface plot of geopolymer binder synthesis with varying replacement level of GGBS versus engineering properties	85
4.23	Effect of GGBS on water absorption rate of geopolymer mortar	87
4.24	One-way ANOVA for replacement level of GGBS in synthesis of geopolymer binder versus water absorption	88

4.25	Effect of PFA:POFA ratio on water absorption of geopolymer mortar	89
4.26	Correlation between compressive strength and water absorption	90
4.27	Effect of GGBS on porosity rate of geopolymer mortar	92
4.28	One-way ANOVA for replacement level of GGBS in synthesis of geopolymer binder versus porosity	93
4.29	Effect of PFA-to-POFA ratio on porosity rate of geopolymer mortar	94
4.30	One-way ANOVA for varying PFA-to-POFA ratio in synthesis of geopolymer binder versus porosity	95
4.31	Positive correlation between water absorption and porosity	96
4.32	Surface plot of geopolymer binder synthesis with varying replacement level of GGBS versus durability performance	97
4.33	Effect of GGBS on capillary absorption of geopolymer mortar	100
4.34	Effect of PFA:POFA ratio on capillary absorption of geopolymer mortar	104
4.35	SEM images of G10F60P30 at 14 days	108
4.36	SEM images of G30F47P23 at 14 days	110
4.37	SEM images of G50F33P17 at 14 days	111
4.38	Partially-dissolved PFA particle found in G50F33P17	112
4.39	SEM images of G70F20P10 at 14 days	113
4.40	Partial-dissolved, broken PFA particle found in G70F20P10	114
4.41	SEM images of G90F7P3 at 14 days	116

LIST OF ABBREVIATIONS

NaOH	Sodium Hydroxide
Na_2SiO_3	Sodium Silicate
GGBS	Ground Granulated Blast-furnace Slag
PFA	Pulverized Fly Ash
POFA	Palm Oil Fuel Ash
OPC	Ordinary Portland Cement
(CO_2-e)	Carbon Dioxide Emission
(C-S-H)	Calcium Silicate Hydrate
(C-A-S-H)	Calcium Aluminosilicate Hydrate
(N-A-S-H)	Sodium Aluminosilicate Hydrate
SiO_2	Silica / Silicon Dioxide
Al_2O_3	Aluminium Oxide
CaO	Calcium Oxide
XRF	X-ray Fluorescence
SEM	Scanning Electron Microscopy
SM	Silicate Modulus
BS	British Standards

LIST OF SYMBOLS

%	Percentage
g	Gram
kg	Kilogram
m	Meter
m^3	Cubic Meter
mm	Millimetre
mm^2	Millimetre Square
μm	Micrometre
MPa	Megapascal
N	Newton
kN	Kilonewton
km/s	Speed
kg/m^3	Density

CHAPTER 1

INTRODUCTION

1.1 RESEARCH BACKGROUND

Geopolymer is an inorganic aluminosilicate-hydroxide polymer synthesized from pozzolanic compound materials which consist essentially of silicon (Si) and aluminium (Al) for instance, Pulverized Fuel Ash (PFA), Ground Granulated Blast-furnace Slag (GGBS) and Palm Oil Fuel Ash (POFA) with alkali activator. Geopolymer is prevailing than ordinary Portland cement in terms of environmentally friendly, carbon footprint and durability. In fact, approximately 1.5 billion tons of carbon dioxide (CO_2) is emitted annually by the production of ordinary Portland cement (OPC). Each ton of cement produces approximately 1 tonne of carbon dioxide (CO_2). Meanwhile, the CO_2 emission from the production of ordinary Portland cement contributes about 5 % to 7 % of total global anthropogenic emission (Turner & Collins, 2013).

Greenhouse gas emissions by Australian geopolymer concrete is estimated about 44 % to 64 % lower than ordinary Portland cement (McLellan *et al.*, 2011). The CO_2 emission by GGBS is only about 7 % of OPC. Each ton of GGBS releases only about 70kg of CO_2 for the equivalent quantity of OPC (Islam et al., 2015).

Geopolymerization comprises three basic stages which are first, dissolution of the aluminosilicate materials, following by gel formation and eventually polycondensation. At the first stage, use of the highly-alkaline solution including sodium hydroxide (NaOH) to dissolve the aluminosilicates in the pozzolanic material into silica solution, alumina solution and aluminosilicate species. Next, gel is formed by the supersaturated aluminosilicate solution as oligomers and eventually forming a three-dimensional network of silicon-aluminates structures with similar strength or even higher than OPC concrete as the gel continues to reorganize and rearrange. Instead of a linear time series, these processes usually occur concurrently throughout the mixture (Soutsos et al., 2016). Furthermore, three different types of structures can be from geopolymerization which is: polysialate (-Si-O-Al-O-), polysialate-siloxo (Si-O-Al-O-Si-O) and polysialate-disiloxo (Si-O-Al-O-Si-O-Si-O-) depending on the resultant chemical bonding and the SiO_2/Al_2O_3 ratio (Part et al., 2015).

The aforementioned gel formation in geopolymerization is differed from the main binding system of traditional hydrated Portland cement. Sodium Aluminosilicate Hydrate (N-A-S-H) gel is the main product of alkali activated system. On the other hand, the hydration of OPC forms Calcium Silicate Hydrate (C-S-H) gel function as the cement pastes. However, the co-existence of N-A-S-H and C-A-S-H gels has been studied and would enhance the gel microstructures and overall compressive strength varying with Calcium (Ca) content, pH value and Si/Al ratio of the mixture (Garcia-Lodeiro et al., 2011).

PFA namely, class F low calcium Pulverized Fly Ash consist abundantly of silicon dioxide (SiO_2) and aluminate oxide (Al) with very low Ca/Si ratio mainly produces N-A-S-H gels. In the contrary, C-A-S-H gel is the main product of alkali activated GGBS due to high Ca content with 1-1.5 Ca/Si ratio and low Al/Si ratio of 0.3-0.4 (Soutsos et al., 2016). Furthermore, Garcia-Lodeiro et al. (2011) investigated the presence of Ca will degrade the three-dimensionally structured designated N-A-S-H gel at high pH (>12) in favor of C-A-S-H gel formation.

1.2 AIMS AND OBJECTIVES

Aim

To develop alkali-activated ternary blended Geopolymer mortar (POFA-GGBS-PFA) at ambient temperature for building component fabrication.

Objectives

- ✓ To study the engineering properties of sodium alkali activated POFA-GGBS-PFA ternary hybrid geopolymer mortar composites at ambient temperature.

- ✓ To study the durability performance of sodium alkali activated POFA-GGBS-PFA ternary hybrid geopolymer mortar composites at ambient temperature.

1.3 PROBLEM STATEMENT

Global ash production is about 500 million tons annually, of which 75 % to 80 % is FA (Ranjbar et al., 2014a). Disposal problems of FA lead to environmental issue due to vast areas of land have been occupied as ash ponds and have led researchers to exploit FA as supplementary material in production of geopolymer and Portland cement. Fly ash ponds will release particulates into the atmosphere and leachates are produced due to infiltration of rainwater, prone to pollute the local aquifers (Voltaggio et al., 2015). In Malaysia, approximately 40 % of electricity is generated by pulverized coal firing, which depletes about 11 million tonnes of coal annually. Yearly, about 3 million tonnes of FA are produced from the thermal power plants with the use of aforementioned powdered coal burning (Yap & Foong, 2013).

Table 1.1: Generation of oil palm kernel shell, oil palm kernel and POFA in year 2011 from Malaysian Palm Oil Board (MPOB) (Yap & Foong, 2013)

Materials	Waste generated (million tonnes)			
	2007	2008	2009	2010
Oil Palm Kernel Shell (OPKS)	2.2	2.4	2.3	2.2
Oil Palm Kernel	4.1	4.3	4.2	4.3
POFA	0.06	0.06	0.06	0.06

Table 1.1 shows that 0.06 million tonnes of POFA is produced in Malaysia annually. POFA which currently disposed to landfill and ash ponds could lead to the environmental problem as well due to low utilization and limited uses (Ranjbar et al., 2014b). In order to minimize the wastage ash disposal to landfill, numbers of researches have been conducted to utilize FA and POFA as cementitious materials in geopolymer or blended cement.

However, conventional PFA or POFA-based geopolymer requires elevated temperature curing (60^{o}C to 80^{o}C) for 24 hours to develop sufficient strength and do not gain any significant strength at ambient curing (Ranjbar et al., 2014a). In the research of Atiş et al. (2015), a dramatically improvement in strength development of geopolymer mortar is observed as the curing temperature increased. Geopolymer mortar cured at 105^{o}C for 24 hours achieved high compressive strength of 110.7 MPa, whereas similar specimen cured at 55^{o}C only developed incredibly low strength of 1.2 MPa. The vast difference in strength development indicates the limitation of geopolymer in terms of ambient curing. The requirement of elevated temperature curing for geopolymer product has limited the application of geopolymer technology in pre-cast manufacture industry, instead of to be adopted for cast in-situ method.

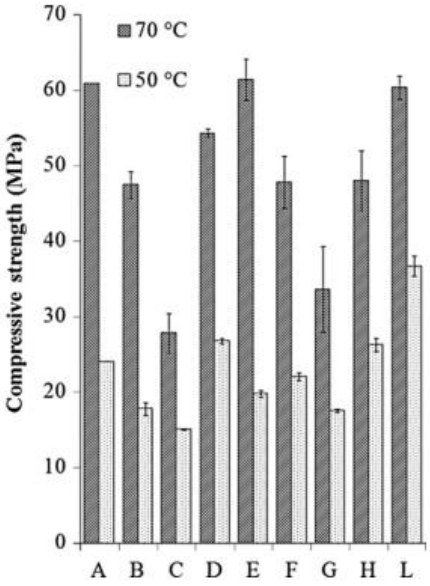

Figure 1.1: Compressive strength of various FA-sources geopolymer at 28 days (Soutsos et al., 2016)

Furthermore, Figure 1.1 indicates the overwhelming strength development in all FA-based geopolymer mortars cured at higher temperature of 70^{o}C over specimens cured at 50^{o}C. Unfortunately, elevated temperature curing plays a crucial role in carbon footprint, where contributed 12.4 % of carbon dioxide emission (CO_2-e) for the geopolymer (Turner & Collins, 2013). Furthermore, Deb et al. (2014) and Salih et al. (2015) have studied the almost linear relationship between the amount of GGBS with ambient curing, the inclusion of GGBS in blended geopolymer increase the compressive strength at 1, 7 and 28 days were cured at room temperature. This can be explained by the presence and contribution of calcium in the system.

Next, to the best knowledge of Yusuf et al. (2014) and Soutsos et al. (2016), very few researches and publications have been done on the properties and performance of alkali activated POFA in binary blended with GGBS, binary blended between FA and GGBS or in ternary blended form, further detailed investigations are needed. Not only that, the effect of calcium mingling with silica and alumina species in POFA-GGBS binary blended geopolymer is still very complex and unclear, further investigations are required to provide better insight (Salih et al., 2015).

Table 1.2: Pollution index by country 2016 mid-year in Asia (NUMBEO, 2016)

Country	Pollution Index	Expected Pollution Index
Vietnam	88.41	158.09
China	88.08	161.07
India	76.65	134.89
Indonesia	76.25	134.07
Thailand	72.84	127.23
Malaysia	67.61	116.78
Hong Kong	67.53	121.68
Taiwan	64.30	112.54
Sri Lanka	62.89	108.76
South Korea	50.28	90.01
Oman	44.20	73.40
Japan	40.90	66.70
Singapore	37.69	64.94

Table 1.2 shows the pollution index and expected pollution index of different countries in Asia. Malaysia is comparatively high with the pollution index of 67.61 and expected pollution index of 116.78. According to Malaysia Infrastructure Report (2013), the pollution index of Hong Kong was ranked on top of Malaysia in 2013, yet currently in Year 2016 Malaysia has surpassed Hong Kong which pollution index of 67.53. The carbon dioxide emission (CO_2-e) from cement is higher than geopolymer during the hydration and chemical reaction process. Therefore, geopolymer is the better alternative to OPC concrete for the advantage of lower global carbon footprint and environmental-friendly.

1.4 SCOPE OF STUDY AND LIMITATION

This research is to study the engineering properties and durability performance of alkali activated ternary blended geopolymer at room temperature. All the specimens were cured at ambient temperature and the result of 3, 7, 14 and 28 days were taken. Furthermore, the fine aggregates in this study are held constant on mining sand and the alkali activator are used of the combination of sodium silicate and sodium hydroxide with constant Na_2SiO_3/NaOH ratio of 2.5 and concentration of 12 M NaOH. The varying composition of binder among GGBS, POFA and PFA are the independent variables of this study for the purpose to study the effect of composition of binder in terms of engineering properties and durability performances of ternary blended geopolymer.

Next, both the engineering properties and durability performance of blended geopolymer are the dependent variables of this study. The engineering properties to be studied in research are compressive strength, density, internal voids of the specimens and microstructure. Besides that, the durability performances are including porosity, water absorption and capillary absorption of the geopolymer. Lastly, the workability of the freshly mixed geopolymers is studied through slump test as well.

The limitation of this research is the reaction and mechanism of geopolymerization process among GGBS, POFA and PFA are not observed. The quantitative data obtained through this research are limited to the effect of engineering properties and durability performance with varying binder composites which did not indicated the rate of hydration and mechanism of geopolymerization process.

1.5 SIGNIFICANT OF STUDY

A thoroughly explanation and better insight on the rate of hardening and strength development of ternary blended geopolymer among GGBS, PFA and POFA with ambient curing can be provided in this research. Therefore, the optimum synthesis of GGBS-PFA-POFA ternary blended geopolymer binder can be obtained throughout the research and the outcome of optimum synthesis can be applied to either concrete or mortar product.

Conventional geopolymer needs of elevated temperature curing to develop significant strength, which results in drawback effect to the environment due to higher emission of carbon dioxide compare to ambient curing. Although studies have proven the positive relationship between the elevated temperatures curing with the compressive strength development of geopolymer mortar, however the prolongation of curing duration would adversely affect microstructural matrix by forming of micro-cracks. This is related to substantially loss of pore fluid and moisture from the geopolymer matrix, which ended up induced rapidly and excessive drying shrinkage during the curing process (Sukmak, P. & Horpibulsuk S., 2013). Through this study, satisfactory strength of ternary blended geopolymer can be developed at ambient temperature. This would facilitate the application of geopolymer technology in the industry as well as able to enhance the confidence level of Malaysia construction industry in geopolymer technology as a satisfactorily in-situ material.

Next, environmental issue can be minimized though this research. Maximizing the utilization of waste products by proving and promoting the waste materials such as FA, POFA and GGBS are of great benefit to building structures in terms of strength and exposure to acid or sulphate attack as well as eco-friendly technology. The University of Queensland's Global Change Institute (GCI), Australia has successfully use of slag/fly ash-based geopolymer concrete for structural purpose (Islam et al., 2015).

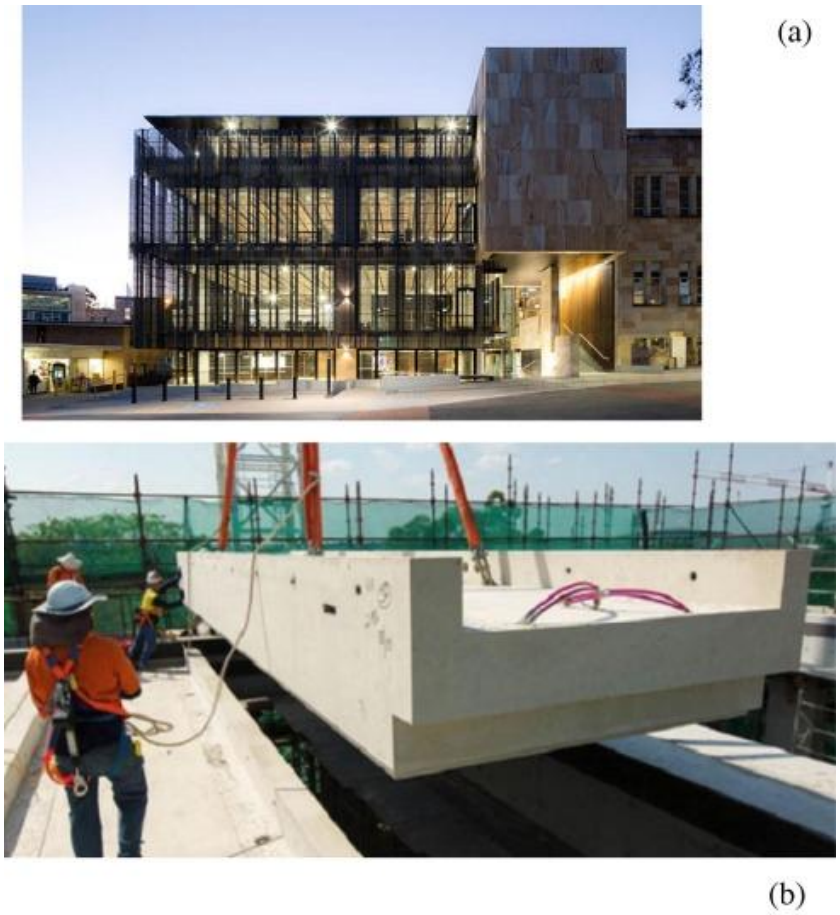

Figure 1.2: University of Queensland's Global Change Institute (Islam et al., 2015)

Instead of disposing FA and POFA in landfill or ash ponds, utilizing them in binary or ternary blended geopolymer as better alternative to ordinary Portland cement concrete for the purpose of reducing wastage and pollution. Not only that, geopolymer contributes to lower the carbon footprint. Approximately 9 % lower in CO_2-e by geopolymer concrete compare to OPC concrete after taking account of treatment, mining, transportation and alkali activators for geopolymer (Turner & Collins, 2013). Therefore, geopolymer has great potential in reducing pollution, climate-changing impact and greenhouse effect.

1.6 RESEARCH FRAMEWORK

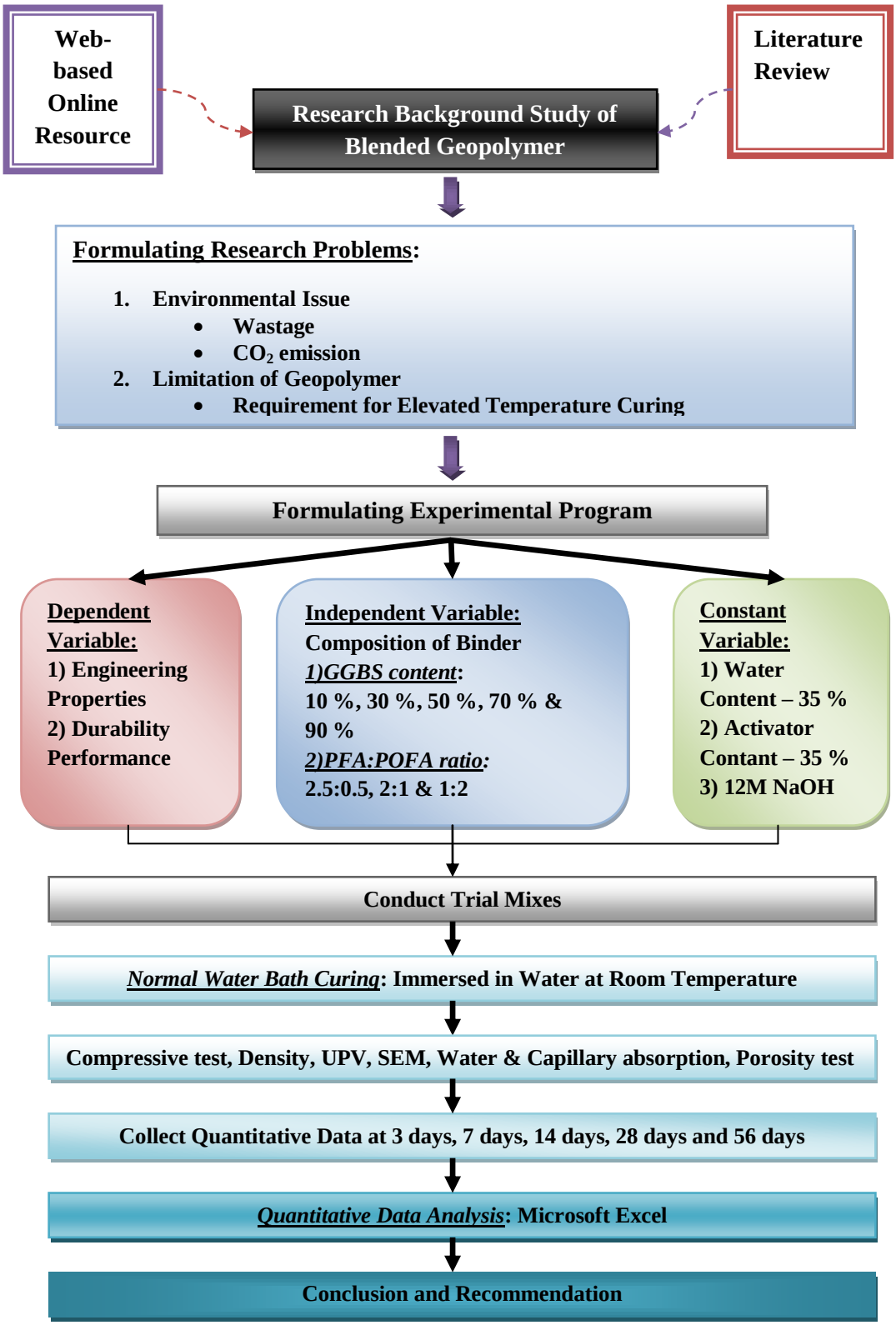

Figure 1.3: Research framework

CHAPTER 2

LITERATURE REVIEW

2.1 INTRODUCTION

This chapter is mainly discussed the factors affect the geopolymerization process and strength development of alkali-activated binary or ternary blended geopolymer (POFA-PFA-GGBS) including concentration of alkali activators and water content. The varying compositions of GGBS, POFA and PFA in binder would determine the dominance of N-A-S-H and C-A-S-H gel in the geopolymer. Next, the factors affecting the engineering properties of blended geopolymer including compressive strength, density and microstructures. Besides that, the water absorption rate, porosity and capillary absorption coefficient, namely durability performance of hybrid geopolymer will be thoroughly discussed in this chapter.

2.2 GEOPOLYMER CONCRETE AND GEOPOLYMERIZATION PROCESS

Geopolymer typically consists of three fundamental poly-sialate oligomer units, namely Poly-sialate with 1.0 Si/Al, Poly-sialate siloxo with 2.0 Si/Al and Poly-sialate disiloxo with 3.0 Si/Al (Mackenzie and Welter, 2014). Geopolymerization mechanism adopts the ion-pair theory which involves chemical reactions between several alumino-silicate oxides with silicates. Upon the highly alkaline conditions, the dissolution and rehydration of Si–Al elements would turn into the sources of geopolymerization (Yang et al., 2008).

These units are tend to condense randomly into ring cross-linked or chains to build up amorphous framework as shown in Figure 2.1 and Figure 2.2. These aluminosilicate source and the reaction conditions including the type and concentration of alkali activator, curing period and temperature are the key factors of varying in compressive strength of geopolymer.

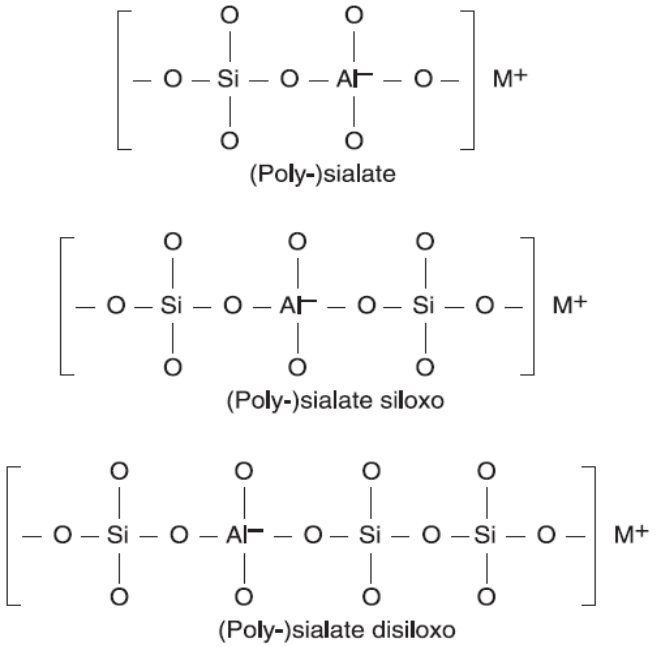

Figure 2.1: Composition of PS, PSS and PSDS (Mackenzie & Welter, 2014)

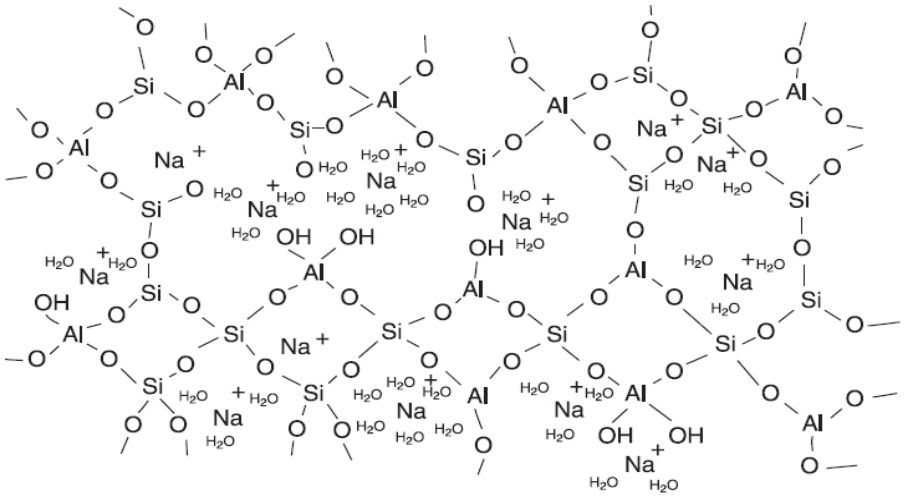

Figure 2.2: Chain diagram of Poly-sialate Oligomer (Mackenzie and Welter, 2014)

GGBS is a by-product waste of the production of iron and it consists chiefly of Al_2O_3, SiO_2 and CaO in amorphous state. It is an ideal alternative to cement in concrete industry with the advantages of lower CO_2 emission and utilization of wastes product. Next, Class F low calcium pulverized fly ash, namely PFA is the by-product from coal fired power station with potential pozzolanic properties. It is fine powder with glassy (amorphous), spherical particles and composes essentially of SiO_2 and Al_2O_3. Normal-Al_2O_3 content (25 % to 45 %) FA developed superior properties compare to low- Al_2O_3 FA due to lower mass loss and higher degree of geopolymerizaton occurred (Zhou et al., 2016). Not only that, POFA is also one of the waste products which obtained from the production of palm oil and is approximately 5 % of solid waste (Islam et al., 2014). It contributes significant amount of Si in the geopolymer. The chemical composition of GGBS, POFA and PFA through X-ray Fluorescence (XRF) analysis is shown in Table 2.1.

Table 2.1: Chemical composition of GGBS, POFA and PFA (Islam et al., 2014)

Chemical compounds	SiO_2	Al_2O_3	CaO	Na_2O	MgO	K_2O
GGBS	32.52	13.71	45.83	0.25	3.27	0.48
POFA	63.41	5.55	4.34	0.16	3.74	6.33
PFA	54.72	27.28	5.31	0.43	1.10	1.00

Furthermore, according to the research of Yusuf et al. (2014), GGBS tend to contribute soluble Ca and resulting mainly formation of calcium-silicate-hydrate (C-S-H) gel in the mix. The inclusion of GGBS in binary blended geopolymer (POFA-GGBS) increased the amorphousness of the geopolymer namely increasing soluble Ca ions, thus more reactive Al are contributed to the system and result in the changes in the characteristic of C-S-H formed to C-A-S-H gel. Higher amount of gels are formed result to higher density due to pores filling effect in the mix. Not only that, Salih et al. (2015) further proven that GGBS contributes to the increment of Ca/Si ratio and the diminishing of Si/Al ratio in the mix due to GGBS increasing the amount of Al to the system. Higher amount of Al ions shifts the C-S-H to C-A-S-H gel.

1) Si + Ca = (C-S-H)

2) Si + Al = (A-S-H)

Next, in the studies of Soutsos et al. (2016), FA-based geopolymer produces mainly of N-A-S-H gel with very low Ca/Si ratio. In the contrast, the main product from 100 % GGBS geopolymer is C-A-S-H gel with Ca/Si ratio of 1-1.5 and a very low Al/Si ratio of 0.3-0.4. The co-existence of both N-A-S-H and C-A-S-H gel could enhance the bonding of microstructure improving the compressive strength.

Furthermore, in the research of Wardhono et al. (2015), two possible mechanism on the hydration reaction between FA and GGBS. Firstly, the hydration reaction of GGBS is precedent to the polymerization of FA, both are occurring separately. In this case, GGBS tend to form a matrix around the FA, and FA fills in the pores subsequently. Secondly, both the hydration reaction and polymerization of GGBS and FA are occurring simultaneously. In this latter case, the reaction of GGBS, activates the FA at ambient temperature. The beneficial effect of GGBS content on compressive strength mainly due to higher reactivity at ambient temperature than FA and thus greater formation of reacted products without heat curing (Gao et al., 2016).

Numbers of studies had proven the contribution of CaO in strength development of geopolymer at room temperature. However, in the research of Puligilla & Mondal (2013) has shown the contribution of GGBS is relatively outstanding performance than mere CaO replacement in FA-based geopolymer. The ultimate strength of specimen added with 1 % of CaO is lower than specimen blended with 1 % of GGBS, despite of the total amount of calcium is the same. Not only that, inclusion of GGBS contributed to reduction in drying shrinkage of geopolymer (Deb, Nath and Sarker, 2015).

The critical difference between the two specimens is the rate of dissolution, and this would create different amount of free calcium ions in the system. The rapid dissolution of CaO is mostly been consumed in the early stage, while the dissolution of GGBS is much slower and thus continuously influencing on the geopolymerization for a longer duration. The reaction of specimens with 1 % of CaO is slowed down at around 210 minutes due to complete consumption of calcium, whereas the reaction of specimen with 1 % GGBS is slowed down after 270 minutes. The availability of free calcium ions in the GGBS promotes the dissolution of FA and formation of geopolymeric gels in the extended time duration (later stage). Besides, GGBS also contributes silicon, aluminum and magnesium which may influence on the compressive strength.

In the studies of Ranjbar et al. (2014a), Al ions contribute to high initial strength due to easier dissolve than Si components, and this allows higher rate of condensation between aluminate and silicate species than mere condensation between silicate species. Therefore, the lower the Si/Al ratio, the higher the initial strength of PFA-POFA blended geopolymer. The greater amount of POFA in the mix, the higher the Si/Al ratio, thus the lower the initial strength. Next, FA-based geopolymer needs of elevated curing temperature to develop significant strength. Curing temperature of 300^{o}C developed the highest compressive strength of PFA-POFA binary blended geopolymer at all level of PFA (0 %, 25 %, 50 %, 75 % and 100 %).

Further proven by Ranjbar et al. (2014b) on FA-POFA blended geopolymer mortar in the same year, lower initial strength development in POFA-based geopolymer with higher Si/Al ratio compare to FA-based geopolymer with lower Si/Al ratio. The varying Si/Al ratio throughout the geopolymerization process is the key factor of strength development at future stage. Therefore, the abundant of Si in POFA prolong the strength development and gradual hardening as the gradual increment of Si for reaction and condensation between silicate and silicon species throughout the geopolymerization process. In the opposite, the Al components in FA contribute to quicker reaction and condensation at the early stage.

2.3 FACTORS AFFECTING GEOPOLYMER STRENGTH DEVELOPMENT

The properties and performance of geopolymer including strength and microstructure development, durability and workability of fresh geopolymer are significantly influenced by composition of blended binder, chemical composite of binder, alkali activator, water content and curing condition. The concentration and dosage of alkali activator affect the rate of geopolymerization and determine the final strength of hardened geopolymer. Besides, the molarity of activator solution would affect by the water content as well. Hydroxyl ions (water) in activator solution contributes to liberation of Si and Al from the geopolymer binder (Williamson & Juenger, 2016). However, excess in water content would dilute the concentration of activator. Therefore, the effect of alkali activator and water content on geopolymer is thoroughly study in this chapter.

2.3.1 ALKALI ACTIVATOR

Alkali activator is added into geopolymer to improve the pH value of geopolymer mix with the primary purpose to enhance the dissolution of geopolymer binder. Therefore the concentration and content of activator would vastly affect the hydration reaction of geopolymer concrete. The binder particles would only partially reacted when the activator modulus is low, yet excessive alkali modulus beyond the optimum level would attribute over-strongly alkaline which so much so affect the crystallized structure of geopolymer and creating cracks. Deb et al. (2014) have investigated the effects of sodium silicate to sodium hydroxide (Na_2SiO_3/NaOH) ratio and alkali activator content on the workability and compressive strength of GGBS-FA blended geopolymer. The Na_2SiO_3/NaOH ratio decreased from 2.5 to 1.5 resulting in increased in compressive strength. Not only that, the strength improved when the activator content increased from 35 % to 40 %, yet reverse effect on the workability.

Therefore, the optimal Na_2SiO_3/NaOH ratio of 1.5 with 40 % activator content is the optimal alkali activator dosage in terms of strength. However, according to the finding of Salih et al. (2014), the compressive strength of POFA-based geopolymer increased by increasing the Na_2SiO_3/NaOH ratio. The Na_2SiO_3/NaOH ratio of 2.5 achieved the maximum strength of 24.48 MPa at 28 days, yet the strength dropped to 23.83 MPa when Na_2SiO_3/NaOH ratio continue increased to 3.0.

In addition, Singh et al. (2016) had further proven the activator-binder ratio of 0.4 developed higher compressive strength than 0.35 activator-binder ratio for blended geopolymer (GGBS-FA). The specimen containing 40 % alkali activator achieved targeted strength of 35 MPa at 28 days whereas lower strength of 30.26 MPa is developed by the specimen containing lower activator content (35 %). Besides, the highest compressive strength of FA-GGBS binary blended geopolymer was obtained at optimum activator concentration of 14M due to higher amount of hydrated gels is produced. Activator with lower concentration (12M), would result in insufficient dissolution of aluminosilicate species and therefore geopolymer gel are unable to fully form at this concentration level. However beyond the optimum concentration, the strength shows decrease trend as increasing in the activator concentration (16M). This can be explained by viscosity of higher molarity of activator solution limits the leaching of Si and Al as well as might lead to formation of sodium carbonate by reaction between excess Na and atmospheric CO_2 (Williamson & Juenger, 2016).

Similar outcome has been proven in the studies of Kazemian et al. (2015), geopolymer mortar activated by 12 M NaOH developed higher compressive strength at 28 days as above 40 MPa than which activated by 4 M and 8 M NaOH of below 15 MPa. Besides, increased in Na_2SiO_3 to NaOH ratio from 0.25 to 1.0 contributed to higher strength of 30 MPa and 40 MPa respectively. Furthermore, low concentration of alkali activator lead to insufficient dissolution of Si and Al ions, resulted in lower degree of geopolymerization and strength development (Nath *et al.*, 2016).

The formula for the specific gravity of combined alkali activator of sodium silicate with sodium hydroxide is provided (Islam et al., 2015).

$$\frac{\mathbf{G}_{\mathrm{NaOH}} \times \mathbf{1}}{\mathbf{1} + \mathbf{2.5}} + \frac{\mathbf{G}_{\mathrm{Na_2SiO_3}} \times \mathbf{2.5}}{\mathbf{1} + \mathbf{2.5}}$$

Moreover, in the research of Al-Majidi et al. (2016), positive relationship is found between the silicate modulus (SM) as well as dosage of alkali activator and the compressive strength. In other words, the compressive strength of geopolymer increased with increasing in activator dosage and SM. Not only that, according to Wang et al. (2015), the higher dosage of alkaline solutions, the higher the compressive strength. The average compressive strength of binary blended geopolymer concrete (GGBS-FA) with 0.5 % alkaline solution is only 46.61 MPa at 28 days, yet the average strength increased to 85.09 MPa and 93.60 MPa when increasing the alkaline solution to 1.0 % and 1.5 %, respectively. This is because of higher alkaline condition increases the polymerization rate and hydration reaction by providing higher pH value to dissolve and destroy the structure of slag. However, additional content of alkaline solution in geopolymer would shorten the setting time due to accelerating the hardening process with higher rate of polymerization at early stage.

Gao et al. (2016) had investigated the effect of activator modulus (M_s) namely, SiO_2/Na_2O molar ratio on workability, setting time, compressive strength and porosity of binary blended geopolymer (GGBS-FA). Targeted M_s is achieved by adding appropriate amount of NaOH into Na_2SiO_3 solution. Increased in M_s indicates higher content of sodium silicate in the activator solution. The slump flows are slightly increased from 16.4cm to 23.6cm and 26.5cm with the increase in M_s from 1.0 to 1.4 and then 1.8, respectively. The explanation on this was due to activator solution with higher proportion of Si benefits the workability due to the nature of silicate group. Not only that, increase in activator modulus would extend the initial and final setting time as well.

The activator modulus decreased from 1.8 to 1.0 so does the initial/final setting time reduced from 60/110 min to 26/69 min. The increased in M_s caused relatively higher proportion of Na2SiO3 to NaOH in the activator solution, thus prolong the hydration reaction. Next, activator modulus of 1.4 indicates the optimum compressive strength in the study. The compressive strength of 80 % GGBS and 20 % FA blended geopolymer at 7 days increased from 61.8 MPa to 68.4 MPa with shifting activator modulus from 1.0 to 1.4, yet lower strength of 65.3 MPa when beyond 1.4 M_s to 1.8 M_s.

However, contrast finding in the studies of Salih et al. (2014), workability of POFA-based geopolymer decrease as the increased in Na_2SiO_3/NaOH ratio. The flow of 243mm for the specimen with 1.0 Na_2SiO_3/NaOH ratio, decreased to 227mm when Na_2SiO_3/NaOH ratio increased to 3.0. Besides, 2.5 ratio of Na_2SiO_3/NaOH is the optimum ratio of activator in terms of strength development.

Table 2.2: Compressive strength at 28 days with ambient curing sources: (Phoo-Ngernkham et al., 2015)

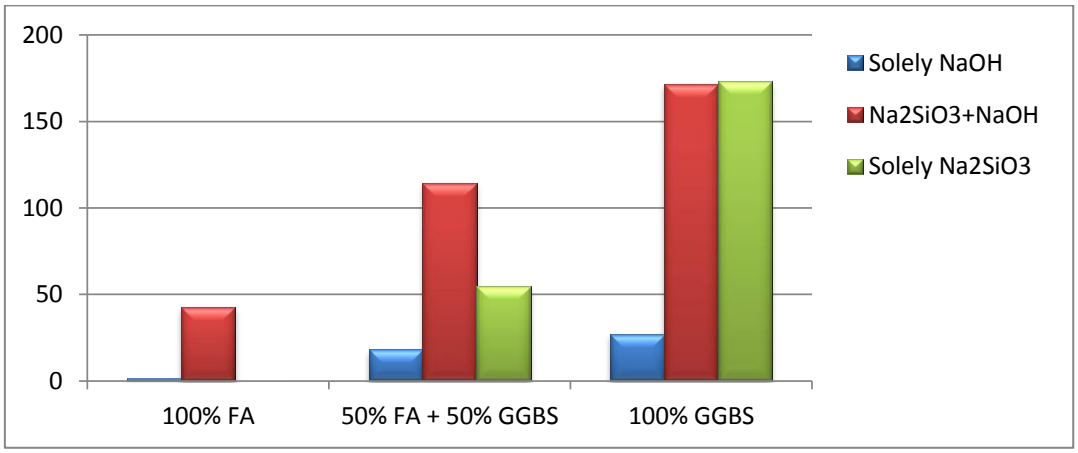

Table 2.2 indicates the effect of different composition in alkali activator as well as blended binder (GGBS-FA) on compressive strength of GGBS-FA blended geopolymer concrete at 28 days. Lowest strength obtained with activated by NaOH solely in all specimens with varying binder ratio. The combined alkaline solution of 2.0 Na_2SiO_3/ NaOH activator shows relatively higher strength in all different binder composites.

Although highest strength of 173.0 MPa is achieved by the 100 % GGBS specimen activated solely by sodium silicate, yet insignificant strength in other specimens composing FA. This mainly due to additional Si in the system, hasten the geopolymerization process (Phoo-Ngernkham et al., 2015).

2.3.2 WATER CONTENT

Water performs as the medium in synthesizing the Si and Al during dissolution, condensation and polymerization stages (Xie & Kayali, 2014). Although previous studies have proven reverse effect between the water-binder ratios and compressive strength, yet somehow water content does contributes to higher rate of geopolymerization. According to Kazemian et al. (2015), low liquid to solid ratio (L/S) below the optimum point would hinder the strength development of geopolymer mortar. A nearly flat curve movement is observed on the strength development of geopolymer with 0.62 L/S. Higher L/S shows upward movement in the strength development over the curing age. Specimen with 0.81 L/S developed above 30 MPa compressive strength at 28 days, while the specimen with 0.62 L/S developed strength below 15 MPa. However, excess in liquid might obstruct the strength development as well. Slightly lower strength of 23 MPa is achieved by the geopolymer mortar with 1.08 L/S compare to 0.8 L/S.

Furthermore, Salami et al. (2016) had investigated the effect of water content and superplasticizer on compressive strength and workability of 100 % POFA-based geopolymer. POFA has high surface area with particle distribution of 1.068μm. This may lead to higher requirement of water to binder ratio for the purpose of desired workability. Three specimens with varying content of water and superplasticizer is studied.

The results show highest compressive strength of 18.2 MPa at 3 days is developed by the specimen with 10 % water content alone, following by around 17.5 MPa by the specimen with combined 5 % water content and 5 % superplasticizer and the lowest compressive strength of about 15 MPa by the specimen with 10 % superplasticizer alone. The flaw in specimen with superplasticizer alone in terms of strength development is due to weakly bound H-O-H scilicet, weak hydrogen bond in the matrix of geopolymerization products and this is determined by the quantity of H^+.

According to Xie & Kayali (2014), the higher the water content, the lower the compressive strength of FA-based geopolymer. Increase in water content would dilute the concentrated alkali activator result in lower hydration reaction due to insufficient alkaline strength to dissolve the Si and Al of FA particles. A vast difference is observed between the strength of specimens at 14 days of 16.16 MPa and 10.81 MPa with water/binder ratio of 0.22 and 0.26, respectively. Greater proportion of unreacted FA particles is identified in the specimen with higher water/binder ratio. Lower water/binder ratio would accelerate the geopolymerization process. Similar outcome is proven is the studies of Aliabdo et al. (2016), compressive strength of approximately 34 MPa at 7 days is reduced to about 26 MPa when additional water content of 10 kg/m^3 is increased to 35 kg/m^3. Besides, the water absorption rate and porosity percentage of FA-based increased as the additional water content increased to the specimens.

2.4 EFFECTS OF GGBS, POFA, PFA ON ENGINEERING PROPERTIES OF GEOPOLYMER CONCRETE

The engineering properties of geopolymer at room temperature are influenced by the different composition of binder among GGBS, POFA and PFA. In this study, the engineering properties of ternary blended geopolymer mortar to be studied are including compressive strength, density, UPV, microstructure and workability.

2.4.1 COMPRESSIVE STRENGTH

The compressive strength of binary or ternary geopolymer is vastly influenced by the composition of binder. Variation in the composition of binder (GGBS-POFA-PFA) would cause varying in Si/Al ratio, Ca/Si ratio and Na/Si ratio which are directly affecting the properties and performance of geopolymer concrete.

Zhou et al. (2016) had investigated the effect of variation in Si/Al ratio and on compressive strength of both low-Al and high-Al FA-based geopolymer. Result indicates optimum Si/Al ratio of 2.0 developed highest 7 days compressive strength of 21.5 MPa at room temperature (20^{o}C), following by Si/Al ratio of 2.5 and then 1.5. The compressive strength dropped dramatically to 11 MPa, when Al content is greater than Si with Si/Al of 1:1.15. Besides, all of these specimens with different in Si/Al ratio, continuously increased the strength when under heat curing up to 80^{o}C.

In the research of Yusuf et al. (2014), the optimum ratio of 20 % GGBS and 80 % POFA found to be highest compressive strength of 44.57 MPa at 28 days, beyond 20 % of GGBS resulted in drawback effect in terms of compressive strength development. However, in the studies of Salih et al. (2015), found that the addition of GGBS in the mix from 10 % up to 50 % increased the strength at all ages, even beyond 20 %. The equal ratio of GGBS and POFA developed the highest strength at 28 days of 78.12 MPa compare to 0 % of GGBS specimen with the strength of 31.04 MPa at 28 days. The inclusion of GGBS contributes to acceleration of hardening process, thus reducing the setting time of the mix.

Furthermore, Islam et al. (2015) had found that the finer the particles size of POFA, the higher the compressive strength due to better filler effect, yet might affect the workability of the mix. Next, the addition of GGBS improved the initial strength at early stage and this could facilitate the reuse of formwork and hasten the construction.

Soutsos et al. (2016) had investigated the linear relationship between the compressive strength at 1, 7 and 28 days with the amount of GGBS in geopolymer which were cured at room temperature. Significant increase in compressive strength was observed from 20 to 50 MPa with only 20 % of GGBS is added. Curing temperature is the essential factor of strength development in FA based geopolymer. Besides, the highest compressive strength of 80 MPa was achieved at 28 days for mortar consist of 80 % GGBS and 20 % FA at room temperature. Similar phenomena is observed in the research of Puligilla & Mondal (2013), GGBS contributes to higher compressive strength at room temperature and hasten the setting time of geopolymer. The presence of soluble calcium dissolved from GGBS accelerates the hardening of geopolymer. Not only that, higher final strength is achieved with greater content of GGBS due to higher rate of geopolymerization of both FA and GGBS particles.

Gao et al. (2015) had investigated the effect of incorporation of nano-silica in GGBS-FA blended geopolymer concrete. The nano-silica composes essentially of SiO_2 (98.68 %), which could be assumed as similar effect for blending POFA into GGBS-FA binary blended geopolymer concrete as POFA consists mainly of Si (63.41 %) too. Increased in nano-silicate content enhanced the compressive strength up to optimum ratio of 2 %. 6.4 % increment in strength when nano-silicate content increased from 0 % to 1 %, but the strength dropped when nano-silicate content reached 3 %. Besides, increased in nano-silicate content resulting slightly delay the initial and final setting times.

In addition, Deb et al. (2014) had investigated the effects of GGBS content, sodium silicate to sodium hydroxide (Na_2SiO_3/NaOH) ratio and alkali activator content on the compressive strength of GGBS-FA blended geopolymer. The compressive strength of geopolymer increased at higher content of GGBS and activator but lower Na_2SiO_3/NaOH ratio of 1.5. The optimum 28 days compressive strength of 51 MPa was achieved by the geopolymer cont2ning 80 % of FA and 20 % of GGBS in the binder and 40 % of activator content with 1.5 Na_2SiO_3 to NaOH ratio.

Furthermore, inclusion of GGBS in FA-based geopolymer from 10 % to 50 % increased the compressive strength at ambient curing from 18.45 to 45 MPa at 28 days with the cost of accelerated hardening and resulting dramatically reduction in setting time as well as high rate of dry shrinkage (Al-Majidi et al., 2016). Next, in the studies of Wang et al. (2015), increase in the FA replacement in GGBS-FA blended geopolymer could bring drawback effect on compressive strength. The greater the replacement of FA the lower the compressive strength at all ages as well as all level of alkaline solutions. The optimal compressive strength of 93.06 MPa is 100 % GGBS with 1.5 % alkaline solution at 28 days. Futhermore, similar results are proven by Gao et al. (2016), the addition in GGBS content contributed to development of higher compressive strength at all ages. The compressive strength specimen with the GGBS/FA ratio of 40/60 at 7 days with activator modulus of 1.4 is 58.4 MPa. It slightly increased to 62.6 and 68.4 MPa when increasing the GGBS proportion to 60 % and 80 %, respectively.

Besides, the compressive strength of geopolymer is very sensitive to curing period, curing temperature, water/binder ratio and alkaline condition as well. The effect of different curing methods including bath curing, sealed curing and exposed curing with varying water-binder ratio of 0.33, 0.45 and 0.5 on the compressive strength of GGBS-based geopolymer has been investigated by Collins & Sanjayan (2008). First for the bath curing, specimens are immersed in saturated lime water at 23^{o}C and specimens are stored in confined space at 23^{o}C for sealed curing. Lastly exposed curing is exposing the specimens at 50 % relative humidity (RH) at 23^{o}C. Results have shown bath curing achieved highest compressive strength despite of shifting the water/binder ratio to all level. In the contrast, exposed curing indicates a decrease trend on compressive strength and developed unideal and lowest strength with all level of water contents. Furthermore, in the research of Xie & Kayali (2014) a positive relationship between compressive strength development of FA-based geopolymer and curing period is observed. Compressive strength of 3.54 MPa at 7 days is subsequently increased to 16.16 MPa at 14 days.

Besides, heat curing could hasten the strength development as well. Specimen with 4 hours elevated temperature curing achieved strength of 15.71 MPa is then increased to 42.07 MPa when subject to 24 hours heat curing. The compressive strength of FA-based geopolymer with 4 hours heat curing is comparable to specimen cured at 7 days. This indicates the important of elevated temperature to FA-based geopolymer during the early stage of curing period. Continuous heat curing over 24 hours would bring opposite effect to strength development of geopolymer.

2.4.2 DENSITY

The measurement of density could indirectly provide an insight to the degree of geopolymerization, presence of voids or porous structure, degree of compactness and compressive strength of geopolymer. Yong et al. (2016) had investigated the effect of changes in density on the compressive strength and pore structures. Form concrete is a ventilation technique by used of lightweight concrete with high degree of voice space (Zhang et al., 2014). In this research, specific volume of foam is added into specimens with density of 1300 and 1500 kg/m^3 respectively. The difference between foam added specimens resulting in reduction in density and normal dense geopolymer is observed. The reduction in density shows decrease trend of compressive strength and an upward trend of pore structure as well as water absorption rate in the FA-POFA blended geopolymer. The compressive strength of formed geopolymer with density of 1300 kg/m^3 at 28 days was 8.3 MPa, yet compressive strength of 13.5 MPa was developed by the formed geopolymer with higher density of 1500 kg/m^3. Hence, it explicitly illustrated the positive correlation between density and compressive strength.

Xie & Kayali (2014) had investigated a decreasing trend in density of FA-based geopolymer over the curing period. The density of 1.77 g/cm^3 is measured for the specimen cured at room temperature at 7 days, subsequently decreased to 1.75 g/cm^3 at 14 days ages. Similar trend is observed when FA-based geopolymer is subjected to heat curing. Density of 1.7 g/cm^3 with 4 hours heat curing is then reduced to 1.69 g/cm^3 after 24 hours of heat curing. Besides, water content is adversely affected the density of geopolymer. Lower density of is measured for the specimen with 0.22 water/binder ratio compared to specimen with higher water/binder ratio of 0.26 in all condition. However, in this case, reduction in density does not indicating lower compressive strength. The reduction of density over curing period is merely due to evaporation of internal moisture.

The higher solid to liquid (S/L) ratio , the higher the density of POFA-based geopolymer paste (Salih et al., 2014). Result has shown variation in the density of 1798.0 kg/m^3 and 1722.4 kg/m^3 with different in S/L ratio of 1.32 and 1.0 respectively. Higher density is obtained on the specimen with higher S/L ratio due to greater amount of binder lead to more compact structure and little porous voids with greater amount of reacted products. Further discuss in the studies of Cheah *et al.* (2016), increased in the replacement level of GGBS from 72 % to 80 % in GGBS-PFA binary blended geopolymer mortar resulted in an upward trending of bulk density from 2182 kg/m^3 to 2236 kg/m^3 at 90 days. This mainly due to denser microstructure was produced in the specimen with higher content of GGBS inclusion.

Furthermore, with reference to the studies of Islam *et al.* (2014), fully GGBS-based geopolymer developed highest oven-dried density of 2163 kg/m^3 at 3 days; oppose to completely fly ash-based geopolymer which found to be lowest 3-day oven-dried density of 2014 kg/m^3. The variance in density was much influenced by the specific gravity and fineness of pozzolanic binders. Besides that, the density could be determined by the filling effect of particles into the voids. POFA has relatively coarser particles as compared to GGBS and FA. Hence, the finer particles of GGBS contributed to enhance its density of about 7.5 % as compared to POFA-based geopolymer mortar.

2.4.3 ULTRASONIC PULSE VELOCITY (UPV)

Ultrasonic pulse velocity (UPV) test is to detect the micro-cracks, voids and cavities within the hardened geopolymer concrete or mortar in order to provide information on the compactness of experimental specimens. Low UPV value shows the presence of cavities, cracks or internal voids in the geopolymer products. Adequate compaction during the casting of geopolymer concrete would enhance the uniformity of hardened concrete and thus lead to higher UPV value (Islam et al., 2015). Next, the effect of alkali activator on UPV value had been studied in the research of Wang et al. (2015), the UPV of GGBS-FA binary blended geopolymer increased from 2187-3300 m/s to 3100-4024 m/s at 28 days as the alkali solution increased from 0.5 % to 1.5 %. This is because of strongly alkaline solution increases the hydration reaction and rate of polymerization, and thus enhancing the compactness of internal structures.

Furthermore, as referred to the studies of Omer, Demirboga and Khushefati, (2015), the UPV values of GGBS-based geopolymer were affected by the Na_2SiO_3/NaOH ratio as well as elevated temperature exposures. An upward trending of UPV values in GGBS-based geopolymer is observed with the increment in Na_2SiO_3/NaOH ratio from 0.25 to 1.5 and to 2.5. The highest UPV value was achieve by the specimens with 2.5 Na_2SiO_3/NaOH ratio at 4385m/s, following by 1.5 and 0.25 Na_2SiO_3/NaOH ratio specimens which of 4255m/s and 4099m/s, respectively. The finding in this study was similar to the research outcome as shown in Figure 4.3.1, whereby the highest UPV value of 4.365 km/s ±0.16 was achieved by G90F7P3 at 28 days. On the other hand, the UPV values in the studies of Omer were reduced as the exposed elevated temperature increased from 200^{o}C to 800^{o}C with every 200^{o}C interval.

Moreover, according to the studies of (Cheah *et al.*, 2016), the 7-days UPV value of binary blended geopolymer mortar with 80 % of GGBS and 20 % of PFA was found to be 4007m/s and subsequently increased to 4029m/s and 4159m/s at 28 and 56 days, respectively. Hence, it can be concluded that satisfactorily UPV value was able to achieve by GGBS-PFA birnary blended geopolymer mortar.

2.4.4 MICROSTRUCTURE

Observing the internal structures that built up a geopolymer concrete could provide an insight to the condition of crystallized and unreacted products of binder particles as well as the presence of porous voids or cracking throughout the curing process. Soutsos et al. (2016) studied that the microstructures of 100 % FA geopolymer are potentially porous and look granular, however for the 100 % GGBS geopolymer looks denser and homogeneous, yet desiccation cracks were found in the gel.

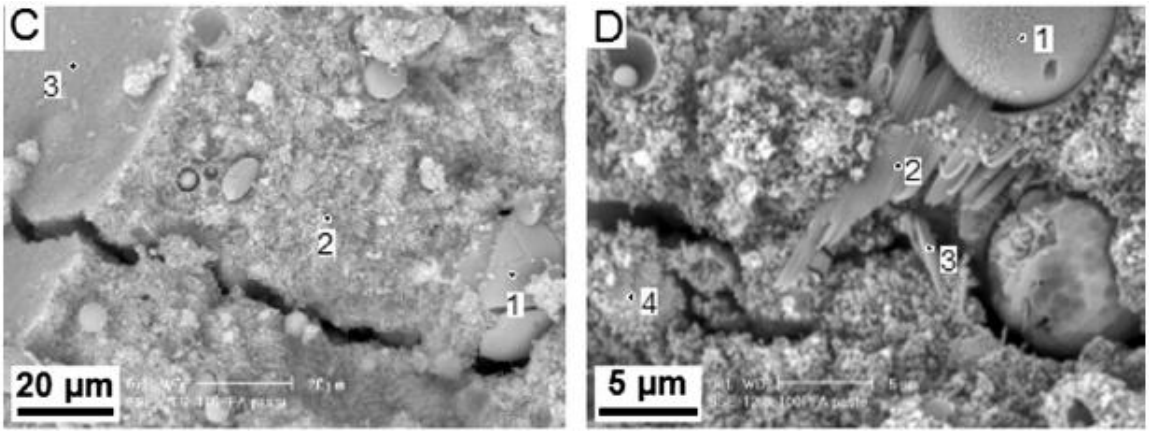

Figure 2.3: SEM image of 100 % GGBS geopolymer paste (Soutsos et al., 2016)

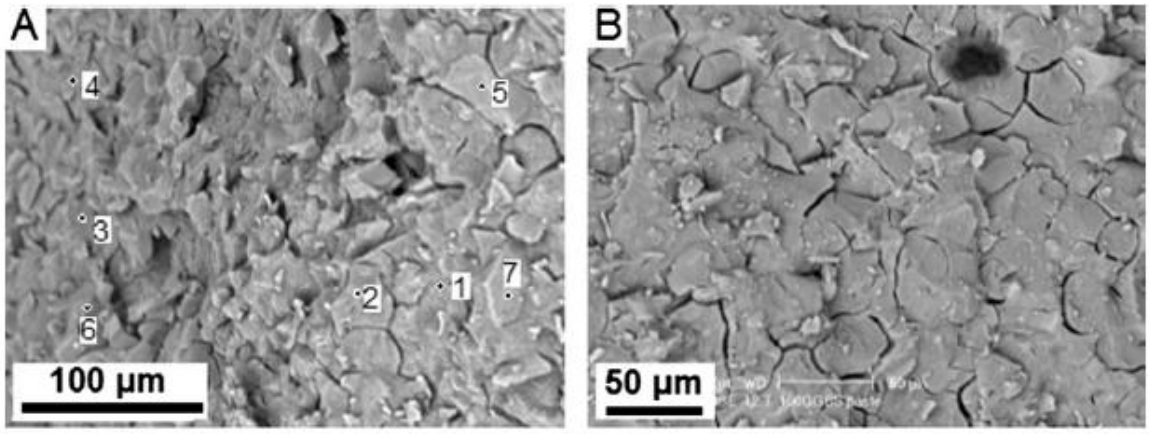

Figure 2.4: SEM image of 100 % FA geopolymer paste (Soutsos et al., 2016)

The microstructures of the equivalent ratio of 50 % GGBS-50 % FA blended geopolymer were found taken the advantages of both pure FA and pure GGBS geopolymer with homogeneous structures, denser-looking and minor cracking. Hence, the coexistence of N-A-S-H and C-A-S-H gels enhances the structures bonding with little micro-cracking.

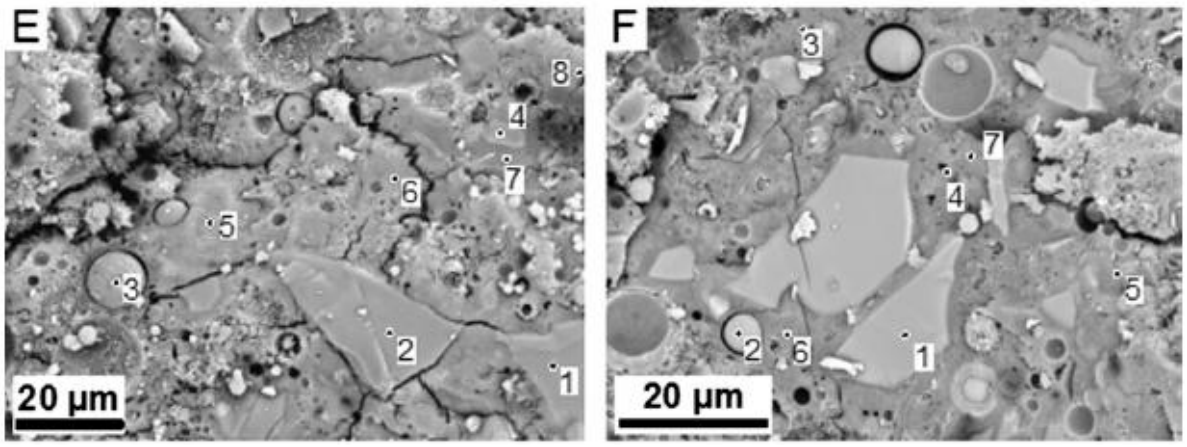

Figure 2.5: SEM images of 50 % GGBS & 50 % FA geopolymer paste (Soutsos et al., 2016)

Although GGBS contributed to high initial strength, yet issue with long-term durability may occur in fully GGBS-based geopolymer product. This is because of GGBS contributed to growth of micro-cracking which lead to increment in porosity and water absorption, thus lower compressive strength. However, addition of FA in the specimen would improve the stability of geopolymer mortar with the cost of elevated curing is usually needed (Wardhono et al., 2015).

Through the observation of the microstructure of GGBS-FA blended geopolymer in the research of Al-Majidi et al. (2016), non-reacted FA particles and less dense structures were found in the specimens which consist of low replacement level of GGBS, however the compactness of geopolymer matrix increased as the GGBS content increased. The spherical micro-particles of PFA binder as well as glassy-looks GGBS particles are clearly shown in Figure 2.6 and 2.7 respectively. Besides, the presence of GGBS enhanced the rate of microstructure development in FA-based geopolymer, thus resulted in higher interconnectivity of gel-like network structure (Puligilla & Mondal, 2013).

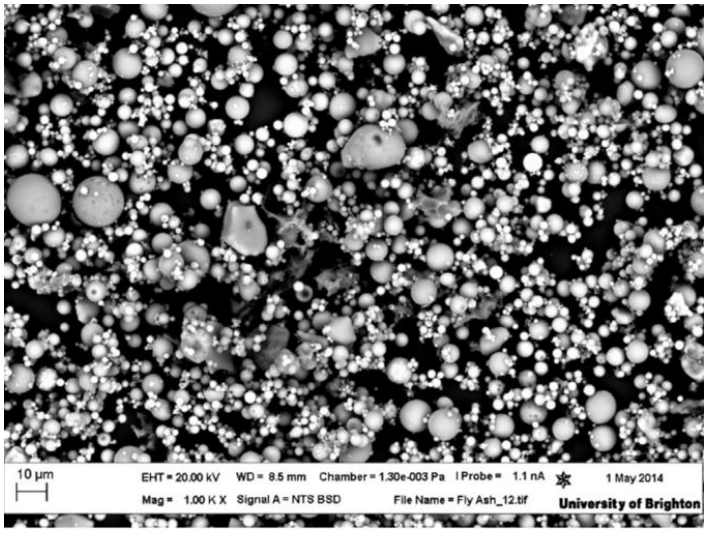

Figure 2.6: SEM image of Pulverized fly ash (PFA) (Al-Majidi et al., 2016)

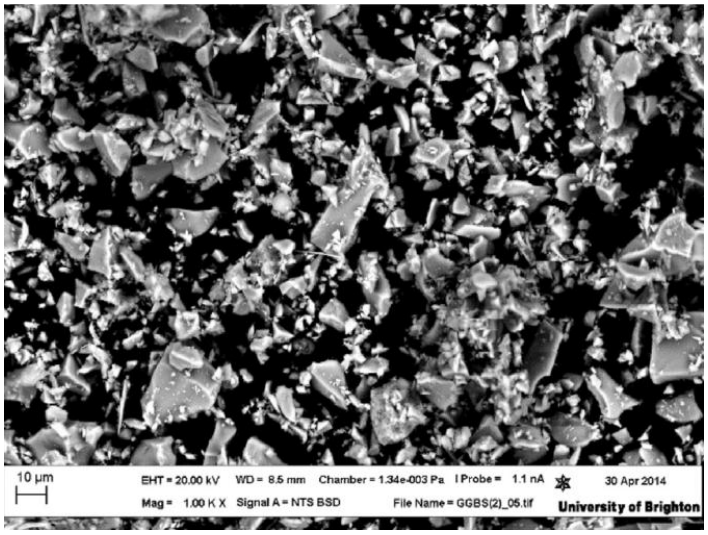

Figure 2.7: SEM image of GGBS (Al-Majidi et al., 2016)

Moreover, the comparison of SEM images between POFA and PFA are shown in Figure 2.8 and 2.9 respectively. Unlike fly ash of spherical and smooth surface particles, POFA particle appears irregular shaping with “rotten” surface (Ranjbar, Mehrali, Behnia, et al., 2014).

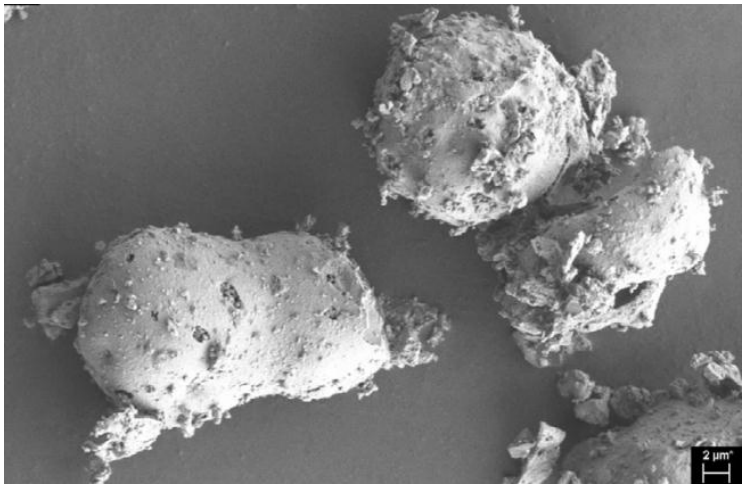

Figure 2.8: SEM image of POFA (Ranjbar, Mehrali, Behnia, et al., 2014)

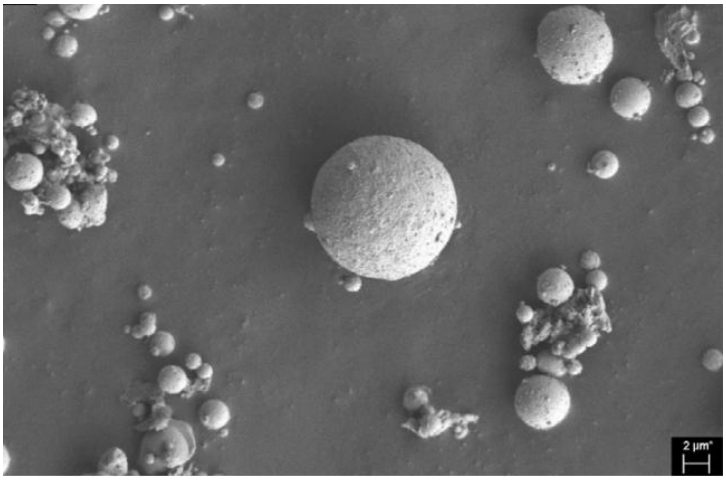

Figure 2.9: SEM image of fly ash (Ranjbar, Mehrali, Behnia, et al., 2014)

Yong et al. (2016) had investigated the prolongation of curing period at 65^{o}C would diminishing the pore sizes in geopolymer and has led to enhancement in compressive strength over the curing period. Next, micro cracks were spotted in the formed geopolymer concrete and this may due to drying shrinkage, mechanical damage during specimen preparation or thermal curing to speed up geopolymerization process.

Micro cracks would restrict the binding capacity of structure and bring negative effect on strength development. Therefore, internal voids and micro-cracking of geopolymer shall be minimized. Infilling of hydrated gels as the result of improving geopolymerization process could overcome the problem of internal voids and micro-cracking. Higher activator concentration of 14 M shows higher rate of hydration reaction than low concentration of 12 M, thus denser microstructure with little micro-cracking is developed (Singh et al., 2016).

The density and compressive strength of geopolymer varying over curing period attributed to varying amount of hydrated binder particles in the microstructure. A higher degree of denser microstructure with lesser pores and micro-cracks had been observed over the curing period in the FA-based geopolymer in real-time basis (Xie & Kayali, 2014). Next, some of the researches have shown relatively higher content of Ca in POFA. According to the research of Salih et al. (2014), the SEM images indicate mainly formation of C-S-H gel in the microstructure of POFA-based geopolymer rather than N-A-S-H gel. This is due to high content of Ca of 11.83 % in the POFA particle compare to Al of 3.53 %. Activator would influence the gels formation as well. Denser paste is spotted on the FA-GGBS blended geopolymer activated by combined activator of sodium silicate and sodium hydroxide than those of activated solely by sodium silicate or sodium hydroxide (Phoo-Ngernkham et al., 2015).

2.4.5 WORKABILITY

Islam et al. (2015) had investigated that beneficial effect of the finer the particles size of POFA on the compressive strength, yet adverse effect was to be found on the workability. The finer the particles of POFA with irregular shape result in higher water absorption rate and thus affecting the workability and flows of geopolymer. Additional POFA content in blended geopolymer require higher water-to-binder ratio for satisfactory workability (Ranjbar et al., 2014a).

Moreover, Deb et al. (2014) had investigated the effects of GGBS content, sodium silicate to sodium hydroxide (Na_2SiO_3/NaOH) ratio and alkali activator content on the workability of GGBS-FA blended geopolymer. Reduction in alkaline solution from 40 % to 35 % improved workability of geopolymer. Next, Wang et al. (2015) studied the workability and slump value of binary blended geopolymer (GGBS-FA) increased as the replacement of FA increased. Besides, when the amount of FA is fixed, the slump value and flow time increased with the dosage of alkaline solutions. Addition in either FA replacement or alkaline solutions content would contribute in improving the liquidity of fresh geopolymer concrete. Gao et al. (2016) stated the higher the GGBS content result in lower workability and slump flow. Next, when the GGBS content is fixed, the higher the activator modulus the better the workability and higher slump flow. The slump value decreased from 18.7cm to 16.4cm when doubling the GGBS content of 40 %. Besides, the slump flow increased from 23.6cm to 26.5cm when the activator modulus increased from 1.4 to 1.8. Similar outcomes have been proven in the research of Nath and Sarker (2014), where both the slump of concrete and flow of mortar were adversely influenced by the inclusion of GGBS in the binder.

Furthermore, GGBS tends to accelerate both initial and final setting times of geopolymer product without input of heat. In the contrast, full fly ash-based geopolymer paste generally prolonged its setting times attributed to slower rate of reaction at ambient temperature. Hence, it could be concluded that positive relationship between fly ash binder and workability of geopolymer product were found in this study, on the contrary to GGBS binder. Next, in the studies of Aliabdo et al. (2016), the higher molarity of NaOH, the lower the slump value of FA-based geopolymer. Slump value of 100mm is reduced to 80mm when shifting the concentration of NaOH from 12 M to 18 M. On the other hand, increased in activator content would positively affect the workability of fresh geopolymer. Slump value of 70mm is increased to 150mm when activator/FA ratio increased from 0.3 to 0.45. Besides, lower Na_2SiO_3/NaOH ratio contributes to better workability. This is because of the viscosity of sodium silicate affect the flow of fresh geopolymer.

2.5 EFFECTS OF GGBS, POFA, PFA ON DURABILITY PERFORMANCE OF GEOPOLYMER CONCRETE

Rate of water absorption, porosity percentage and capillary absorption coefficient are the aspects which would affect the durability performance of geopolymer mortar. Therefore, the aforementioned factors are the dependent variables to be thoroughly discussed in this chapter with different composition of geopolymer binder (GGBS, POFA, PFA).

2.5.1 POROSITY

GGBS plays a vital role in reduction of total porosity of geopolymer by contributing soluble Ca which tend to enhance pore filling effect and thus providing a denser structure. The porosity of GGBS-FA blended geopolymer after 28 days with 10 % of GGBS is around 30 %, yet the porosity reduced to 18.3 % as the GGBS content increased to 40 % (Al-Majidi et al., 2016).

Similar result had proven by Gao et al. (2016), higher replacement level of GGBS into the composite (FA-GGBS) exhibited lower porosity. The porosity of specimen containing 80 % of GGBS with 1.0 Ms was only 21.4 %, and increased to 23.6 % when half of the GGBS replacement level been reduced (40 %). A slight decreased in porosity over the curing age of 7 days to 28 days. Besides, increase in activator modulus would gradually reduce the porosity of geopolymer. The aforementioned porosity of 21.4 % (with 1.0 Ms) was then reduced to 20.6 % and 20.1 % with increase in the activator modulus to 1.4 and 1.8, respectively whereas constant replacement level of GGBS at 80 %. The explanation for this trend is because of additional Si are provided by higher proportion of sodium silicate and eventually contributed as part of the reaction products with pore filling effect.

Increase in water content would lead to higher porosity in the POFA-based geopolymer. These pores were created through the evaporation of water which initially filled in the voids within the paste. In other words, these pores can be known as the remnants of the added water (Salami et al., 2016). Next, study has proven a nearly equal trend between the porosity and water absorption rate of geopolymer when subjected to variations in water content, molarity of NaOH, Na_2SiO_3/NaOH ratio and content of alkali activator (Aliabdo et al., 2016). A study of reduction in porosity by blending nano-silicate in FA-GGBS geopolymer is done by Gao et al. (2015). The porosity of approximately 52 % is reduced to about 46 % when 1 % of nano-silicate content is added to the binder. Not only that, the porosity continuously decreased to nearly 43 % when nano-silicate content of 2 % is added. This can be explained by pore filling effect and greater reacted products as greater amount of Si.

2.5.2 WATER ABSORPTION RATE

Aliabdo et al. (2016) had studied the effects of additional water content, molarity of sodium hydroxide solution, activator content and Na_2SiO_3/NaOH ratio on water absorption rate of FA-based geopolymer. The increased in additional water content in the mixing stage could lead to higher water absorption rate of the hardened geopolymer. This can be explained by greater amount of pores is created in the hardened geopolymer which initially filled with initial water content. Evaporation of internal moisture result in more pores in the microstructure and thus higher absorption rate. Next, the higher concentration and content of alkali activator would reduce the water absorption rate up to the optimum level of 16M NaOH and activator content of 40 %. Beyond the optimum level would enhance the water absorption rate. A diminishing trend in water absorption percentage is observed from 5.80 % to 5.30 % and then 5.09 % with increase in activator content of 0.3, 0.35 and 0.4, respectively. However, the absorption percentage rebounded upward to 5.15 % when activator content inceased to 45 %. Next, the lower the Na_2SiO_3/NaOH ratio, the higher the absorption rate of FA-based geopolymer.

Next, with reference to the studies of Görhan and Kürklü (2014), a reduction trend in water absorption of fly ash-based geopolymer mortar with increase in NaOH concentration was observed. The 7-days geopolymer specimen activated by 6M NaOH were observed to achieved the optimum condition with lowest water absorption and porosity values of approximately 15.8 % and 25.5 % respectively with elevated temperature curing at 85^{o}C for 24 hours.

2.5.3 CAPILLARY ABSORPTION COEFFICIENT

Capillary absorption is the ingress of water through micro-cracks and fractures in the geopolymer, especially the aggregate-paste transition zones are the critical path of ingress of water (Collins & Sanjayan, 2008). Capillary suction is the convective-induced mechanism that allows the entry of water all the way from the external surface of geopolymer concrete. A continuous-path is essential for capillary action. Researches had proven that high porosity geopolymer product has the high tendency in capillary absorption if and only if the internal voids or micro cracks had interconnected to one another which so much so to be formed a continuous-path for capillary action.

Collins & Sanjayan (2008) had investigated the influence of varying water-binder ratio and different curing methods of alkali activated GGBS geopolymer concrete on the capillary uptake of water. Specimens were cured with different curing methods including bath curing, sealed curing and exposed curing and with varying water-binder ratio of 0.33, 0.45 and 0.5, respectively are tested. Result indicates reverse influence of the water content on water absorption and capillary absorption of GGBS-based geopolymer. Specimen with 0.5 water/binder ratio is the highest absorption rate and following by specimens with water/binder ratio of 0.45 and 0.33, respectively. Besides, exposed curing shows a network of visible micro-cracking on the surface of specimen and has resulted in higher degree of water spreads along the capillary pores.

2.6 SUMMARY AND CONCLUSION OF LITERATURE REVIEW

Geopolymer is used of waste products with pozzolanic properties and reacted under strongly alkaline condition. High pH would dissolve the oxides of the geopolymer binder including Si, Al and Ca eventually lead to formation of crystallized aluminosilicate structure. However, previous studies have shown strong alkalinity is insufficient to accelerate the geopolymerization process and typically heat curing is required, especially FA-based geopolymer. Dissolution of Si compound is more difficult than Al, and therefore the development of ultimate strength of geopolymer with high Si/Al ratio is always been delay. This would obstruct the utilization of in-situ geopolymer. Increase the calcium content in geopolymer would not only contribute to formation of dual gels (C-A-S-H and N-A-S-H), but also hasten the strength development at early stage as well as room temperature.

Ca^{+} acts as the charge-balancing agent and would integrate into the geopolymeric network (N(C)-A-S-H). Besides, the other mechanism of Ca^{+} is contribution to formation of C-S-H gel which could coexist with geopolymeric gel (N-A-S-H). Therefore, the author hypothesized increase the composition of GGBS in blended geopolymer would enhance the compressive strength at room temperature. However, sole GGBS-based geopolymer would forgive the beneficial effect of co-existence of dual gels. Therefore, ternary blended geopolymer (GGBS-POFA-PFA) able to achieve optimum composition of Si, Al and Ca.

Besides, the molarity and dosage of alkali activator would significantly affect the strength development of geopolymer. Based on the previous study, lower molarity of NaOH is insufficient to accelerate the geopolymerization, yet over-concentrated of activator would contribute to micro-cracking. Therefore, the author hypothesized the optimum activator ratio of 35 % of combined sodium silicate and 12M sodium hydroxide with Na_2SiO_3/NaOH ratio of 2.5 in terms of strength development and satisfactory durability performance. Besides, water content would affect the strength development and workability as well.

Lower water content contributes to higher strength but would affect the workability of geopolymer. Irrational reducing the water content for the benefits of higher strength yet compromised the workability and flowability of geopolymer mortar, would eventually affect the compressive strength due to inadequate and non-uniformly compaction and greater amount of air in the internal structure of geopolymer is produced. Therefore, the author fixed the water/binder ratio constant at 0.35.

CHAPTER 3

RESEARCH METHODOLOGY

3.1 INTRODUCTION

This chapter is to outline the experiment program and the flow for the research. The details of the materials used will be discussed in this chapter as well as all the experimental tests. Compressive test, UPV test, density test and scanning electron microscopy (SEM) test are used to study the engineering properties of the specimens. While water absorption test, porosity test and capillary absorption test are to investigate the durability performance of the specimens. Next, trial mix will be conducted before the casting the experimental specimens.

3.2 MATERIALS

The materials used in this research are including GGBS, POFA, PFA, mining sand and combined alkali activator of sodium silicate and sodium hydroxide. The physical properties of the materials will be explained in this chapter.

3.2.1 GGBS

The GGBS comply with MS EN 15167-1 were obtained from YTL Cement Sdn Bhd, Malaysia. The specific surface area is 405m^2/kg, specific gravity of 2.89g/cm^3 and 1mm soundness. Table 3.1 has shown the chemical composition of GGBS. It is off-white in colour (as shown in Figure 3.1) and consists essentially of CaO and SiO_2 for about 45.83 % and 32.52 % respectively, following by 13.71 % of Al_2O_3.

3.2.2 PFA

The PFA namely, class F low calcium (CaO < 10 %) FA comply with BS EN 450 were obtained from YTL Cement Sdn Bhd, Malaysia. It is grey in colour (as shown in Figure 3.1) with 341m^2/kg specific surface area and specific gravity of 2.4 g/cm^3. FA comprises high SiO_2/Al_2O_3 ratio of 2.0 with 54.72 % and 27.28 % of silicon dioxide and aluminum oxide respectively.

3.2.3 POFA

POFA is potentially to be used as pozzolanic material as it rich in silicon dioxide (SiO_2). It is typically dark in colour (as shown in Figure 3.1) and with specific gravity of 2.2. In this research, POFA was oven-dried at 80^oC for at least 24 hours to remove the moisture and sieved through 300 μm prior to the mixing process.

Table 3.1: Physical properties of GGBS, PFA and POFA

Materials	Properties
GGBS	Specific surface area: 405m^2/kg
	Specific gravity: 2.89
	Soundness: 1mm
	Colour: Off-white
PFA	Specific surface area: 341m^2/kg
	Specific gravity: 2.4
	Colour: Grey
POFA	Specific surface area: 172m^2/kg
	Specific gravity: 2.2
	Colour: Dark

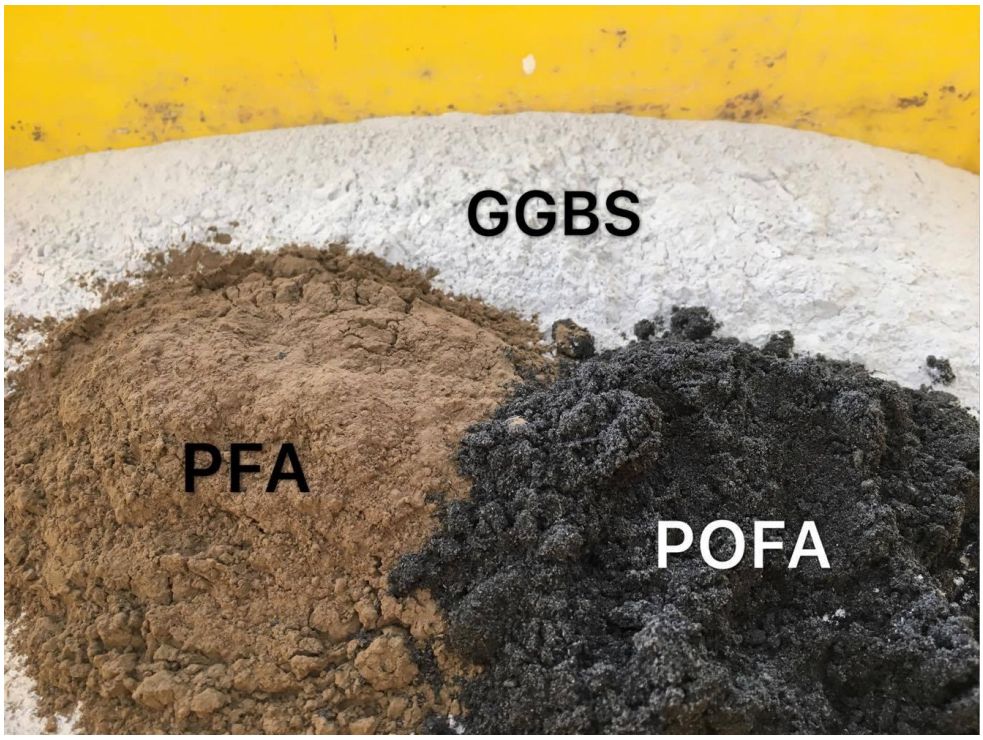

Figure 3.1: GGBS, PFA and POFA binders

3.2.4 MINING SAND

Sieve analysis was carried out to determine the size distribution of fine aggregates that used in this research. The fine aggregates for the geopolymer mortar were used of mining sand which obtained from UTAR. The passing rate of sand particles is shown in Figure 3.1. Throughout the sieve analysis, it clearly indicating the larger portion of sand was at the range of 0.3mm to 0.6mm and following by the range of 2.36mm to 1.18mm, as shown in Table 3.2.

Table 3.2: Sieve analysis for mining sand

Sieve Size Range	**Sieve Fraction**		**Nominal Aperture Size**	**Cumulative Undersize**
mm	gram	% by mass	mm	% by mass
> 4.75	0	0	4.75	100
4.75 - 2.36	153	15	2.36	85
2.36 - 1.18	207	21	1.18	64
1.18 – 0.600	169	17	0.600	47
0.600 – 0.300	310	31	0.300	16
0.300 – 0.150	101	10	0.150	6
< 0.150	55	6		
Total	995	100		

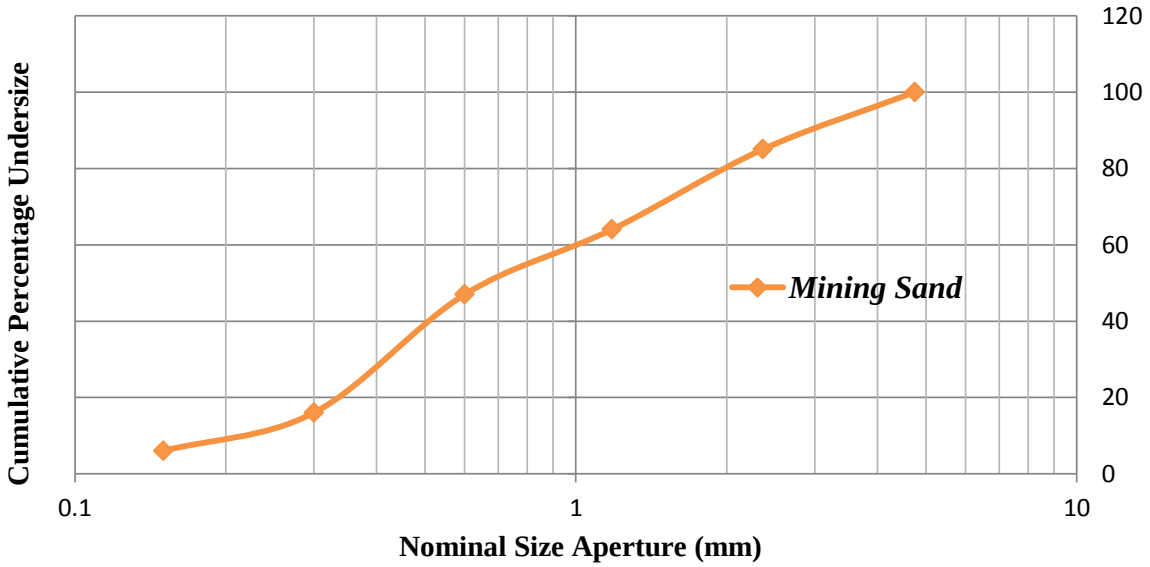

Figure 3.2: Particle size distribution chart

3.2.5 ALKALI ACTIVATOR

The alkali activator in this study was used to combination of sodium silicate (SS) and sodium hydroxide (SH) with the constant Na_2SiO_3/NaOH ratio of 2.5 and fixed dosage at 35 %. Both the Na_2SiO_3 solution and NaOH pellets were obtained from Avantis Scientific Lab Sdn. Bhd. The Na_2SiO_3 solution comprises 5 % of water with pH above 11.5. The concentration of NaOH was fixed constant at 12 M. The specific gravity of combined alkali activator of sodium silicate with sodium hydroxide is provided (Islam et al., 2015). The NaOH solution was prepared one day prior to the synthesis of geopolymer. The concentration of NaOH solution is manipulated by mixing specific mass of NaOH pellets with distilled water. After that, the NaOH solution was left to cool for overnight and sealed to prevent from reaction with atmospheric CO_2. After the NaOH solution become uniformly homogeneous, the preparation of alkali activator was done by adding sodium silicate into the prepared sodium hydroxide solution.

(a) Sodium Hydroxide (b) Sodium Silicate (c) Preparation of NaOH

Figure 3.3: Alkali activator

3.3 EXPERIMENTAL PROGRAM

This research is to investigate the varying composition of binder as independent variable on the engineering properties and durability performance of ternary blended geopolymer mortar. A trial mix is conducted prior to the casting of experimental specimens. The control variable of this research is the variation in binder composite, total five mortar samples were casted with increasing GGBS content of 10 %, 30 %, 50 %, 70 % and 90 %. While the remaining contents was two-third of PFA and one-third of POFA, as shown in Table 3.3. A further study of PFA:POFA ratio had conducted after obtained the optimum replacement level of GGBS. Besides, water-to-binder ratio, sand-to-binder ratio as well as activator-to-binder ratio was remained constant as shown in Table 3.4.

Table 3.3: Mix proportion of geopolymer mortar for optimum GGBS content

Mix designation	**GGBS**	**PFA**	**POFA**	**W/B ratio**	**Mining Sand**	**Na_2SiO_3**	**NaOH**
G10F60P30	0.1	0.6	0.3	0.35	2.5	0.25	0.1
G30F47P23	0.3	0.47	0.23	0.35	2.5	0.25	0.1
G50F33P17	0.5	0.33	0.17	0.35	2.5	0.25	0.1
G70F20P10	0.7	0.2	0.1	0.35	2.5	0.25	0.1
G90F7P3	0.9	0.07	0.03	0.35	2.5	0.25	0.1

Table 3.4: Mix proportion of geopolymer mortar for optimum PFA:POFA ratio

Mix designation	**GGBS**	**PFA**	**POFA**	**W/B ratio**	**Sand**	**Na_2SiO_3**	**NaOH**	**SP**
PFA2.5:POFA0.5	0.9	0.083	0.017	0.35	2.5	0.25	0.1	0.01
PFA2:POFA1	0.9	0.067	0.033	0.35	2.5	0.25	0.1	-
PFA1:POFA2	0.9	0.033	0.067	0.35	2.5	0.25	0.1	0.01

Table 3.5: Control and constant variable

Variable	
Constant Variable	Control Variable
Water/binder ratio: 0.35 Binder-Sand ratio: 1:2.5	<u>GGBS content</u> (10 %, 30 %, 50 %, 70 %, 90 %)
Alkali dosage: 0.35 $Na_2SiO_{3/}$ NaOH = 2.5	<u>PFA:POFA ratio</u> i. 2.5 : 0.5 ii. 2 : 1 iii. 1 : 2
Curing method: Water bath curing	

3.3.1 PREPARATION OF SPECIMENS

Binder (GGBS, POFA, PFA) was blended prior to mixing of mortar. Each material was weighted precisely according to the experimental program to ensure the accuracy of mixing proportion. After that, the blended binder was further mixed with fine aggregate (mining sand). The mixing process continued until the binder and sand were uniformly blended. Alkali activator and water were then added into the prepared binder to form the geopolymer fresh mortar.

Figure 3.4: Preparation of geopolymer mortar

Demoulding oil was coated on the steel moulds prior to the moulding process to ensure the ease of demoulding process of hardened specimens, in order to prevent any damage occurred to the specimens. Next, adequate compaction on the specimen during the moulding process until a smooth and leveled surface is achieved to minimize the presence of trapped air voids within the fresh mortar. The specimens were then placed for hardening process at room temperature for 24 hours. After that, all the hardened geopolymer mortars were demoulded on the next day, and cured with water bath curing method by immersed the specimens inside water at ambient temperature.

Figure 3.5: Application of demoulding oil prior to specimen casting

The prepared experimental specimens are illustrated in Figure 3.6 and 3.7, the colour of specimens turned darker and darker as the POFA content increased. Besides, the engineering properties and durability performance of specimens were tested at different ages of curing (3, 7, 14, 28 and 56 days), as shown in Table 3.5. Furthermore, the flow of experimental program is shown in Figure 3.7 and 3.8.

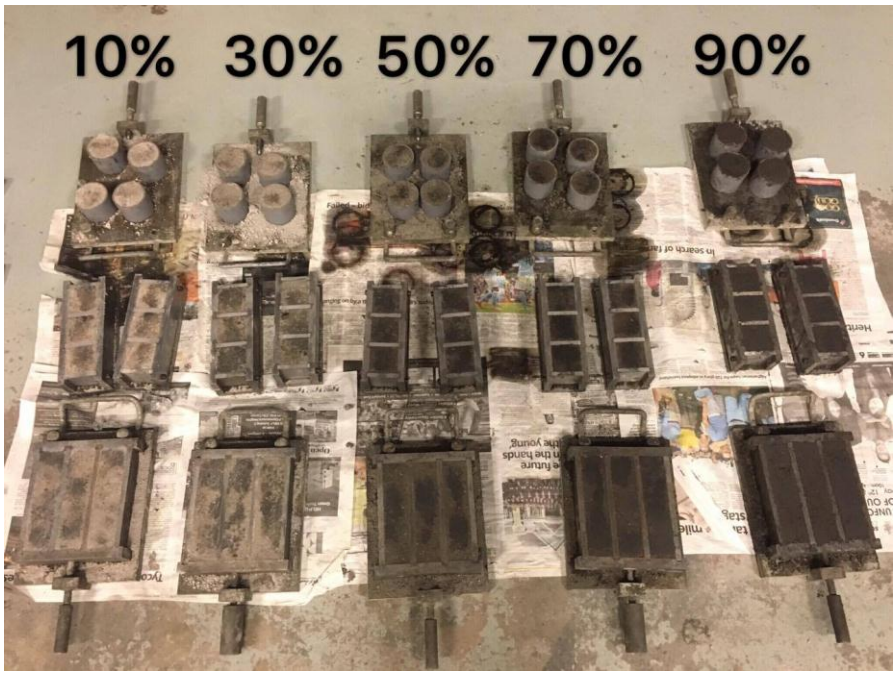

Figure 3.6: Experimental specimens with varying replacement level of GGBS

Figure 3.7: Experimental specimens with varying PFA:POFA ratio

Figure 3.8: Ternary blended GGBS-PFA-POFA geopolymer mortar specimens

Table 3.6: Test program schedule

Properties	Type of Test	Age of Specimen	Type of Specimen
Fresh Properties	Flow table test **(BS EN 12350-5:2009)**	-	-
Engineering Properties	Compressive test **(BS EN 12390-3:2009)**	3, 7 ,14,28 and 56 days	Mortar cube with 50m x 50mm x 50mm dimension
	Density test **(BS EN 12390-7:2009)**	3, 7, 14, 28 and 56 days	Mortar cube with 50m x 50mm x 50mm dimension
	UPV test **(BS EN 12504-4:2004)**	3, 7, 14, 28 and 56 days	Mortar cube with 50m x 50mm x 50mm dimension
	SEM analysis	14 days	Crushed mortar
Durability Performance	Water absorption test **(BS 1881-122:2011)**	7, 14, 28 and 56 days	Cylinder with 45mm diameter and 40mm height
	Porosity test **(RILEM 1984)**	7, 14, 28 and 56 days	Cylinder with 45mm diameter and 40mm height
	Capillary absorption test **(BS EN 1015-18:2002)**	7 days	Prism mortar with dimension of 50mm x 50mm x 200mm

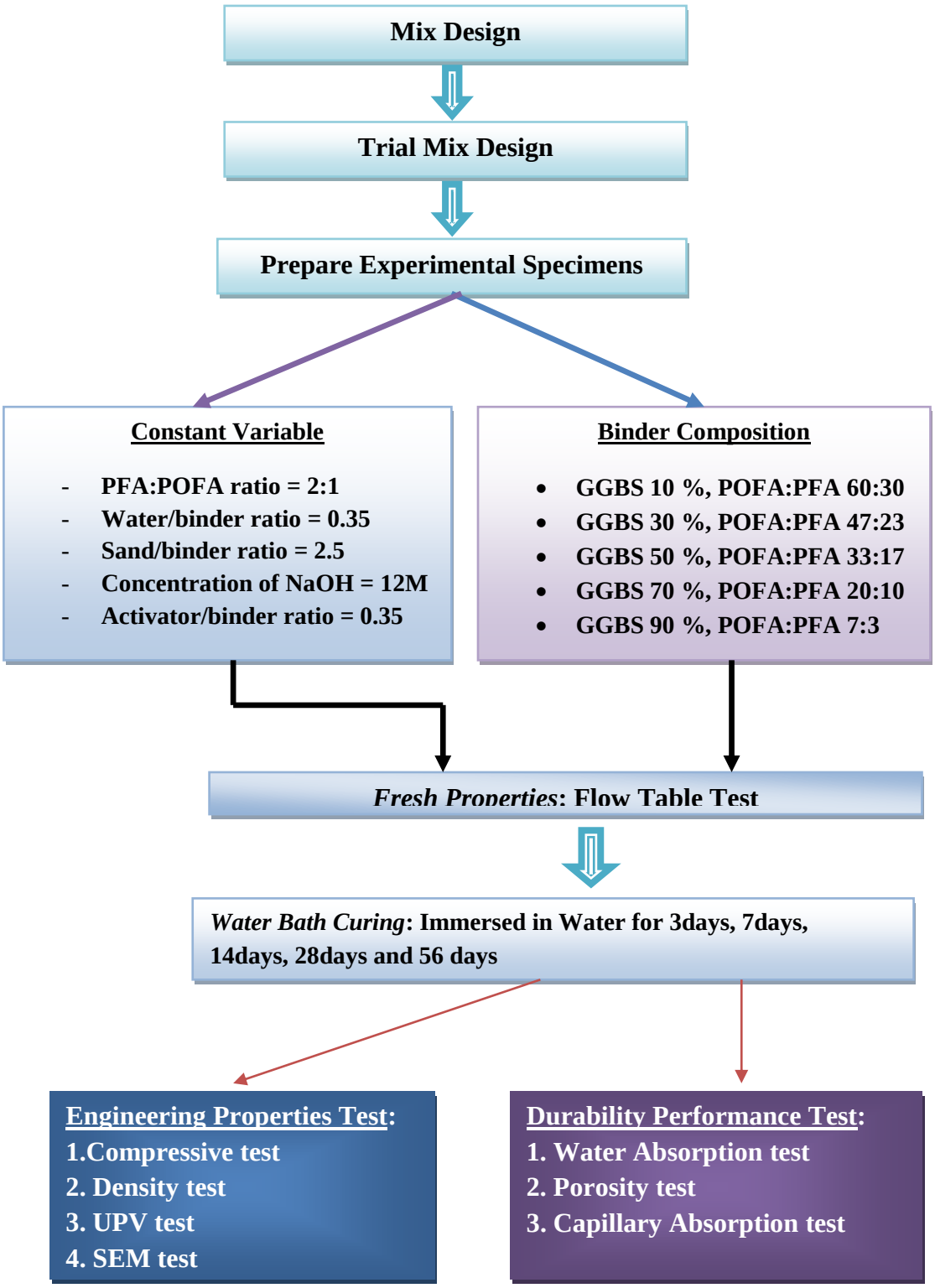

Figure 3.9: Experimental program flow chart for optimum replacement level of GGBS

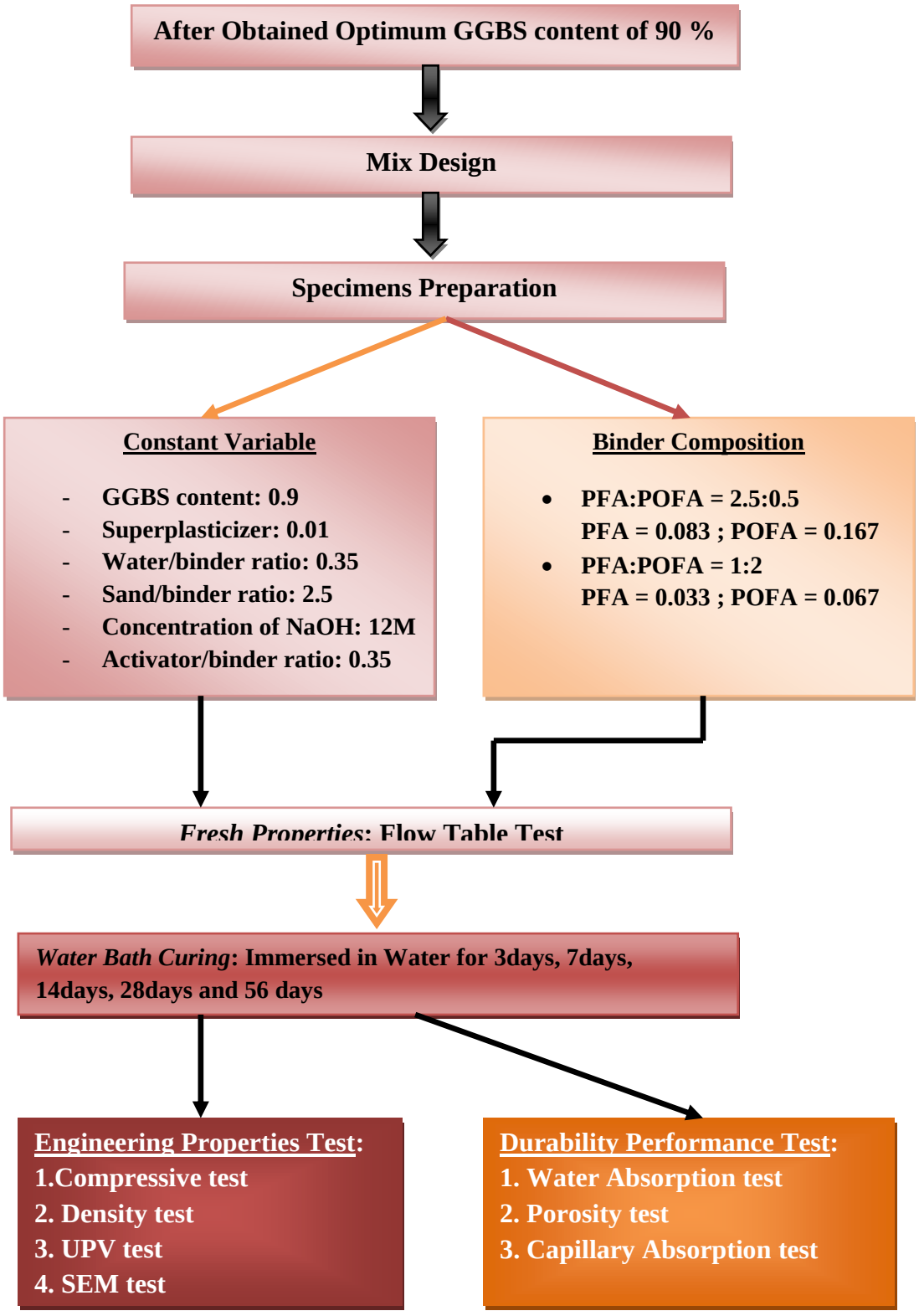

Figure 3.10: Experimental program flow chart for optimum PFA:POFA ratio

3.4 Experimental Testing Method

The engineering properties of alkali-activated (POFA-GGBS-PFA) ternary blended geopolymer mortar were tested by several tests, including compressive test, UPV test and density test as well as scanning electronic microscopy (SEM) examination. Besides, water absorption test, porosity test and capillary absorption test were conducted in order to analyse the durability performance of alkali-activated ternary hybrid geopolymer mortar with varying replacement level of GGBS as well as varying PFA-to-POFA ratio. Finally, flow table test were carried out to study the flow ability of readily mixed fresh geopolymer mortar.

All the tests above were conducted in compliance to procedures of British Standards testing method. The engineering properties of geopolymer mortar were collected at day 3, 7, 14, 28 and 56 by used of 50mm mortar cube specimen. On the other hand, 7, 14, 28 and 56 days results were collected for durability performance test by used of 40mm height with 45mm width cylinder specimens. However, prism specimens were casted to conducted capillary absorption test after 7 days cured onwards.

3.4.1 Compressive Test

The compressive strength of specimens was tested by compressive test in accordance with BS EN 12390-3:2009 at 3, 7, 14 and 28 and 56 days. It is performed under the loading rate of 45kN per minute on the 50mm cube specimen until the failure occurred. The compressive strength value was obtained by the average of three specimens. Ensure the specimen is centered and the seated platen is free to move. Run the test and record the maximum force loaded on the specimen.

Figure 3.11: Kenco compressor testing machine

3.4.2 Density Test

The test in accordance with BS EN12390-7:2009 to develop data required for conversion between volume and mass for concrete, thus determine the density, percent void and percent absorption in hardened concrete. Density of specimens is indicating the degree of compactness and internal void of the hardened mortar. Two different mass types have to be taken in order to measure the density of specimen, which are the mass in the air as well as the mass of specimen immersed in water as shown in Figure 3.12. After collecting the data, formula for quantify the density of specimen is shown in below.

Figure 3.12: Measurement of mass in air as well as mass submersed in water

Calculation:

$$\rho_m = \frac{m_a \times \rho_w}{m_a - m_w}$$

Where:

m_a = Mass of mortar in air

m_w = Mass of mortar submersed in water

ρ_w = Density of water

ρ_m = Density of mortar

3.4.3 Ultra-sonic Pulse Velocity (UPV) Test

UPV test is used to determine the propagation velocity of longitudinal wave pulses through the concrete in order to investigate the uniformity and relative quality of hardened specimen, thus to detect the presence of internal voids and cracks. The lower the velocity indicates the presence of voids or cracks within the concrete. Besides, it is also applicable to estimate the severity of cracking or deterioration of concrete and mortar. The UPV test in this study was complied with the standard procedure of BS EN 12504-4:2004. The measurements are obtained by measuring the travel time of the ultra-sonic pulse between transducers on opposite ends of the specimen, which known as "direct method".

Figure 3.13: Ultrasonic pulse velocity testing machine

3.4.4 Scanning Electron Microscopy (SEM) Analysis

SEM analysis is to characterize the microstructure of the specimens with varying composition of binder, thus understanding the contribution of each material (GGBS, PFA and POFA) to the product formed. It is able to provide a high resolution image of specimens at magnifications from 15-50,000× to make pertinent observations and measurements.

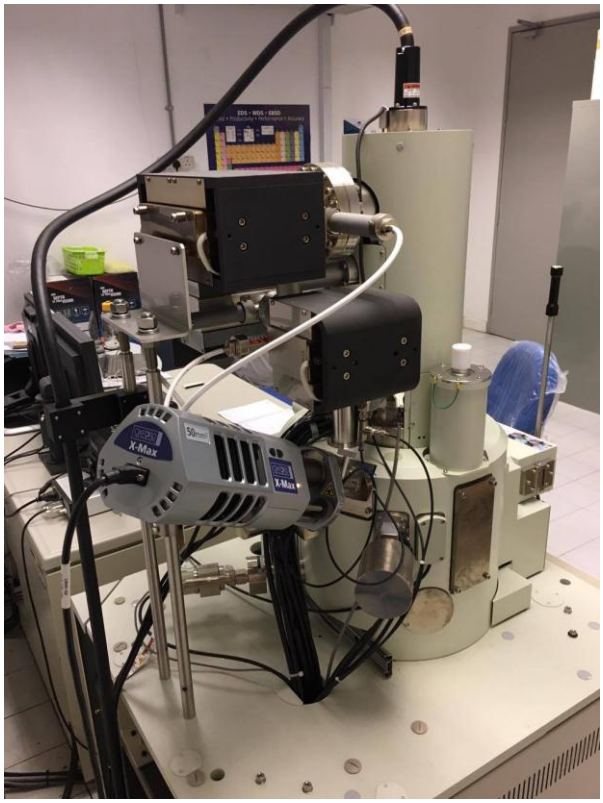

Figure 3.14: Scanning electron microscopy machine

3.4.5 Water Absorption Test

The water absorption test in this research was performed in accordance to BS 1881-122:2011. The weight of specimen after oven-dried at 105°C for 48 hours (m_d) and the weight after 30 minutes of immersion in water (m_w) are measured. Formula is applied to calculate the percentages of absorption rate of specimens.

Calculation:

$$Water\ Absorption = \frac{m_w - m_d}{m_d} \times Correction\ factor \times 100\ \%$$

Where:

m_w = Mass of oven-dried mortar after 30 minutes immersed in water

m_d = Mass of oven-dried mortar

Correction factor = 0.576

$$Correction\ factor = \frac{\text{Volume}}{\text{Surface area} \times 12.5}$$

Where:

Volume $= \pi\ r^2\ h$

$= \pi \times (22.5mm)^2 \times 40mm$

Surface area $= [\ 2\pi rh + 2\pi r^2\ ]$

$= [\ 2(\pi\ 22.5mm \times 40mm)\ ] + [\ 2\pi(22.5mm)^2\ ]$

3.4.6 Porosity Test

The porosity of geopolymer mortar was measured according to standard method of RILEM 1984. Throughout the test, three different weights were measured for the specimens with 50mm cube dimension, including mass of specimen after oven dried, mass of saturated-mortar in air and mass of saturated-mortar immersed in water. Specimens were placed into a vacuum-pressure vessel as shown in Figure 3.15 and vacuumed for approximately 15 minutes, repeated vacuuming process after 2 hours interval. After that, the specimens were then left for 24 hours in order to achieve full saturation or total absorption of dense geopolymer mortar to enable the estimation of porosity by collecting the air weight and immersed weight of saturated geopolymer mortar as shown in Figure 3.12.

Calculation:

$$Porosity = \frac{m_s - m_a}{m_s - m_w} \times 100\ \%$$

Where:

m_s = Saturated mass of mortar in air

m_a = Mass of mortar in air

m_w = Saturated mass of mortar submersed in water

Figure 3.15: Vacuum-pressure vessel for obtaining saturated mass

3.4.7 Capillary Absorption Test

Capillary absorption coefficient indicates the absorption rate by capillary suction of concrete during the initial contact with water. The capillary absorption test in this study was complied with BS EN 1015-18:2002, "Methods for determination of water absorption coefficient due to capillary action of hardened mortar" After cured for 7 days, the plastic-wrapped prism specimens were immersed into 5mm depth water with standing position in order to measure the capillary action of water through the specimens, as shown in Figure 3.16. The deviation in mass by the absorption of water was then measured at several time intervals.

Calculation:

$$Capillary\ Absorption\ Coefficient = \frac{g/cm^3}{\sqrt{time}}$$

Figure 3.16: Prism specimens for capillary absorption test

3.4.8 Flow Table Test

The flow rate and workability of fresh geopolymer mortar was studied through flow table test is complied with BS EN 1015-3:1999. The readily mixed geopolymer mortar was repeatedly tapped for 25 times on a leveled surface, in order to observe the spreading level of fresh mortar. Result was then collected by measuring the length and width of spread mortar. The wider the spreading indicates the higher the flowability of geopolymer mortar, thus better workability performance.

Figure 3.17: Flow table testing apparatus

CHAPTER 4

RESULT AND DISCUSSION

4.1 INTRODUCTION

This chapter is to assess the quantified data obtained throughout the experimental programs as well as to analyze the degree of influence towards various dependent variables, to investigate and discuss the leading factors. Study on the correlation between the independent and dependent variables in order to conclude the finding with reliable proof. In this research, dependent variables of which: Compressive strength, Density, Ultra-sonic pulse velocity, Microstructural matrix, Flow-ability, Water absorption rate, Porosity rate and Capillary absorption coefficient of ternary blended geopolymer mortar have been thoroughly studied with the manipulating variables of varying synthesis of binder composition, which are GGBS content as well as PFA-to-POFA ratio.

4.2 WORKABILITY

Workability of the readily mixed fresh geopolymer mortar was studied by flow table test. Flow table test is used to observe the spreading of fresh geopolymer mortar by repeatedly tapping for 25 times on a levelled surface. Throughout the experiment, the rapid setting of GGBS-based geopolymer mortar was noticed which so much so that presented two distinct phases of fresh mortar. The fresh mortar began to set within about one and a half minute right after thoroughly mixing process. The width of mortar spreading is shown in Table 4.1.

Table 4.1: Flow table test of geopolymer mortar

Variables	Spreading Width (cm)	Figure
G10F60P30	25cm	4.1.1
G30F47P23	23cm	4.1.2
G50F33P17	20cm	4.1.3
G70F20P10	19cm	4.1.4
G90F7P3 / PFA2:POFA1	22cm (Phase 1) & 13cm (Phase 2)	4.1.5
PFA2.5:POFA0.5	22cm	4.1.6
PFA1:POFA2	24cm	4.1.7

Descending trend in the spreading widths is observed with the increase in replacement level of GGBS. Higher GGBS replacement exhibits faster initial and final setting times of geopolymer mortar. Hence, GGBS contributed in reducing the workability and accelerate the geopolymerization of specimen (Gao, Yu and Brouwers, 2016). Alkali activated GGBS contributes higher strength at ambient temperature but issues related to hasten the setting times, thus insufficient workability along with high values of dry shrinkage (Al-Majidi *et al.*, 2016). Lower workability achieved by GGBS attributed to the abundant content of CaO, thus accelerate the geopolymerization as its rapid reaction with alkaline activator (Khan *et al.*, 2016).

The difference between distinct phases in setting time was explicitly shown in Figure 4.2 to 4.9 with varying replacement level of GGBS. The initial flow table result for G90F7P3 was 22cm as shown in Figure 4.6, however repeated the flow table test on the same specimen right after less than one minute, vast difference was observed as shown in Figure 4.7. The spreading width of subsequent repeated flow table test on F90F7P3 was then found to be reduced to 13cm. This can be explained by rapid dissolution of CaO as reacted with activator, thus instant initial setting was observed which so much so to reveal two distinct phases of fresh mortar. On the other hand, inclusion of fly ash prolong the setting times due to slow rate of decomposition in fly ash particles at ambient temperature (Wang, Wang and Lo, 2015). Hence, it can be concluded that higher content of PFA will positive impact on the workability and flow ability of geopolymer mortar, yet addition in GGBS content will adversely affect the flowability of geopolymer mortar.

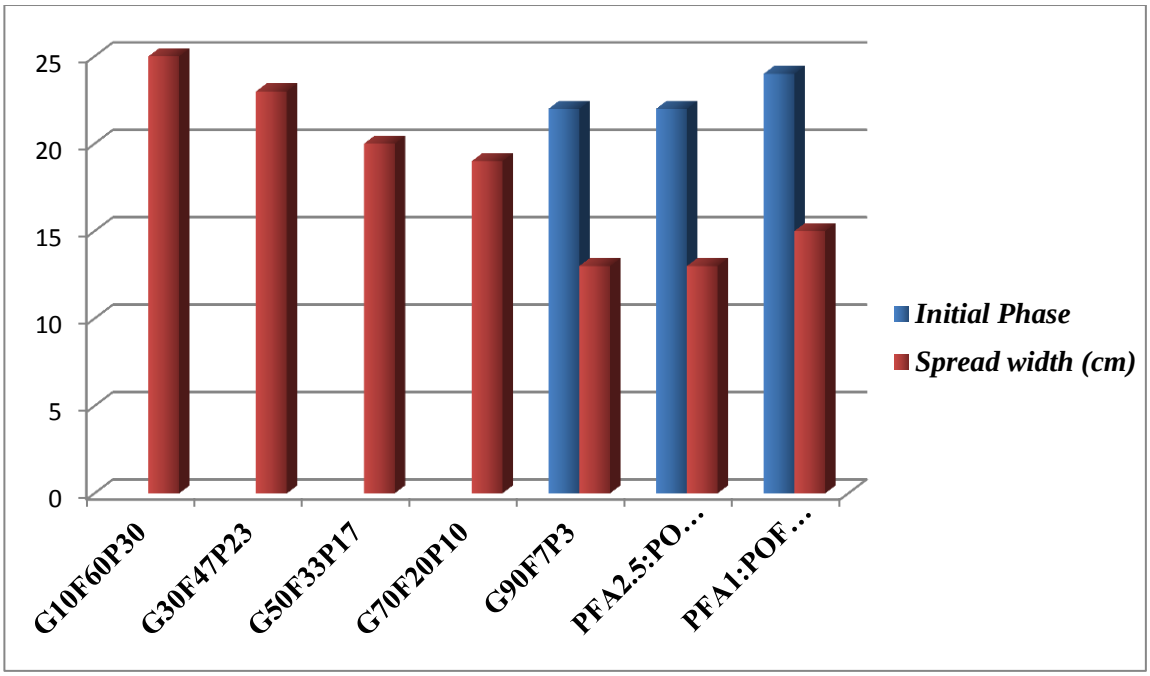

Figure 4.1: Flow ability of geopolymer specimens

Figure 4.2: Flow table of G10F60P30

Figure 4.3: Flow table of G30F47P23

Figure 4.4: Flow table of G50F33P17

Figure 4.5: Flow table of G70F20P10

Figure 4.6: Flow table of G90F7P3 at first phase

Figure 4.7: Flow table of G90F7P3 at second phase

Figure 4.8: Flow table of PFA2.5:POFA0.5 with inclusion of superplasticizer

Figure 4.9: Flow table of PFA1:POFA2 with inclusion of superplasticizer

4.3 COMPRESSIVE STRENGTH

The compressive strengths of ternary blended geopolymer mortar have shown in Table 4.2. All the data have been averaged by three numbers of specimens with the standard deviation among the different specimens. This proved the reliability of each of the data collected without significant outlier. Typical cement product develops higher compressive strength over the curing period, none exception to geopolymer. As shown in Table 4.2, all the geopolymer developed higher strength over the longer period of curing time. The increment in strength has been illustrated in Figure 4.10 and 4.12.

Table 4.2: Compressive strength with varying replacement of GGBS, PFA and POFA

	Compressive Strength (MPa)				
Variable	**3 days**	**7 days**	**14 days**	**28 days**	**56 days**
G10F60P30	15.82 ±2.55	16.92 ±2.31	28.23 ±1.42	28.64 ±0.19	30.71 ±1.78
G30F47P23	17.56 ±2.50	26.14 ±1.98	30.67 ±0.60	35.34 ±3.03	36.38 ±3.19
G50F33P17	23.28 ±1.39	35.32 ±2.78	36.09 ±2.99	42.16 ±2.32	42.25 ±1.72
G70F20P10	39.18 ±1.34	42.94 ±2.85	46.27 ±1.68	48.32 ±1.13	51.01 ±4.92
G90F7P3 & PFA2:POFA1	39.27 ±2.11	46.78 ±2.40	51.46 ±0.33	53.54 ±2.10	55.02 ±6.51
PFA2.5:POFA0.5	39.38 ±0.63	41.75 ±2.08	47.54 ±3.38	52.56 ±1.78	53.05 ±3.67
PFA1:POFA2	37.42 ±1.15	37.49 ±0.72	45.10 ±1.08	49.78 ±1.99	52.68 ±1.48

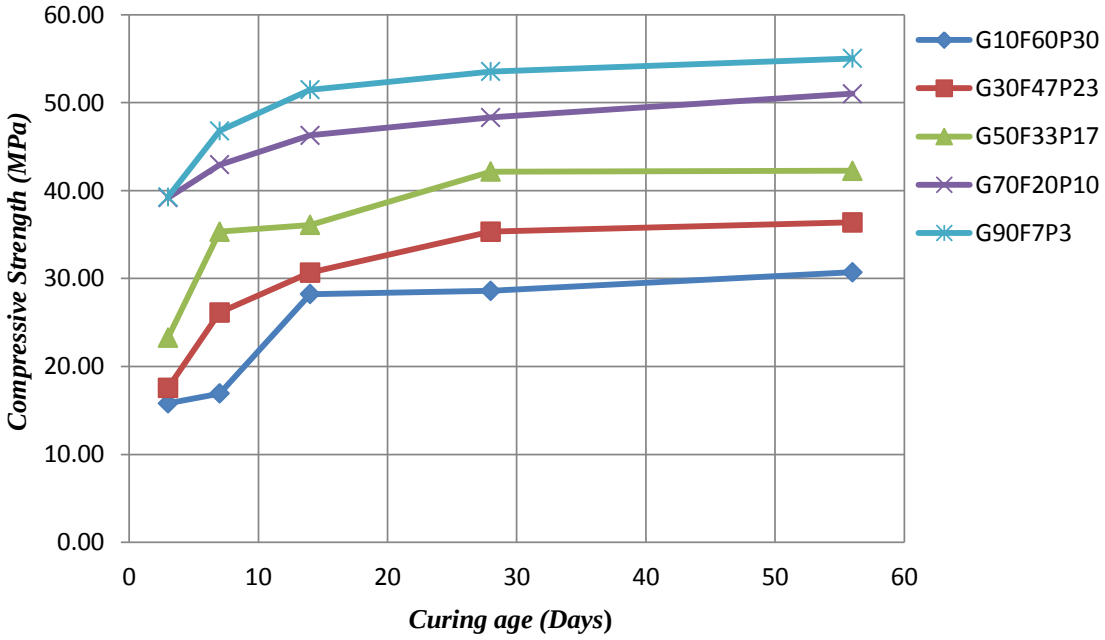

Figure 4.10: Effect of GGBS on compressive strength of geopolymer mortar

With reference to the Figure 4.10, an upward trend in compressive strength was observed with the increase in replacement level of ground granulated blast-furnace slag (GGBS). Highest compressive strength achieved was G90F7P3 of 55.02 MPa at 56 days. As the GGBS contents increased from 10 % to 90 % at every 20 % interval, the compressive strength have increased by 23.39 %, 19.30 %, 14.61 % and 10.80 %, respectively at 28 days. This can be explained by addition in GGBS content, contributed higher rate of Ca^{2+} ions in the geopolymer matrix (Nath and Sarker, 2014). Hence higher rate of geopolymerization in forming calcium-alumina-silicate-hydrate gel (C-A-S-H) with higher Ca/Si ratio (Soutsos *et al.*, 2016). Not only that, GGBS dissolved high amount of Ca^{2+} and Al ions to the system, allowed the substitution of Al into (C-S-H) chain, thus turned into (C-A-S-H) matrix. Hence, it may lead to formation of complex matrix with crosslinking between the tobermorite chains (Salih *et al.*, 2015).

The 7-days compressive strength of G90F7P3 and G70F20P10 had achieved 87.37 % and 88.87 % of the 28 days strength. Higher initial strength development in G90F7P3 and G70F20P10 attributed to high reactivity of GGBS as a Ca bearing material accelerated the dissolution and hydration process of geopolymer at early stage (Nath and Kumar, 2013). In the contrary, lowest initial strength achieved of 15.82 MPa at 3 days found to be G10F60P30, which about 51.51 % of its 56-days strength. Approximately 40.29 % lower in 3-days compressive strength as in compared to G90F7P3. The synthesis of chemical composition in G10F60P30 was high in SiO_2/Al_2O_3 and low Ca/SiO_2 ratio attributed to abundant of Si in POFA. Silicon component tend to dissolve in slower rate as compared to Al component, resulting in gradual strength development (Ranjbar, Mehrali, Alengaram, *et al.*, 2014).

Furthermore, with reference to Figure 4.10, very little or none compressive strength was developed in G10F60P10, the strength development can only be seen from 14^{th} day. This can be explained by low reactivity of fly ash binder at ambient temperature retarded the dissolution and polymerization of reaction product as well as strength development at early ages (Lee and Lee, 2013). Therefore, geopolymer with high SiO_2/Al_2O_3 ratio tends to prolong its final strength development to later stage, by condensation between silicates species due to different rate of dissolution with Al and Ca components (Yusuf *et al.*, 2014a). However, G30F47P23 and G50F33P17 developed higher initial strength at 3 days with relatively high replacement level of PFA at ambient temperature can be explained by the two possible mechanism of geopolymer hydration reaction. Firstly, the high reactivity of GGBS particles tend to accelerate the hydration process, thus separate hydration reaction from one another can be seen by formation of GGBS matrix around the unreacted fly ash, which was much likely to be seen in G10F60P30 as shown in Figure 4.35. Secondly, both of the binders' reactions had occurred simultaneously, whereby the reactions of GGBS particles have activated the fly ash at ambient temperature.

One-way ANOVA: Compressive strength versus Replacement level of GGBS

```
Source                     DF      SS      MS      F      P
Replacement level of GGB    4  6473.3  1618.3  35.30  0.000
Error                      65  2980.3    45.9
Total                      69  9453.6

S = 6.771   R-Sq = 68.47%   R-Sq(adj) = 66.53%


                                Individual 95% CIs For Mean Based on
                                Pooled StDev
Level       N    Mean  StDev  ---------+---------+---------+---------+
G10F60P30  15  24.056  6.749  (--*---)
G30F47P23  13  28.984  7.680      (---*---)
G50F33P17  14  35.368  7.455              (--*---)
G70F20P10  14  45.728  4.941                       (---*--)
G90F7P3    14  49.054  6.766                          (---*---)
                                ---------+---------+---------+---------+
                                        30        40        50        60
```

Figure 4.11: One-way ANOVA for replacement level of GGBS in synthesis of geopolymer binder versus compressive strength

The p-value in the analysis of variance table indicates whether the level means are significantly different from each other. If the p-value is less than the α-level, one or more means are significantly different. If the p-value is larger than the α-level, the means are not significantly different. The output of one-way ANOVA illustrated that p-value of 0.000 which lower than selected α-level of 0.05. Thus, it is reasonable to conclude that there are significant influences on the compressive strength attributed to varying compositions of geopolymer binder.

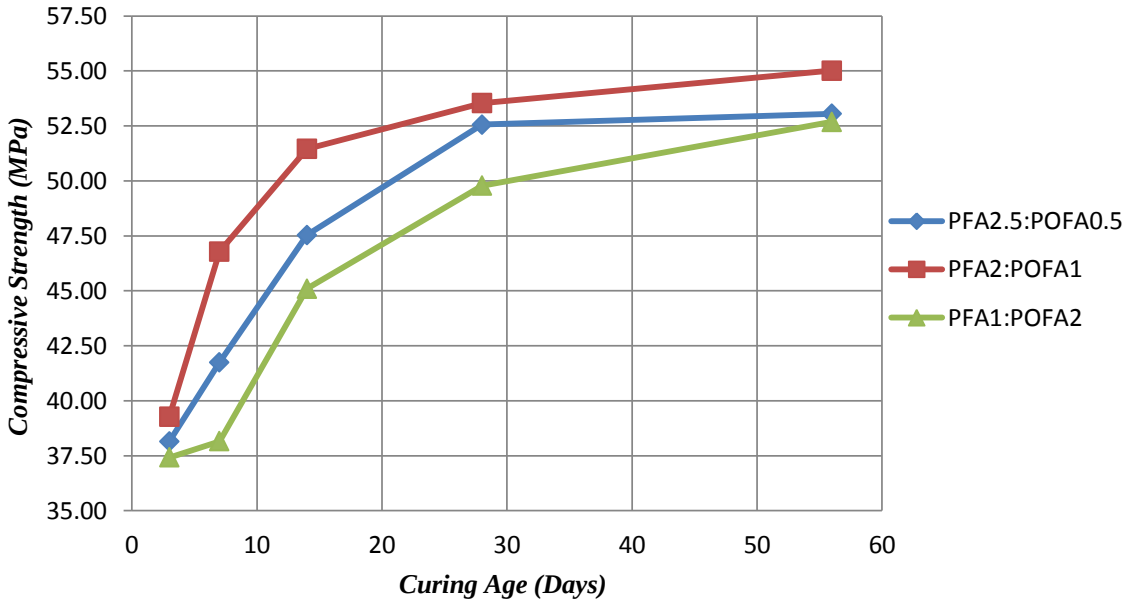

Figure 4.12: Effect of PFA:POFA on compressive strength of geopolymer mortar

Next, further study the effect of variation in PFA and POFA compositions on the compressive strength has been carried out and tabulated in Table 4.2. Increased in fly ash content from 3.33 % to 6.67 % has positive effect on the compressive strength with about 7.55 % improvement, however further addition of fly ash to 8.33 % would adversely affect the compressive strength of geopolymer mortar, causing approximately 1.86 % reduction in strength. This can be explained by low reactivity of fly ash at ambient temperature, thus lead to presence of unreacted fly ash particles in the microstructure as shown in Figure 4.35. On the other hand, further increased in POFA content from 3.33 % to 6.67 % caused a falling trending on compressive strength of about 7.55 % reduction. Increased in POFA content contributed to higher SiO_2/Al_2O_3 ratio, resulting lower leaching of Al^{3+} for condensation (Ranjbar, Mehrali, Alengaram, *et al.*, 2014). Besides, this may be due to untreated-coarse POFA was used in this experiment, whereby the treated and ultrafine-POFA tends to higher reactivity than untreated POFA. The fineness of particle directly contributed to the reactivity of binder (Yusuf *et al.*, 2014a).

Not only that, low in loss on ignition (LOI) has direct relationship with the pozzolanic activity of POFA, while LOI of POFA can be reduced drastically after the removal of unburned carbon by thermal treatment such as incineration (Chandara *et al.*, 2012). Therefore, the relatively poor performance achieved by the specimen with higher content of POFA may be attributed to the nature of untreated POFA. In a nutshell, the optimum synthesis of ternary blended geopolymer binder was achieved at 90 % replacement of GGBS with 2-to-1 ratio of PFA and POFA.

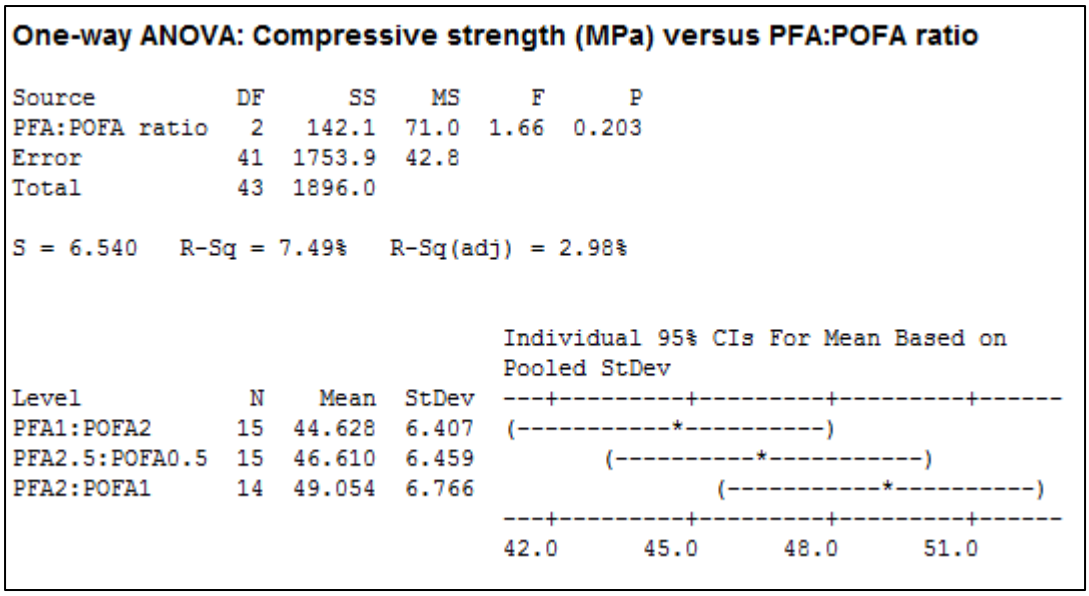

One-way ANOVA: Compressive strength (MPa) versus PFA:POFA ratio

Source	DF	SS	MS	F	P
PFA:POFA ratio	2	142.1	71.0	1.66	0.203
Error	41	1753.9	42.8		
Total	43	1896.0			

S = 6.540 R-Sq = 7.49% R-Sq(adj) = 2.98%

Individual 95% CIs For Mean Based on Pooled StDev

Level	N	Mean	StDev	---+---------+---------+---------+------
PFA1:POFA2	15	44.628	6.407	(-----------*----------)
PFA2.5:POFA0.5	15	46.610	6.459	(----------*----------)
PFA2:POFA1	14	49.054	6.766	(----------*----------)

---+---------+---------+---------+------
42.0 45.0 48.0 51.0

Figure 4.13: One-way ANOVA for varying PFA-to-POFA ratio in synthesis of geopolymer binder versus compressive strength

On the contrary to replacement level of GGBS, the output of one-way ANOVA as shown in Figure 4.13 indicated the variation of PFA-to-POFA ratio has insignificant effect on the compressive strength of geopolymer mortar as indicated by the p-value of 0.203 which is greater than selected α-level of 0.05. Hence, it could be reasonably concluded that GGBS found to be the major factor which determined the compressive strength rather than PFA nor POFA.

4.4 DENSITY

Studies proven that the bulk density of the geopolymer mortar increased with an increase in the curing times. This mainly due to the increasing in reacted products over the curing period of times. Besides, an adverse relationship between density and porosity has been proven over the past studies (Görhan and Kürklü, 2014). Porous structure tends to present larger amount of air voids which very much likely contribute to retaining of water. The density of all the specimen in mean value with varying replacement of GGBS as well as PFA-to-POFA ratio over the curing times have been demonstrated in Table 4.3 as well as the standard deviation among the various specimens.

Table 4.3: Density with varying replacement of GGBS, PFA and POFA

	Density (kg/m^3)				
Variable	**3 days**	**7 days**	**14 days**	**28 days**	**56 days**
G10F60P30	2130 ±9.00	2135 ±4.58	2137 ±6.24	2148 ±2.31	2159 ±10.97
G30F47P23	2145 ±21.07	2154 ±20.74	2159 ±13.86	2163 ±8.72	2165 ±8.96
G50F33P17	2159 ±13.86	2181 ±20.81	2183 ±19.97	2189 ±22.23	2190 ±22.52
G70F20P10	2188 ±19.60	2193 ±19.67	2196 ±20.50	2199 ±20.52	2200 ±20.07
G90F7P3 & PFA2:POFA1	2218 ±4.93	2229 ±4.62	2229 ±5.77	2237 ±4.16	2237 ±4.16
PFA2.5:POFA0.5	2210 ±5.03	2219 ±5.51	2221 ±5.57	2225 ±5.29	2226 ±5.69
PFA1:POFA2	2191 ±4.95	2201 ±5.66	2204 ±4.95	2207 ±3.54	2210 ±2.12

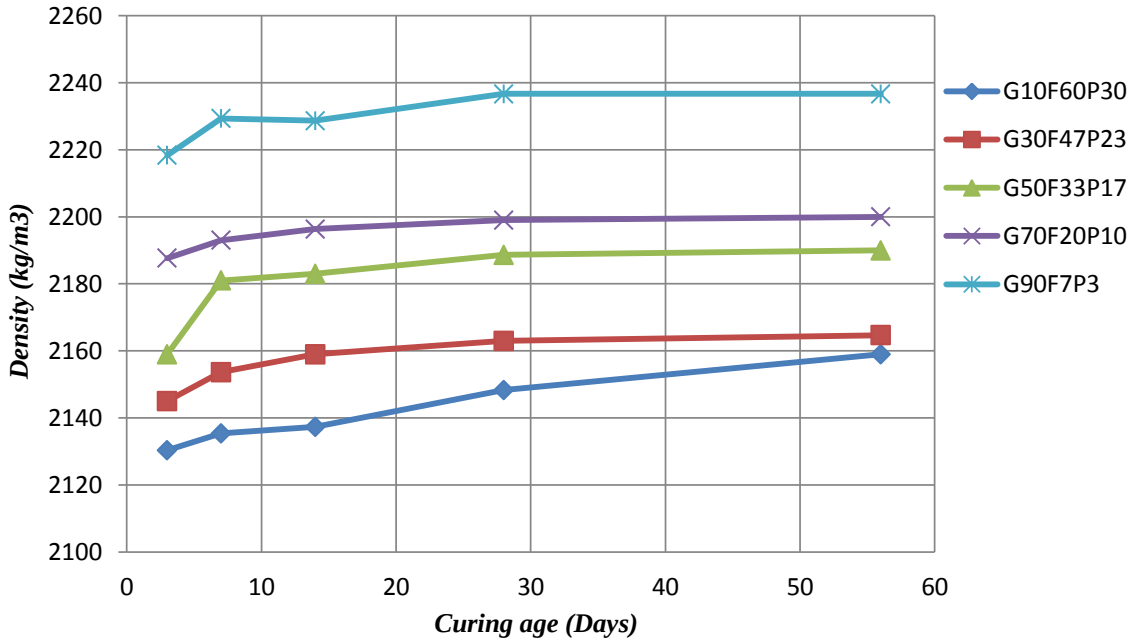

Figure 4.14: Effect of GGBS on density of geopolymer mortar

Figure 4.14 illustrates the density of geopolymer mortar with varying GGBS content. Skyward movement is found in the density from 2159 kg/m^3 to 2165 kg/m^3, consecutively increased to 2190 kg/m^3, 2200 kg/m^3 and 2237 km/m^3 as the replacement of GGBS increased from 10 % to 30 %, subsequently to 50 %, 70 % and 90 % at 56 days. The highest density of 2237 kg/m^3 was achieved by G90F7P3 at 56 days. This can be explained by high degree of dissolution of Ca ion contributed to increase in reacted product, thus a denser geopolymer mortars were achieved. Ca does not solely contribute to compressive strength development but also increases the density of microstructure through the pore filling effects (Yusuf *et al.*, 2014b). Therefore, denser microstructures were developed in the specimens with higher replacement level of GGBS, further proven in the SEM images as shown in Figure 4.41. On other hand, the low density result had cross confirmed the high porosity value as shown in Figure 4.27 due to the effect of porous POFA thus developed lower density (Ranjbar, Mehrali, Behnia, *et al.*, 2014). The low density as well as porous structures in G10F60P30 had been further proven in SEM image as shown in Figure 4.35.

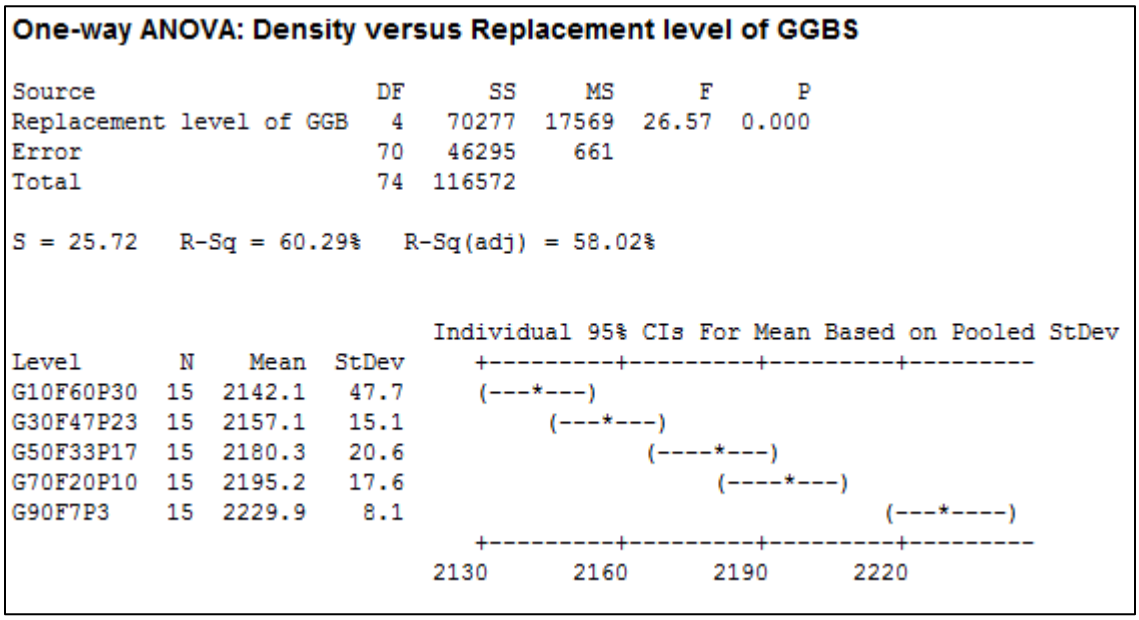

One-way ANOVA: Density versus Replacement level of GGBS

Source	DF	SS	MS	F	P
Replacement level of GGB	4	70277	17569	26.57	0.000
Error	70	46295	661		
Total	74	116572			

S = 25.72 R-Sq = 60.29% R-Sq(adj) = 58.02%

Level	N	Mean	StDev
G10F60P30	15	2142.1	47.7
G30F47P23	15	2157.1	15.1
G50F33P17	15	2180.3	20.6
G70F20P10	15	2195.2	17.6
G90F7P3	15	2229.9	8.1

Individual 95% CIs For Mean Based on Pooled StDev

2130 2160 2190 2220

Figure 4.15: One-way ANOVA for replacement level of GGBS in synthesis of geopolymer binder versus density (kg/m^3)

Figure 4.15 illustrated the one-way ANOVA test conducted to analyze the amount of variance in density attributed to the effect of variation in geopolymer binder synthesis with different level of replacement in GGBS. Absolute significant impact by the replacement level of GGBS can be interpreted by the zero p-value as shown in Figure 4.15.

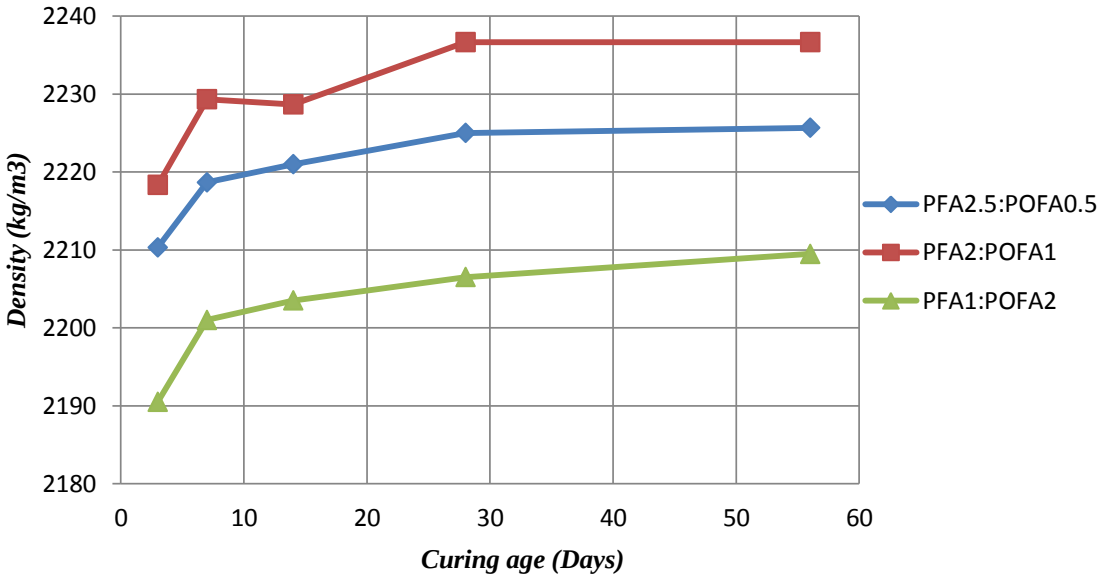

Figure 4.16: Effect of PFA-to-POFA ratio on density of geopolymer mortar

Furthermore, the increment in replacement level of PFA from 3.33 % to 6.67 % caused the density of geopolymer mortar to be increased from 2210 kg/m^3 to 2237 kg/m^3 at 56 days, yet further increased the replacement of PFA to 8.33 % had converse effect on the density and fell to 2226 kg/m^3. However, increased in replacement of POFA resulted in reduction in the specimen density (Ranjbar, Mehrali, Alengaram, *et al.*, 2014). About 1.22 % dropped in density as the POFA dosage increased from 3.33 % to 6.67 %. This may be due to gradual dissolution of POFA as well as lesser amount of Al ion available in the system. Not only that, this may also due to the drawback effect by used of untreated POFA with high loss on ignition (LOI) to the pozzalanic reaction of POFA (Chandara *et al.*, 2010). Besides, fly ash-based geopolymer pastes generally take significantly longer time to set attributed to slower rate of chemical reaction at low ambient temperature (Nath, Sarker and Rangan, 2015).

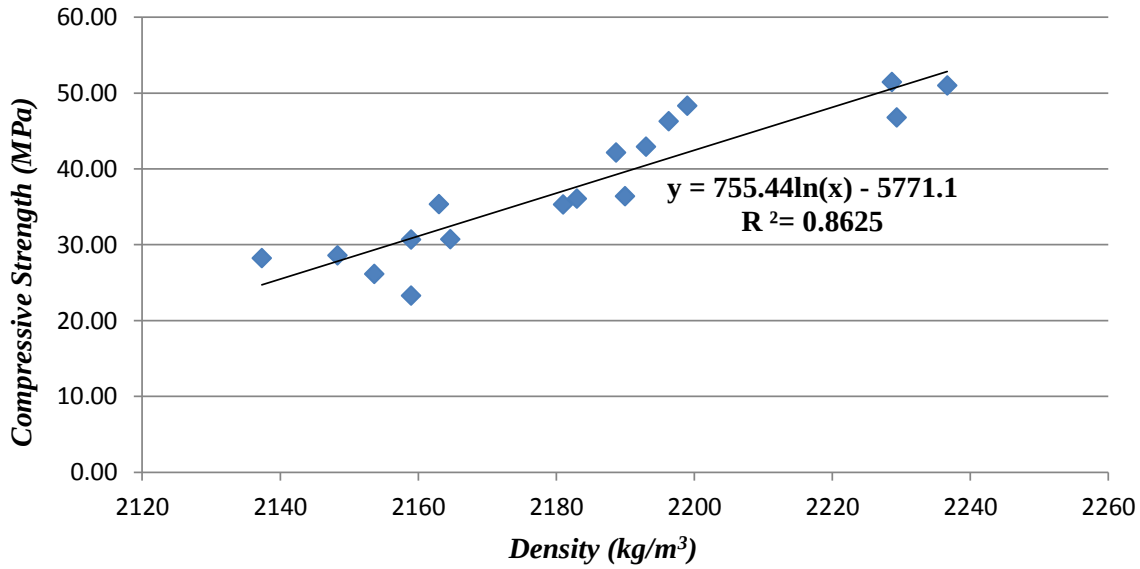

Figure 4.17: Linear correlation between compressive strength and density

The positive linear relationship between the compressive strength and density of GGBS-PFA-POFA ternary-hybrid geopolymer mortar was explicitly shown in Figure 4.17 with R^2 value of 0.8625. This can be interpreted by the higher the dissolution and hydration rate of pozzolanic binders, the denser the reacted products been produced, thus resulted in higher density and compressive strength.

4.5 ULTRASONIC PULSE VELOCITY (UPV)

UPV measurements are to gauge the internal structures of the geopolymer specimen. This test is used to assess the existence of any cracks, voids, damage, internally discontinuities and the level of deterioration of geopolymer specimen (Omer et al., 2015). The higher the level of velocity indicates higher degree of compactiveness and density of geopolymer mortar.

Table 4.4: Quality assessment on UPV value (Civil Engineering Portal, 1992)

Pulse Velocity (km/s)	**Quality Grading**
Above 4.5	Excellent
3.5 to 4.5	Good
3.0 to 3.49	Medium
Below 3.0	Doubtful

Table 4.5: UPV value with varying replacement GGBS, PFA and POFA

	UPV (km/s)				
Variable	**3 days**	**7 days**	**14 days**	**28 days**	**56 days**
G10F60P30	2.893 ±0.01	3.148 ±0.11	3.540 ±0.07	3.810 ±0.08	3.910 ±0.06
G30F47P23	3.443 ±0.06	3.623 ±0.14	3.890 ±0.04	4.018 ±0.02	4.153 ±0.04
G50F33P17	3.747 ±0.01	3.778 ±0.14	3.985 ±0.04	4.208 ±0.02	4.273 ±0.04
G70F20P10	3.885 ±0.01	3.970 ±0.04	4.157 ±0.18	4.227 ±0.01	4.312 ±0.11
G90F7P3 & PFA2:POFA1	3.875 ±0.05	4.022 ±0.01	4.151 ±0.06	4.365 ±0.16	4.438 ±0.12
PFA2.5:POFA0.5	3.838 ±0.04	3.995 ±0.03	4.087 ±0.05	4.250 ±0.01	4.297 ±0.02
PFA1:POFA2	3.822 ±0.03	3.955 ±0.09	4.078 ±0.04	4.227 ±0.03	4.303 ±0.04

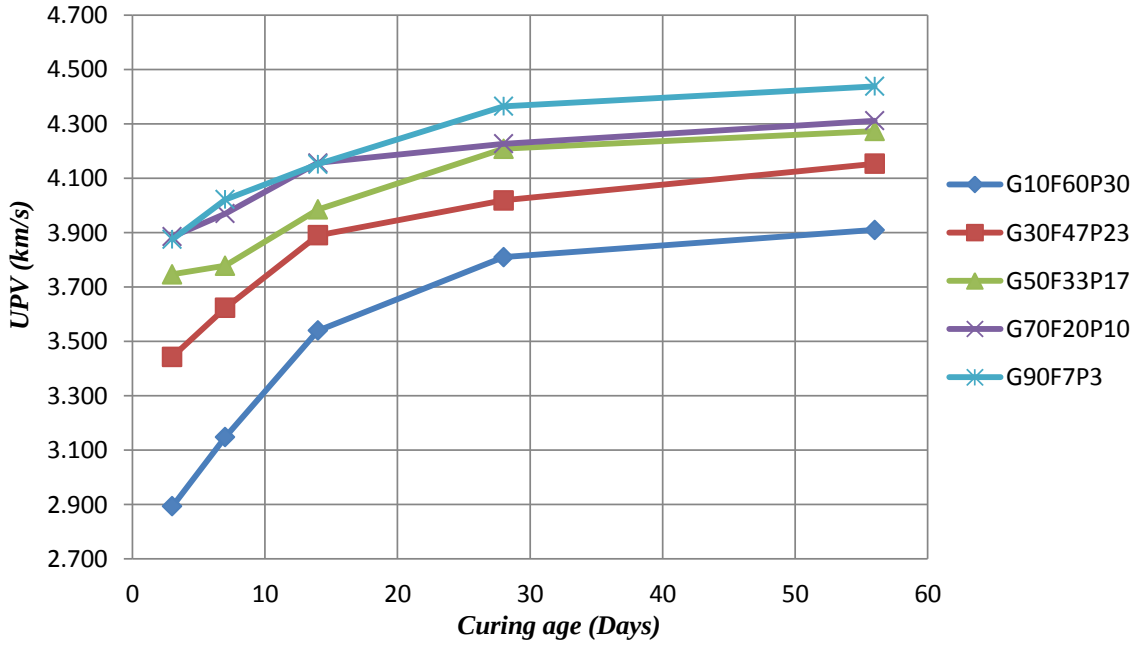

Figure 4.18: Effect of GGBS on UPV value of geopolymer mortar

With reference to Figure 4.18, an upward trending of UPV values with the increase in ground granulated blast-furnace slag content in a perfectly ascending order is observed. The optimum result of 4.438 km/s ±0.12 at 56 days was obtained in G90F7P3 which approximately 13.50 % higher than G10F60P30. This can be explained by higher degree of compactiveness in the microstructural matrix as shown in Figure 4.41. Following by G70F20P10, which was only about 2.92 % lower than G90F7P3. Micro-cracking, void and pores in the internal structure would prolong reception of ultrasonic pulse (Omer et al., 2015). On the other hand, the lower UPV value was obtained in G10F60P30 of 3.540 km/s ±0.07 at 14 days can be explained by the presence of micro-cracking, loose matrix formation and number of unreacted fly ash particles in the microstructure as shown in Figure 4.35. Besides, only about 14.53 % variance between 3-days and 56days UPV values achieved by G90F7P3, however approximately 35.15 % variance is obtained in G10F60P30. The vast difference in variances explicitly indicated the rate of geopolymerization process at early stage between both specimens. High CaO would accelerate the reaction at early stage; while POFA-based geopolymer with higher SiO_2 would prolong the final strength as well as promote continuous reaction in geopolymer to the much later stage (Mijarsh, Megat Johari and Ahmad, 2015).

One-way ANOVA: Ultrasonic pulse velocity versus Replacement level of GGBS

```
Source                    DF       SS      MS      F      P
Replacement level of GGB   4   4.8722  1.2180  16.02  0.000
Error                     70   5.3211  0.0760
Total                     74  10.1933

S = 0.2757   R-Sq = 47.80%   R-Sq(adj) = 44.81%


                              Individual 95% CIs For Mean Based on
                              Pooled StDev
Level       N    Mean   StDev -------+---------+---------+---------+--
G10F60P30  15  3.4603  0.4055 (----*-----)
G30F47P23  15  3.8257  0.2745               (-----*-----)
G50F33P17  15  3.9983  0.2301                      (-----*-----)
G70F20P10  15  4.1100  0.1845                           (----*-----)
G90F7P3    15  4.1703  0.2309                             (-----*----)
                              -------+---------+---------+---------+--
                                   3.50      3.75      4.00      4.25
```

Figure 4.19: One-way ANOVA for replacement level of GGBS in synthesis of geopolymer binder versus UPV value

Similar to the afore-conducted ANOVA tests as on compressive strength and density, varying replacement level of GGBS in synthesis of geopolymer binder had significant influence on the variance of UPV response as the p-value found to be 0.000 which below the selected α-level of 0.05, as shown in Figure 4.19. The output of ANOVA has further proven the beneficial contribution of GGBS to development of higher degree of compactness microstructure as shown in Figure 4.41 credited to larger amount of Ca ion available in the geopolymerization system.

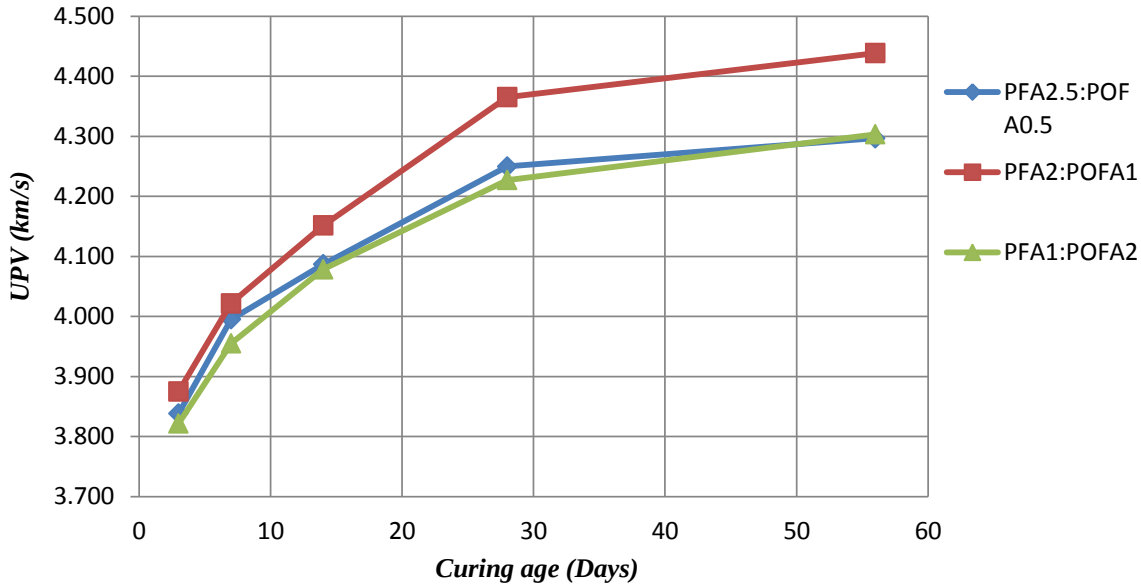

Figure 4.20: Effect of PFA-to-POFA ratio on UPV value of geopolymer mortar

Next, further study of optimum synthesis of ternary blended geopolymer mortar with varying PFA:POFA ratio, highest UPV value was achieved by PFA2:POFA1 of 4.438 km/s at 56 days, following by PFA2.5:POFA0.5 which was 2.71 % lower and lastly PFA1:POFA2 which was 3.26 % lower than PFA2:POFA1 at 28 days. This can be explained by further increment in PFA binder, resulting in higher number of unreacted fly ash particles at ambient temperature, thus emphasizing the presence of micro-cracking, pores and voids in the geopolymer matrix.

On the other hand, further increase of POFA binder in PFA1:POFA2 increased the SiO_2/Al_2O_3 ratio. Higher SiO_2/Al_2O_3 ratio causes the reaction of aluminate species in the early stages and therefore resulting in scarcity of Al ions for further reactions at the later stages (Ranjbar, Mehrali & Behnia, et al., 2014). However, PFA1:POFA2 subsequently achieved about 0.14 % higher in UPV values than PFA2.5:0.5 at 56 days. This can be explained by continuously reaction of Si ion with silicate elements to later stage attributed to high SiO_2 content in POFA (Mijarsh, Megat Johari and Ahmad, 2015).

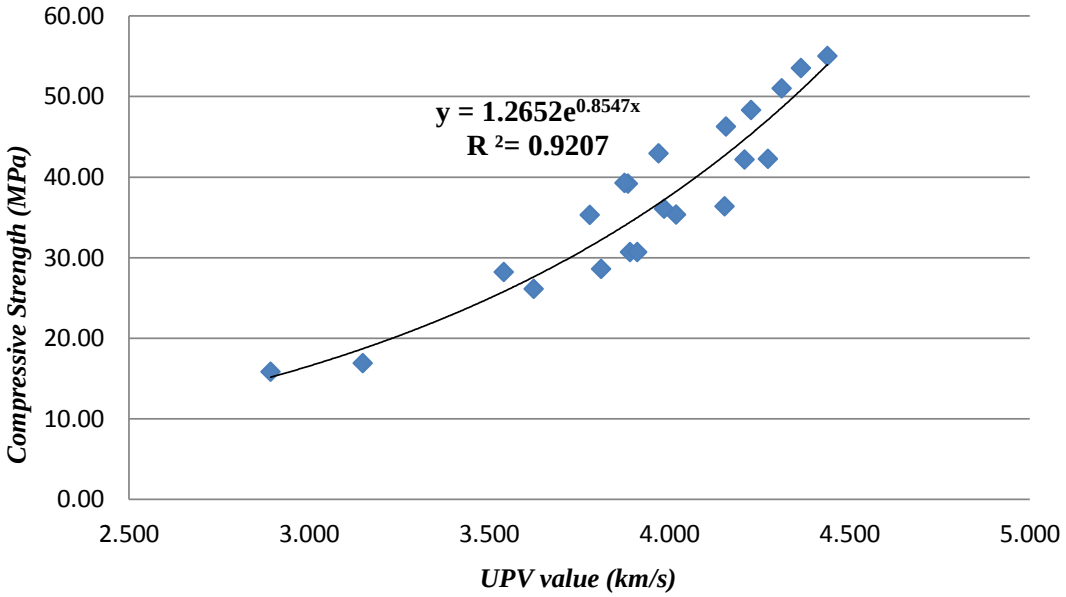

Figure 4.21: Positive correlation between compressive strength with UPV values

Positive relationship between compressive strength and UPV values is illustrated in Figure 4.21 with the R^2 value of 0.9207. The high R^2 value indicated significant variance in the response of one factor attributed to variation in the other. Higher compressive strength of geopolymer mortar attributed to a well-pack, denser microstructural system with minimum crack, void or internal damage ended up with higher UPV value and lower porosity. Hence, UPV values may be an accurately estimators of compressive strength for geopolymer mortar (Omer, Demirboga and Khushefati, 2015). The ternary relationship between compressive strength, UPV and replacement level of GGBS has been further illustrated in Figure 4.22.

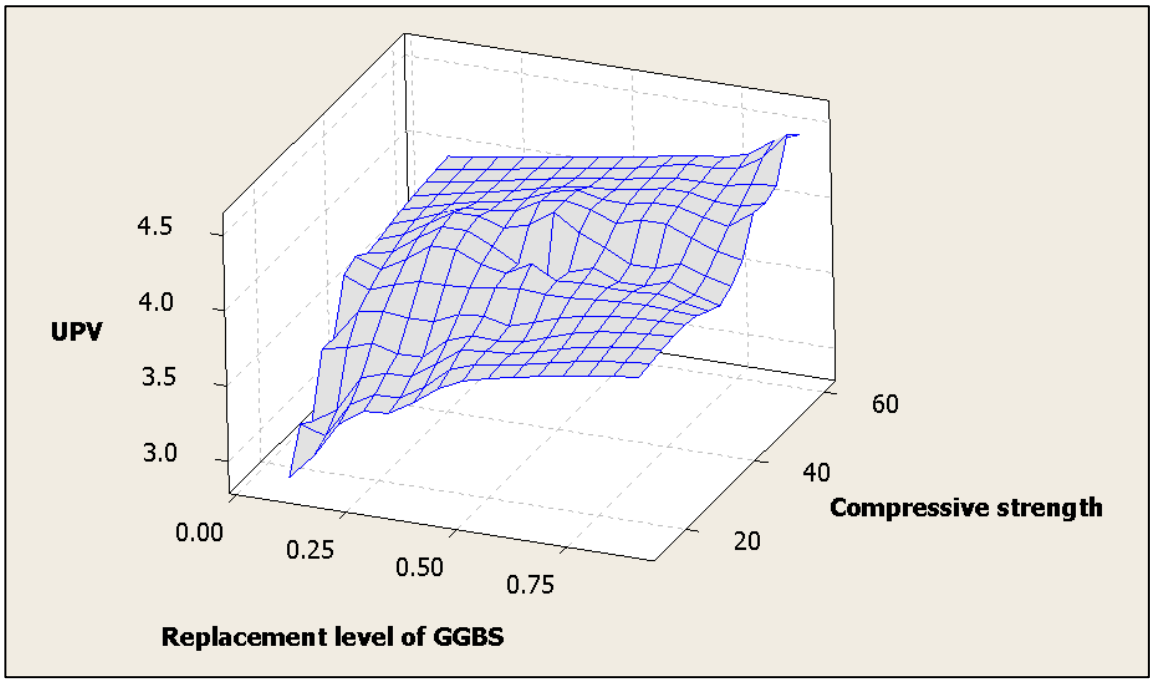

Figure 4.22: Surface plot of geopolymer binder synthesis with varying replacement level of GGBS versus engineering properties

The three dimensional surface plot of varying replacement level of GGBS in geopolymer binder versus compressive strength and UPV can be observed in Figure 4.22. The integration of Y-axis as UPV, Z-axis as compressive strength and X-axis as binder composite demonstrated an upward tilting towards to opposite end. This had further proven the positive ternary relationship among the factors as illustrated in Figure 4.10 and 4.17. The peak of the surface plot was found at specimens with maximum replacement level of GGBS with highest compressive strength of 55.02 MPa as well as UPV values of 4.438 km/s.

4.6 WATER ABSORPTION

Table 4.6 illustrates the water absorption rate of geopolymer specimens with different composition of binder which been cured at 3, 7, 14, 28 and 56 days. The overall variance of 82.09 % in water absorption rate within the range of between 3.63 to 6.61 % was manipulated by the varying composition of geopolymer binder comprise of GGBS, PFA and POFA.

Table 4.6: Water absorption with varying replacement of GGBS, PFA and POFA

	Water Absorption rate (%)			
Variable	**7 days**	**14 days**	**28 days**	**56 days**
G10F60P30	6.61 % ±0.36	6.47 % ±0.18	6.23 % ±0.08	6.05 % ±0.21
30F47P23	5.83 % ±0.26	5.71 % ±0.35	5.51 % ±0.41	5.36 % ±0.11
G50F33P17	5.44 % ±0.17	5.14 % ±0.43	4.93 % ±0.40	4.62 % ±0.36
G70F20P10	5.10 % ±0.39	4.79 % ±0.11	4.58 % ±0.13	3.73 % ±0.25
G90F7P3 & PFA2:POFA1	4.76 % ±0.44	4.63 % ±0.26	4.32 % ±0.27	3.57 % ±0.26
PFA2.5:POFA0.5	4.80 % ±0.12	4.74 % ±0.07	4.44 % ±0.21	3.64 % ±0.20
PFA1:POFA2	4.85 % ±0.08	4.78 % ±0.13	4.61 % ±0.17	3.63 % ±0.09

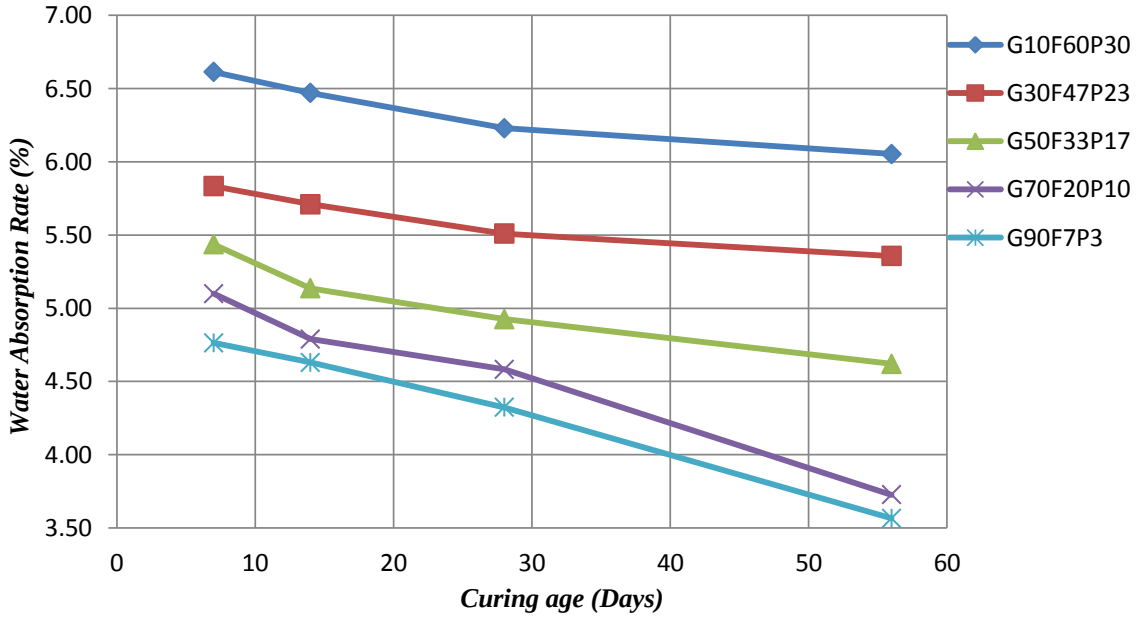

Figure 4.23: Effect of GGBS on water absorption rate of geopolymer mortar

The decreasing trend of water absorption rate is observed with the increase of GGBS content is explicitly shown in Figure 4.23. G10F60P30 has the highest sorptivity rate of 6.05 % at 56 days, yet dropped to 5.36 % when 20 % of GGBS replacement had added into the binder composition. Consecutive decreased to 4.26 %, 3.73 % and 3.57 % with further increasing in replacement of GGBS at every 20 % interval up to G90F7P3. The can be explained by the degree of geopolymerization as well as the resultant product. Fly ash is relatively low reactivity at ambient curing, yet inclusion of GGBS could accelerate the dissolution of fly ash particle (Yusuf *et al.*, 2014b). Large amount of unreacted fly ash particles were spotted in G10F60P30 as it contained lowest dosage of GGBS, as shown in Figure 4.35. The unreacted particles very often are found in hollow cavities and it tends to create pores in the geopolymeric paste (Ranjbar, Mehrali, Alengaram, *et al.*, 2014). However, about 30.95 % reduction in water absorption for G50F33P17 attributed to 40 % higher in GGBS replacement. However, numbers of partially reacted particles were found in G50F33P17 as shown in Figure 4.38. The partially-dissolved spherical PFA particles with widespread-scattered pores allowed water to be retained in the geopolymer matrix (Ranjbar, Mehrali, Alengaram, *et al.*, 2014). In the contrary, G90F7P9 developed denser microstructure with minimal pores (as shown in Figure 4.41), prohibited the penetration of water into the paste.

One-way ANOVA: Water absorption versus Replacement level of GGBS

Source	DF	SS	MS	F	P
Replacement level of GGB	4	32.219	8.055	39.66	0.000
Error	55	11.171	0.203		
Total	59	43.391			

S = 0.4507 R-Sq = 74.25% R-Sq(adj) = 72.38%

Level	N	Mean	StDev	Individual 95% CIs For Mean Based on Pooled StDev
G10F60P30	12	6.3417	0.2993	(---*--)
G30F47P23	12	5.6025	0.3219	(---*---)
G50F33P17	12	5.0300	0.4322	(---*---)
G70F20P10	12	4.5500	0.5727	(---*---)
G90F7P3	12	4.3208	0.5546	(---*--)

Pooled StDev: 4.20, 4.90, 5.60, 6.30

Figure 4.24: One-way ANOVA for replacement level of GGBS in synthesis of geopolymer binder versus water absorption

With reference to the 0.000 p-value demonstrated in Figure 4.24, it is clearly indicated significant variance of the water absorption attributed to composition of geopolymer binder with varying replacement level of GGBS as it lower than selected α-level of 0.05. This can be explained by better filling effect to voids by the GGBS binder with higher specific gravity and thinner fineness of particles.

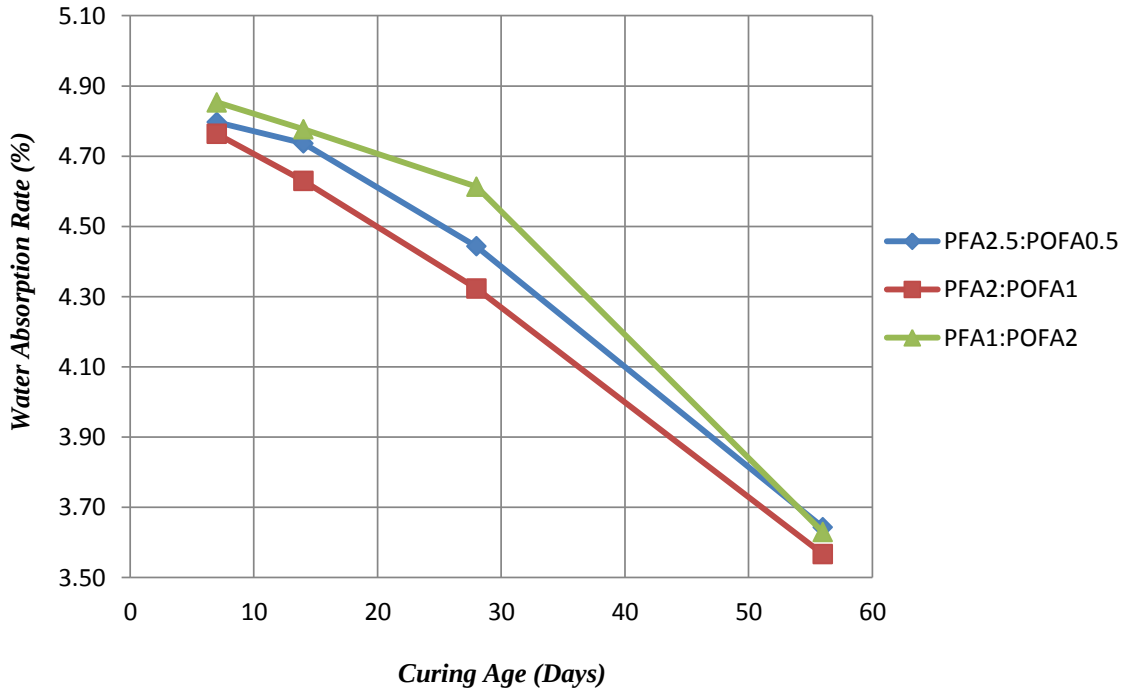

Figure 4.25: Effect of PFA:POFA ratio on water absorption of geopolymer mortar

PFA2:POFA1 with 6.67 % in PFA achieved the low water absorption rate of 4.32 % at 28 days, following by PFA2.5:POFA0.5 and PFA1:POFA2 of 4.44 % and 4.61 %, respectively. Increase in replacement of PFA from 3.33 % to 6.67 % resulted 6.71 % reduction in water absorption, yet rebound effect of 2.77 % increment in water absorption rate is observed when further increased PFA content to 8.33 %. However, the water absorption rate of PFA1:POFA2 has subsequently dropped lower than PFA2.5:POFA0.5 as further curing at 56 days, about 0.01 % lower in water absorption value. This can be explained by higher SiO_2/Al_2O_3 ratio in PFA1:POFA2 prolonged the final setting of geopolymer mortar, thus further extended the reaction and condensation process between leached silicon with silicate component (Mijarsh, Megat Johari and Ahmad, 2014). In a nutshell, based on the result as shown in Table 4.6, it can be concluded that the optimum synthesis of ternary hybrid geopolymer binder is 90 % of GGBS, 6.67 % of PFA and 3.33 % of POFA.

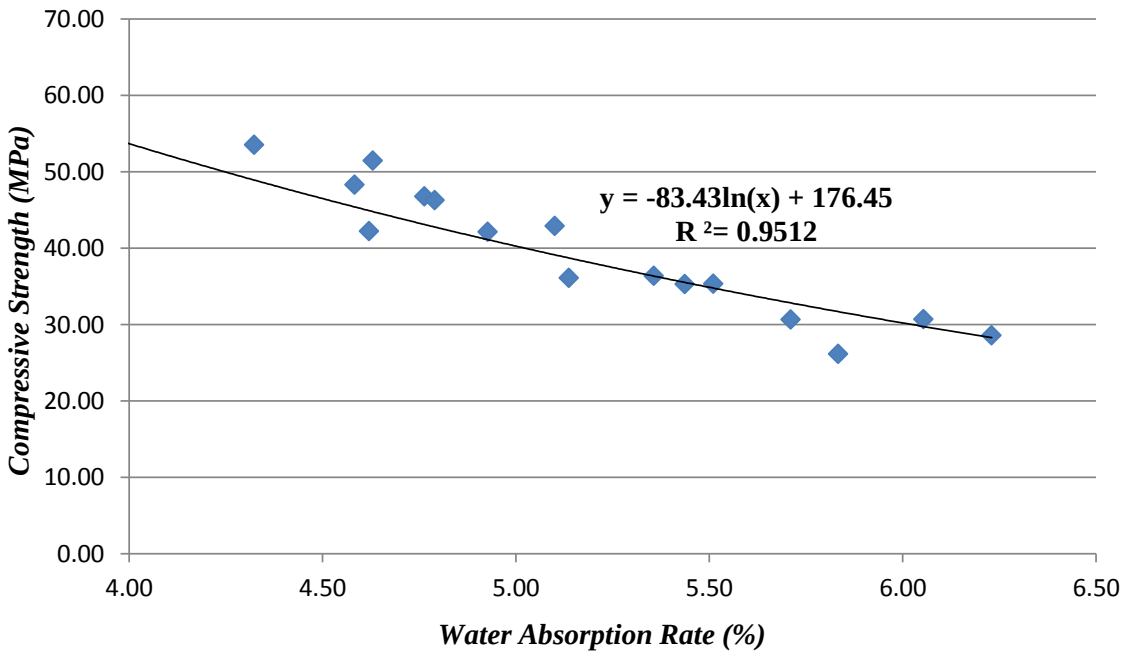

Figure 4.26: Correlation between compressive strength and water absorption

The negative correlation between water absorption and compressive strength is shown in Figure 4.26. Water absorption test indicates the volume of permeable voids, water sorptivity and the presence of crack or damage in the geopolymer mortar. Geopolymer mortar with high water absorption attributed to development of porous microstructure and/or presence of micro cracks and voids which ended up lead to lower compressive strength. Taken G10F60P30 as an example, loose and porous microstructure as shown in Figure 4.35 had resulted low compressive strength as shown in Figure 4.10 as well as high water absorption as shown in Figure 4.23. Hence, water absorption is one of the indicators of compressive strength (Shaikh, 2016).

4.7 POROSITY

Resistance of geopolymer mortar towards acid attack and penetration of chloride ions is vastly rely on the porosity and inter-connectivity of the pore system (Shaikh, 2016). High porosity of geopolymer mortar is prone to deterioration by chemical attacks, thus leading to loss of weight attributed to formation of cracking and scaling (Okoye, Prakash and Singh, 2017).

Table 4.7: Porosity values with varying replacement of GGBS, PFA and POFA

	Porosity (%)			
Variable	**7 days**	**14 days**	**28 days**	**56 days**
G10F60P30	25.25% ±0.54	25.12% ±0.54	24.75% ±0.83	21.67% ±4.54
G30F47P23	23.42% ±0.52	22.00% ±0.68	21.68% ±0.96	21.08% ±0.60
G50F33P17	21.97% ±1.07	21.64% ±0.60	21.32% ±0.59	20.58% ±1.84
G70F20P10	21.50% ±1.24	21.41% ±1.23	21.27% ±1.21	20.21% ±0.31
G90F7P3 & PFA2:POFA1	21.79% ±1.04	21.39% ±0.60	21.20% ±1.20	20.02% ±1.12
PFA2.5:POFA0.5	21.81% ±0.71	21.44% ±0.76	21.25% ±0.60	20.21% ±0.75
PFA1:POFA2	22.00% ±0.77	21.57% ±0.60	21.29% ±0.44	20.15% ±1.25

Table 4.7 indicates the porosity values of geopolymer mortar with varying replacement level of GGBS. The highest porosity value was obtained in G10F60P30 of 24.75 % at 28 days, following by G30F47P23, G50F33O17, G70F20P10 and the lowest of G90F7P3, with the porosity values of 21.68 %, 21.32 %, 21.27 % and 21.20 %, respectively. This scenario has further proven the aforementioned contribution of leaching Ca ion from GGBS lead to high degree of geopolymerization and better pore filling effect, thus minimize the presence of micro-crack and void in the system.

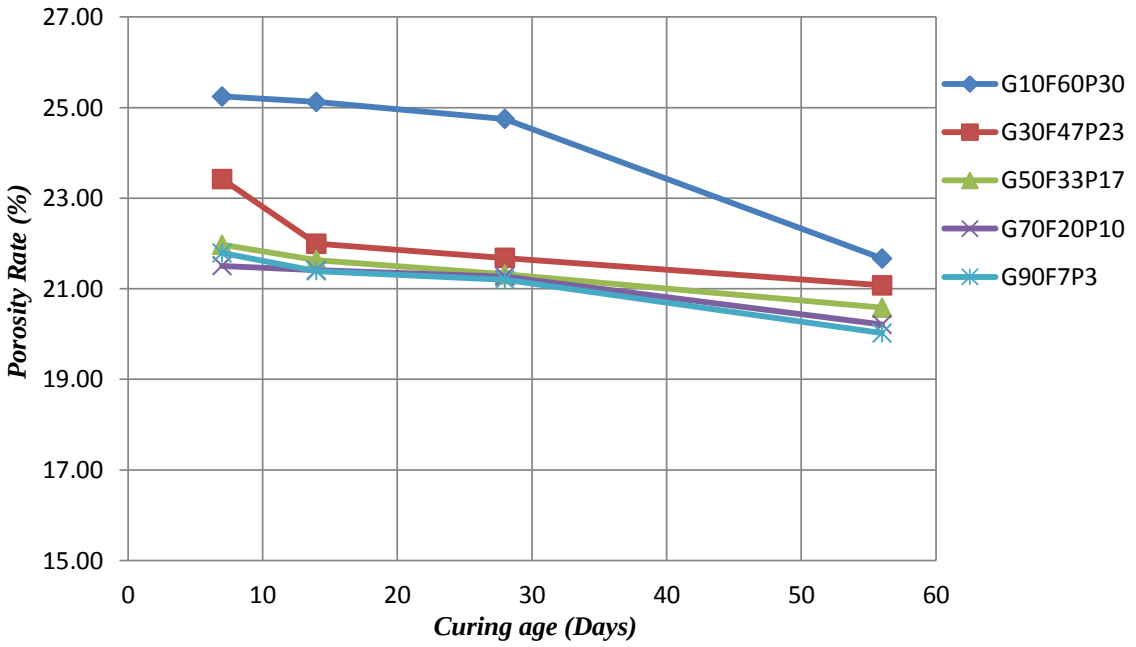

Figure 4.27: Effect of GGBS on porosity rate of geopolymer mortar

A standardized range of variation between the porosity values and addition of GGBS content is observed from G30F47P23 to G90F7P3. As the replacement of GGBS increased from 30 % to 50 %, 70 % and 90 %, the porosity values dropped approximately 1.69 %, 0.24 % and 0.33 %, respectively. However, significant difference is observed in G10F60P30. The porosity value increased about 14.16 % as the replacement of GGBS reduced from 30 % to 10 %. The reason for this scenario may due to the presence of unreacted or partially dissolved particles in the geopolymeric matrix as shown in Figure 4.35. Typically, unreacted particles have been found in hollow cavities as well as the partially-dissolved spherical particle, and it tends to create porosity in the matrix which contained highly dispersed tiny sized pores (Ranjbar, Mehrali, Alengaram, *et al.*, 2014). The reduction in porosity does enhance the compressive strength of geopolymer pastes (Singh *et al.*, 2015). Therefore, the declining trending in porosity has cross-proven the upward movement in compressive strength as shown in Figure 4.10.

One-way ANOVA: Porosity versus Replacement level of GGBS

```
Source                     DF      SS     MS     F      P
Replacement level of GGB    4   81.90  20.48  9.01  0.000
Error                      52  118.14   2.27
Total                      56  200.04

S = 1.507   R-Sq = 40.94%   R-Sq(adj) = 36.40%


                              Individual 95% CIs For Mean Based on
                              Pooled StDev
Level        N    Mean  StDev  -----+---------+---------+---------+----
G10F60P30   12  24.196  2.519                       (-----*-----)
G30F47P23   12  22.044  1.084         (-----*-----)
G50F33P17    9  21.288  1.189   (------*------)
G70F20P10   12  21.098  1.070   (-----*----)
G90F7P3     12  21.100  1.022   (-----*----)
                              -----+---------+---------+---------+----
                                21.0      22.5      24.0      25.5
```

Figure 4.28: One-way ANOVA for replacement level of GGBS in synthesis of geopolymer binder versus porosity

With reference to Figure 4.28, replacement level of GGBS in ternary blended geopolymer mortar has significant effect on the porosity as proven by the output of one-way ANOVA as indicated by the 0.000 p-value with selected α-level of 0.05. On the contrary, insignificant influence to porosity was to be found in varying PFA-to-POFA ratio as shown in Figure 4.29.

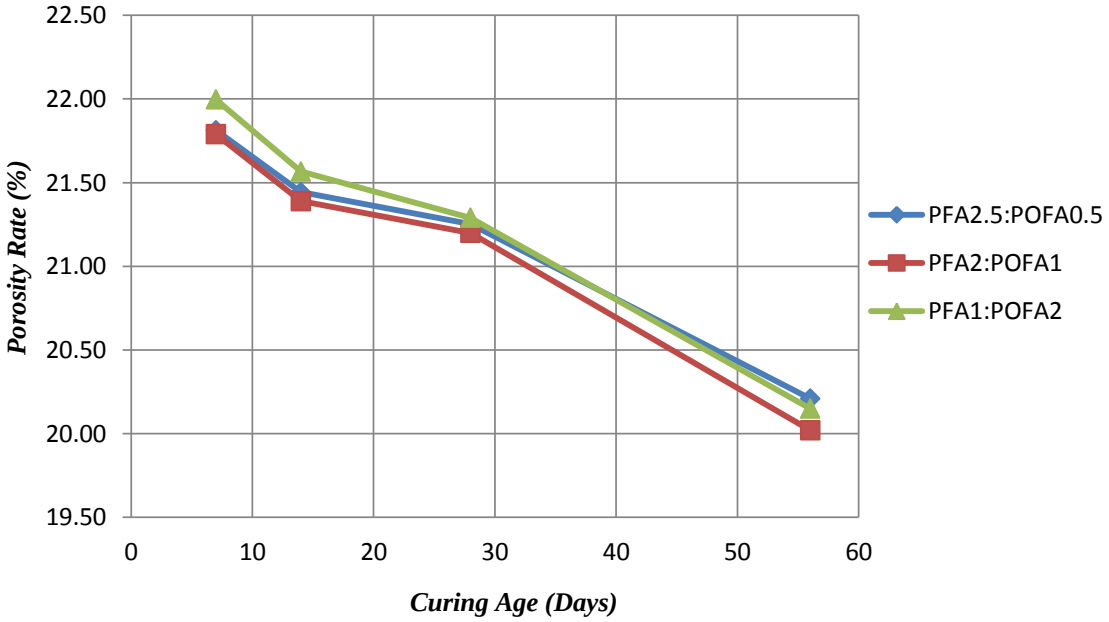

Figure 4.29: Effect of PFA-to-POFA ratio on porosity rate of geopolymer mortar

0.96 % downturn movement of porosity value is observed as the replacement of PFA increased from 3.33 % to 6.67 %. However, reversed effect on the porosity value of 0.09 % increment is spotted with the further increase in PFA to 8.33 %. The changes in PFA-to-POFA ratio had little or implicit effect on the porosity, this is because of insignificant replacement of only 10 % for blended PFA and POFA in the binder composite. The difference in porosity values among the variables was within the range of standard deviation. Gao, Yu and Brouwers (2016) have concluded that porosity is not the only indication of strength. This can be further proven by ANOVA analysis as shown in Figure 4.30.

One-way ANOVA: Porosity (%) versus PFA:POFA ratio

Source	DF	SS	MS	F	P
PFA:POFA ratio	2	0.137	0.068	0.08	0.922
Error	33	27.706	0.840		
Total	35	27.842			

S = 0.9163 R-Sq = 0.49% R-Sq(adj) = 0.00%

Level	N	Mean	StDev	Individual 95% CIs For Mean Based on Pooled StDev
PFA1:POFA2	12	21.251	0.889	(----------*----------)
PFA2.5:POFA0.5	12	21.180	0.827	(----------*----------)
PFA2:POFA1	12	21.100	1.022	(----------*----------)
				20.65 21.00 21.35 21.70

Figure 4.30: One-way ANOVA for varying PFA-to-POFA ratio in synthesis of geopolymer binder versus porosity

Variation in PFA-to-POFA ratio has no significant effect on the porosity with reference to the output of one-way ANOVA (as shown in Figure 4.30) as explicitly indicated by the p-value of 0.922 which so much so even higher than as on compressive strength of 0.203. Although both variances were insignificant, yet somehow the changes in PFA-to-POFA ratio contributed higher degree of variance to compressive strength than porosity. Thus, further proven that porosity is not the only indication of compressive strength (Gao, Yu and Brouwers, 2016).

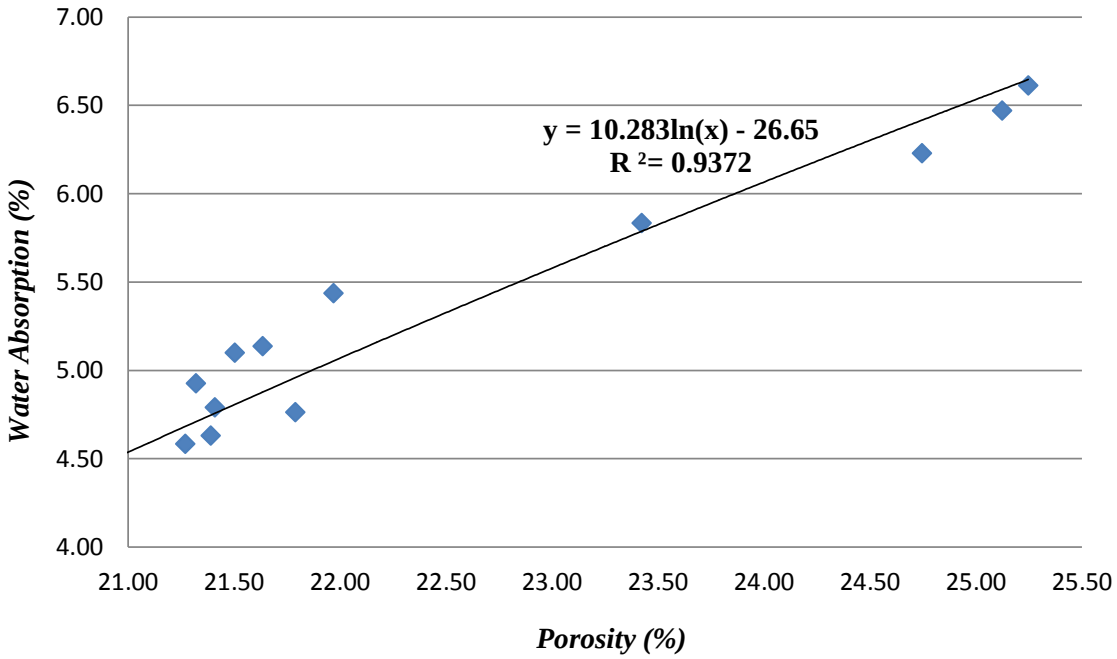

Figure 4.31: Positive correlation between water absorption and porosity

Furthermore, the positive correlation between water absorption and porosity of geopolymer mortar has been illustrated in Figure 4.31. This indicates the presence of crack, void and pores in the geopolymer structure allow the penetration of water, thus prone to acid attack and ingress of chloride ions. Both water absorption test and porosity test used to measure the absorption rate of geopolymer mortar, yet the only different are: porosity test emphasizes on the total absorption volume of a specimen in total saturated condition; whereby water absorption test focus on the degree of initial absorption within a specific duration of time.

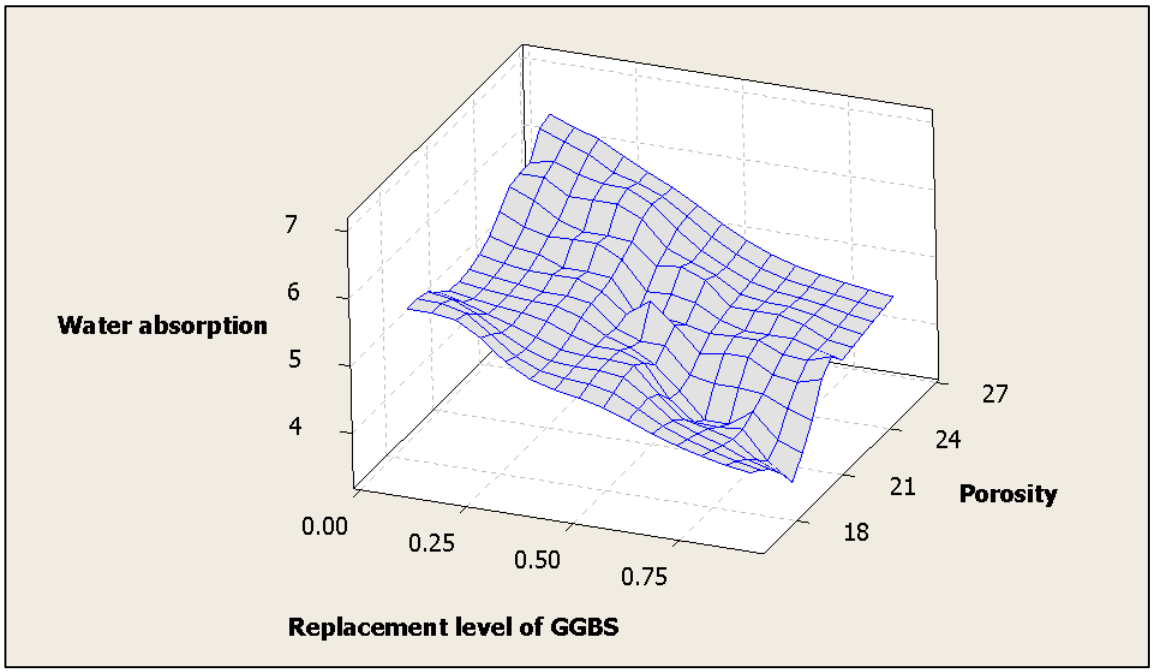

Figure 4.32: Surface plot of geopolymer binder synthesis with varying replacement level of GGBS versus durability performance

The three dimensional surface plot of varying replacement level of GGBS in geopolymer binder versus water absorption and porosity can be observed in Figure 4.32. The integration of Y-axis as binder synthesis, Z-axis as water absorption and X-axis as porosity illustrated a downward slanting towards to end of Y-axis. This has explicitly demonstrated downhill movements in both the water absorption and porosity as the replacement level of GGBS increased. Hence, it has cross-proven the inverse relationships between the water absorption and porosity toward the replacement level of GGBS, as illustrated in Figure 4.23 and 4.27. With reference to Figure 4.32, the nadir of surface plot was found to be specimen with highest replacement level of GGBS, whereas lowest porosity of 20.02 % as well as water absorption of 3.57 % at 56 days.

4.8 CAPILLARY ABSORPTION COEFFICIENT

Capillary action is the ability of liquid to flow through the narrow spaces in between the mortar paste without the assistance of external force or even oppose to gravity force and typically through any crack, voids or pores within the mortar structures. The rate of capillary absorption is depends on the degree of connectivity in voids, cracks or pores within the geopolymer mortar which so much so to form a continuous-path which resulted in facilitates capillary action. A continuous-path is crucial in determination of capillary absorption rate of geopolymer mortar. Studies had proven none correlation occurs between porosity and capillary absorption in concrete. Researches had proven that high porosity geopolymer product has the high tendency in capillary absorption if and only if the internal voids or micro cracks had interconnected to one another which so much so to be formed a continuous-path for capillary action.

This is critically serious to the building components which expose to underground water or saline environment. The penetration of water through capillary action may allow the ingress of sodium chloride, thus causing internal expansion and crack to the geopolymer mortar due to crystallization. Therefore, the water absorption rate of alkali-activated ternary blended geopolymer mortar through capillary action was studied in this research. The amount of water been absorbed by the geopolymer mortar prism over a specific period of time at several intervals, has been recorded and translated into presentable graphs as shown in Figure 4.33 and 4.34.

Table 4.8: Capillary absorption coefficient with varying replacement of GGBS

	Average Mass (g)				
Time(hour)	*G90F7P3*	*G70F20P10*	*G50F33P17*	*G30F47P23*	*G10F60P30*
Oven-dried	568.5	568.33	538.33	563.67	553
0.25	577	574.67	550.67	581	568
0.50	582.5	579.67	558	585.33	573.33
0.75	587.5	583.67	563	589	578.33
1.0	592	587.33	567	592	581
1.25	596	589.67	570	594.33	584.67
1.50	599	593.67	573.33	597.33	587.67
1.75	602.5	596.33	576.33	599.33	591
2.0	604	599.33	579	602	594.33
2.50	608	603	582.33	605	598.33
3.0	610	606	586.33	607	602
3.50	614	609.33	589.67	608.33	605
4.0	616	613	593	611.33	605
5.0	619	617	597.67	613.00	607.33
6.0	621	619	600	614.33	607.33
7.0	624	623.33	601.33	615.67	607.33
8.0	624.33	625.33	602.67	616.00	607.67
48	628	629.67	604.67	618.67	612.33
72	629.5	631.33	606	620.67	614.33
96	630	632.67	607	622	616
120	630.67	633.33	607.67	622.33	617.33
144	631	633	607.33	622.00	618.00
168	631	633	607.33	621.67	617.67
192	631.33	633	607	622	617.67
216	631	632.67	607.33	621.33	618
240	631	633	607	621.00	617.33
264	631.33	633.33	607	621.33	618
288	631.33	633.67	607	621.67	617.67
312	631.33	633.67	607.33	621.33	618.00
336	631.33	633.67	607.33	622	617.67
360	631.33	633.67	607.33	622	618

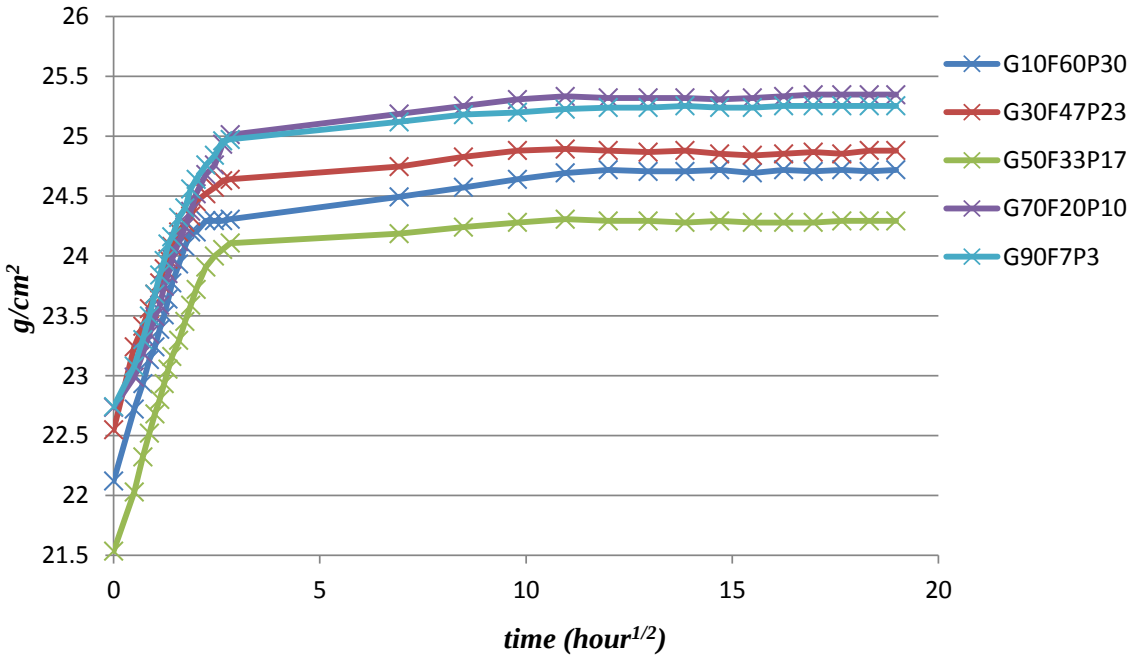

Figure 4.33: Effect of GGBS on capillary absorption of geopolymer mortar

Table 4.9: Gradient of capillary action graph with varying replacement of GGBS

Variables	***Gradient [(g/cm²)/√time]***	
	Oven-dried to 2nd day	***Oven-dried to 15th day***
G10F60P30	0.34	0.137
G30F47P23	0.32	0.123
G50F33P17	0.38	0.145
G70F20P10	0.35	0.138
G90F7P3	0.34	0.132

With reference to Figure 4.32, a dramatically growth in mass is observed in all the specimens at the initial stage, this is due to the continuously absorption of oven-dried geopolymer mortar at the beginning 8 hours. Next, steady growth is found beginning from the second day to fifth day, and subsequently almost flat movement is spotted after the fifth day at all specimens. Two different gradients were taken for the purpose of analyzing the degree of capillary absorption over a specific period of time, which are:

1. Between the oven-dried and 2nd day, indicates the initial absorption with the first turning point,
2. Between oven-dried and 15th day, indicates the total absorption over the entire time frame.

Both gradients for initial and total capillary absorption of G90F7P3, G70F20P10 and G50F33P17 increased from 0.34 to 0.35, and to 0.38 as well as from 0.132 to 0.138 and to 0.145 respectively with the decrease in replacement of GGBS at 20 % interval. The explanation for the negative trending above is because GGBS contributed larger amount of reacted products and their filling effect, thus minimized the sizes and numbers of voids, cracks or pores. Alkaline-activated GGBS-based mortar contains greater in gel pores and fewer capillary pores even in compare to ordinary Portland cement mortar (Yang *et al.*, 2008).Water tends to seep through any least-resistance path, hence the connectivity of mortar paste plays crucial role in capillary absorption. GGBS-based geopolymer developed denser and well-pack microstructure with minimum cracks; this created an impermeable barrier to capillary action, as shown in Figure 4.41.

On the other hand, sudden drop in capillary absorption to 0.32 and 0.34 were found at G30F47P23 and G10F60P10. This may due to absence of continuous-path with in structure, although porous voids were found in both specimens. Studies had proven that there is no absolute correlation between capillary absorption and porosity in concrete. Positive relationship between porosity and capillary absorption occurs if and only if those porous voids within geopolymer structure are continuously interconnected. This is because of capillary action takes place through the least-resistance, continuous-path of voids or crack within the geopolymer structures. Furthermore, relatively lower capillary absorption values in G30F47P23 and G10F60P30 can be explained by higher replacement level of PFA exhibited higher degree of both finer and bigger pores filling effect. Hence, geopolymer mortar with higher replacement level of PFA tends to achieve desired pore structure with lowest capillary absorption value for both bigger and finer pore filling phases (Cheah, Part and Ramli, 2017).

Besides that, alternative explanation might be due to better workable mortars, as shown in Figure 4.2 and Figure 4.3, tend to undergo higher degree of well-compaction and bonding during casting of specimens. Therefore, perfectly smooth and concealed surfaces were achieved by better workable mortar, thus minimized the capillary pores in the mortar paste. Furthermore, though both G90F7P3 and G10F60P30 have the similar initial absorption of 0.34, however higher total absorption of 0.137 was recorded at G10F60P30, this indicated the continuous and prolongation in absorption rate.

Table 4.10: Capillary absorption coefficient with varying PFA:POFA ratio

	Average Mass (g)		
Time(hour)	*PFA2.5:POFA0.5*	*PFA2:POFA1*	*PFA1:POFA2*
Oven-dried	568.5	568.5	538.33
0.25	577	577	550.67
0.50	582.5	582.5	558
0.75	587.5	587.5	563
1.0	592	592	567
1.25	596	596	570
1.50	599	599	573.33
1.75	602.5	602.5	576.33
2.0	604	604	579
2.50	608	608	582.33
3.0	610	610	586.33
3.50	614	614	589.67
4.0	616	616	593
5.0	619	619	597.67
6.0	621	621	600
7.0	624	624	601.33
8.0	624.33	624.33	602.67
48	628	628	604.67
72	629.5	629.5	606
96	630	630	607
120	630.67	630.67	607.67
144	631	631	607.33
168	631	631	607.33
192	631.33	631.33	607
216	631	631	607.33
240	631	631	607
264	631.33	631.33	607
288	631.33	631.33	607
312	631.33	631.33	607.33
336	631.33	631.33	607.33
360	631.33	631.33	607.33

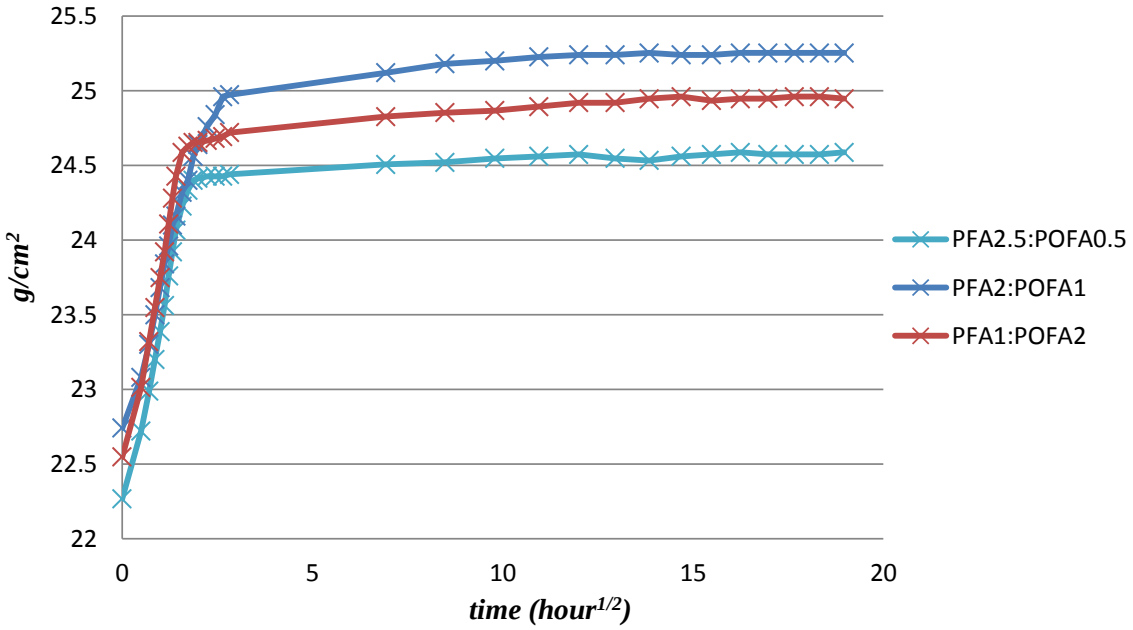

Figure 4.34: Effect of PFA:POFA ratio on capillary absorption of geopolymer mortar

Table 4.11: Gradient of capillary action graph with varying PFA:POFA ratio

Variables	***Gradient [(g/cm²)/√time]***	
	Oven-dried to 2nd day	***Oven-dried to 15th day***
PFA2.5:POFA0.5	0.32	0.122
PFA2:POFA1	0.34	0.132
PFA1:POFA2	0.33	0.126

Next, further the studies into the effect of varying PFA-to-POFA ratio to the capillary absorption coefficient of geopolymer mortar, as shown in Figure 4.34. Similar changes in mass among the three variables were found throughout the research. This can be explained by similar amount of reacted product produced with look-alike microstructures were developed among the three specimens.

PFA2.5:POFA0.5 with higher replacement of fly ash achieved minimum capillary absorption in both initial and final absorption rate of 0.32 and 0.122. Follow by PFA1:POFA2 which achieved initial and final capillary absorptions of 0.33 and 0.126. Although PFA2:POFA1 had achieved overwhelming durability performance in water absorption and porosity tests, however, it attained the highest initial as well as final capillary absorptions of 0.34 and 0.132. This can be due to discontinuous-path of voids in PFA2.5:POFA0.5 and PFA1:POFA2. The rate of capillary absorption is depends on the degree of connectivity in voids, cracks or pores within the geopolymer mortar which so much so to form a continuous-path which resulted in facilitates capillary action. Therefore, based on the result as shown in Table 4.11, it has explicitly indicated relatively higher degree of connectivity in continuous-voids developed in PFA2:POFA1 than PFA1:POFA2 and following by PFA2.5:POFA0.5.

4.9 SCANNING ELECTRON MICROSCOPY (SEM) EXAMINATION

Scanning electron microscopy (SEM) observation is to investigate the microstructure of alkali-activated ternary blended geopolymer mortar and the effect of changes in synthesis between GGBS, PFA and POFA to the morphology of geopolymeric paste formation at ambient temperature. 14-days cured specimens were taken to conduct SEM test. The SEM images of G10F60P30, G30F47P23, G50F33P17, G70 and G90F7P3 were shown in Figure 4.35, 4.35, 4.36, 4.38 and 4.40, respectively. The morphology and formation of microstructure indicates the degree of geopolymerization, dissolution and condensation of reacted product as well as presence of micro-crack, voids or pores which contributed to high water absorption and porosity in geopolymer mortar.

4.9.1 SEM images of G10F60P30

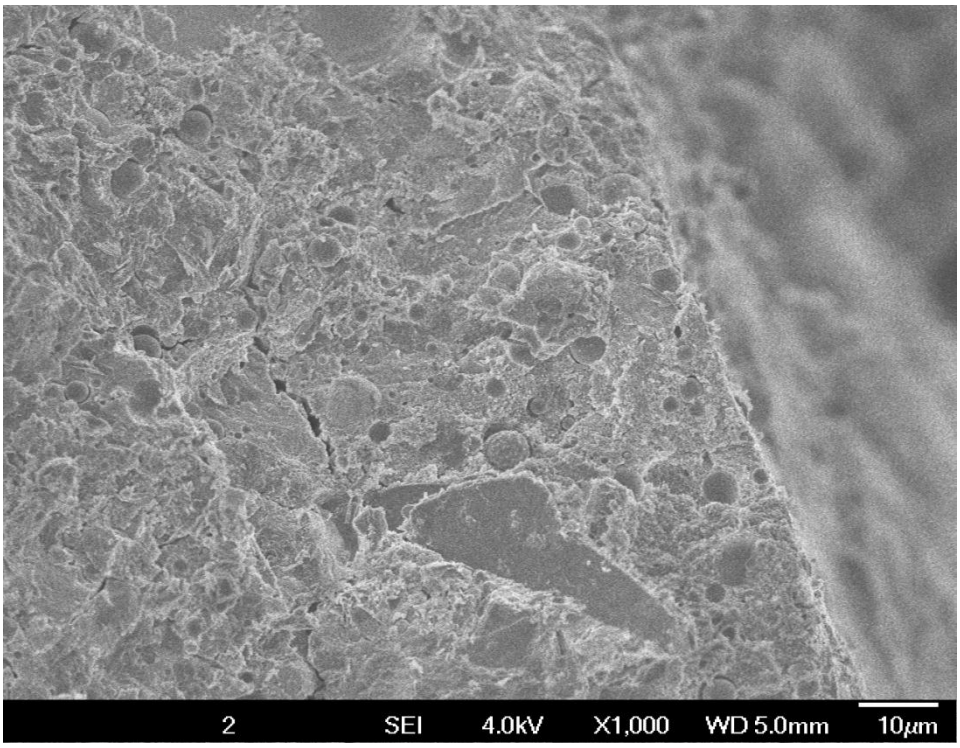

(a) SEM images at ×1,000 magnification

(b) SEM images at ×2,000 magnification

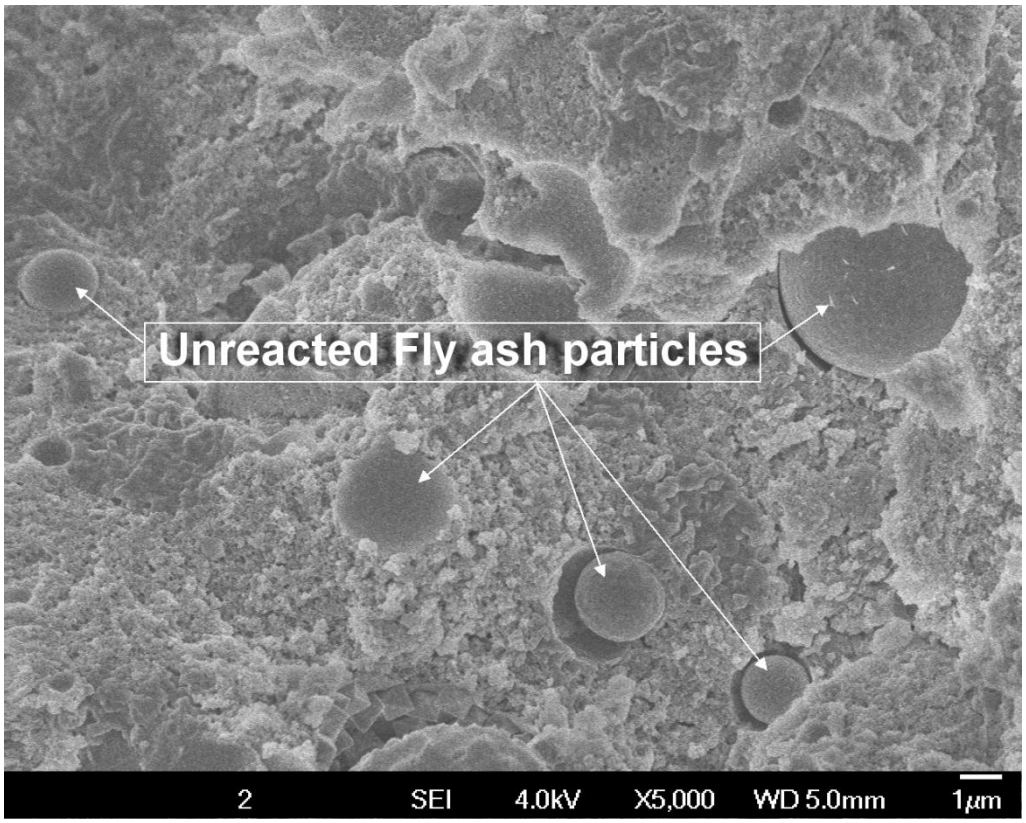

(c) SEM images at ×5,000 magnification

Figure 4.35: SEM images of G10F60P30 at 14 days

Large numbers of non-reacted fly ash and partially reacted PFA particles embedded in the matrix. Fly ash has relatively slower reaction rate at ambient temperature, and therefore numbers of unreacted fly ash particles were spotted in Figure 4.35. Without thermal force of external heat, reaction might not completed and certain amount of unreacted fly ash particles would still spherical in nature solely activated by alkaline solution (Assi *et al.*, 2016). The unreacted fly ash particles were embedded by reacted product with noticeably present porosity. NaOH-activated fly ash based geopolymer tends to show cluster-like morphology of the reaction products with clearly presentable pores (Komljenovic, Bascarevic and Bradic, 2010). Therefore, it cross-proven the highest water absorption and porosity values as shown in Table 4.6 and 4.7. Not only that, the larger amount of unreacted particles and broken particle with loose matrix resulted low compressive strength and UPV values.

4.9.2 SEM images of G30F47P23

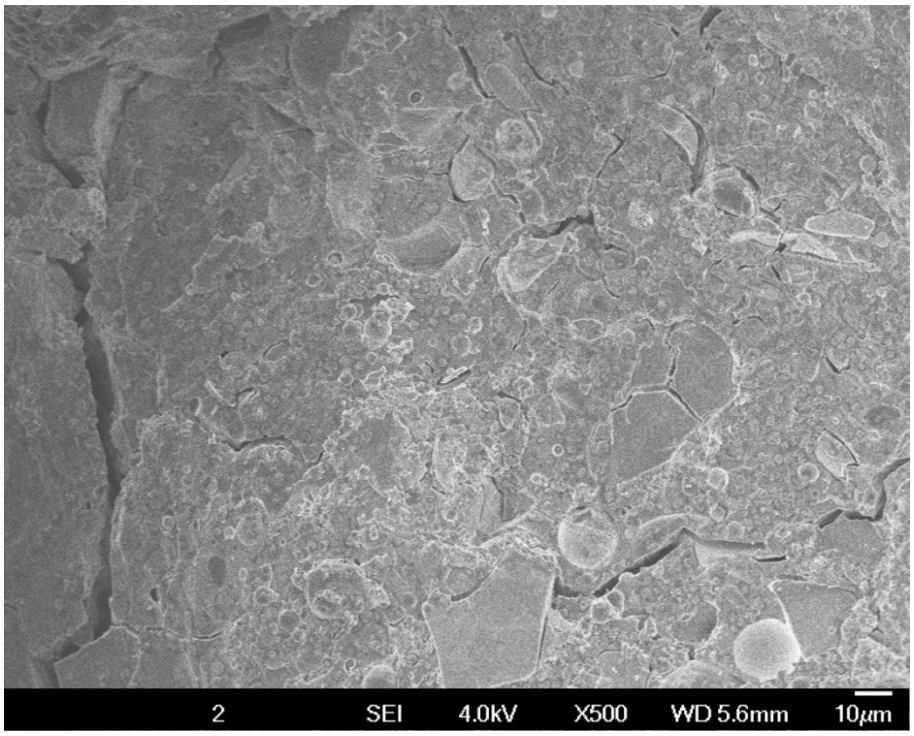

(a) SEM image at ×500 magnification

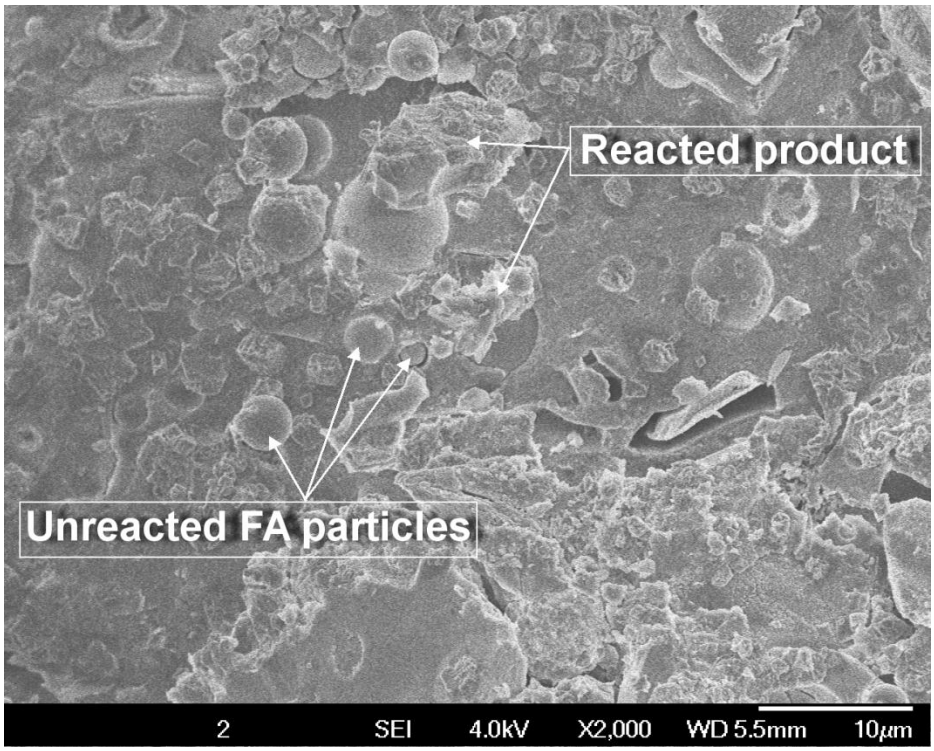

(b) SEM image at ×2,000 magnification

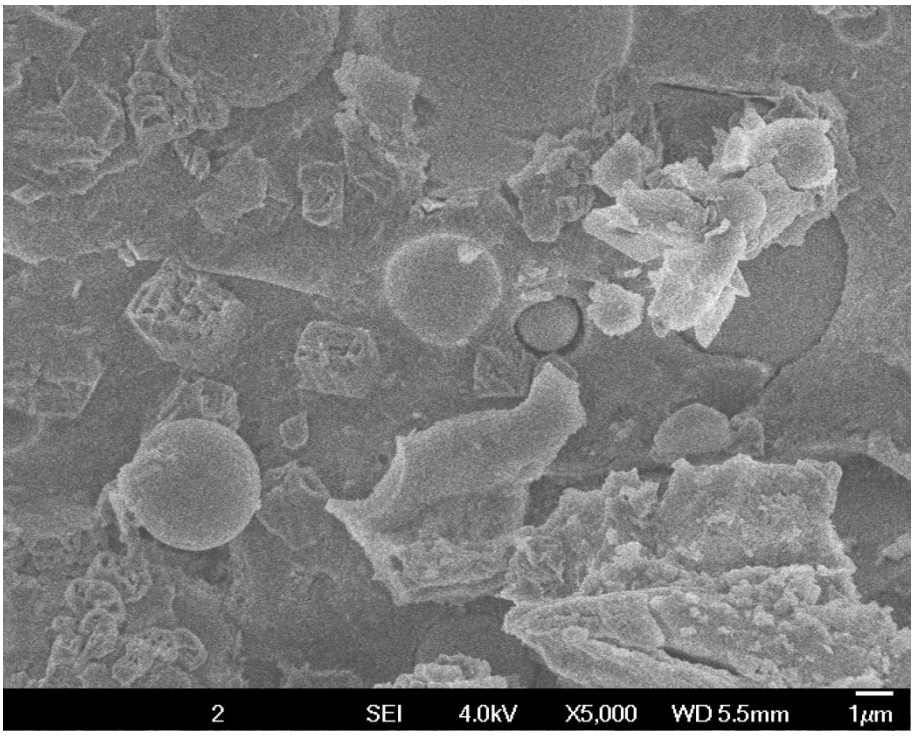

(c) SEM image at ×5,000 magnification

Figure 4.36: SEM images of G30F47P23 at 14 days

Reacted pastes between POFA, PFA and GGBS were spotted in Figure 4.36, somehow non-reacted fly ash particles were still presentable in the images. Loose matrix and porous microstructure was formed in G30F47P23 with visible micro-crack. However, relatively low amount of unreacted fly ash spheres were observed as compare to G10F60P30. This indicates the inclusion of GGBS enhanced the reactivity of PFA particles at ambient temperature.

4.9.3 SEM images of G50P50F33P17

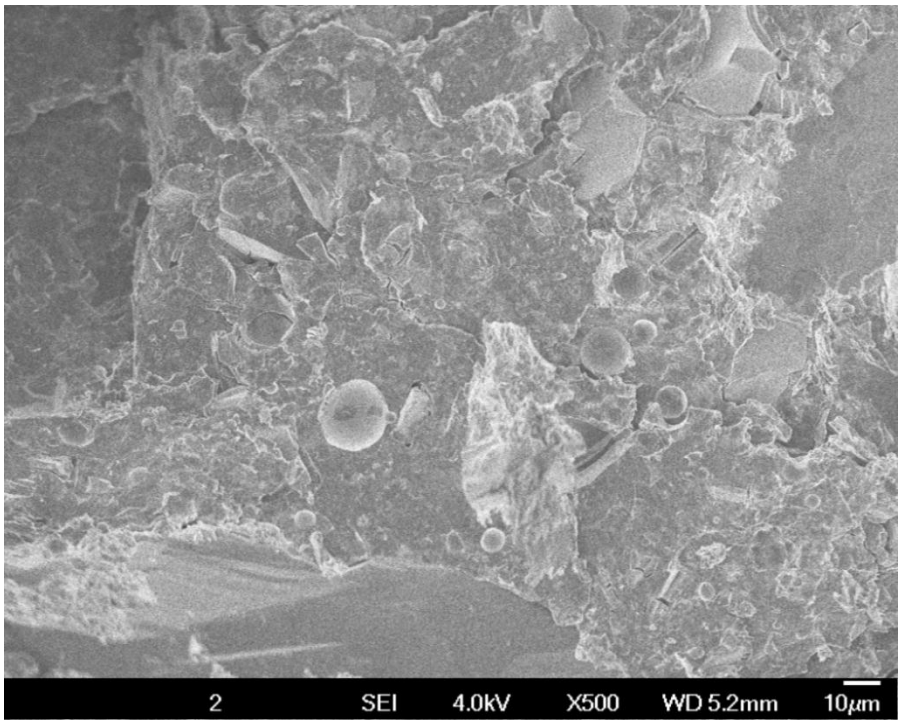

(a) SEM image at ×500 magnification

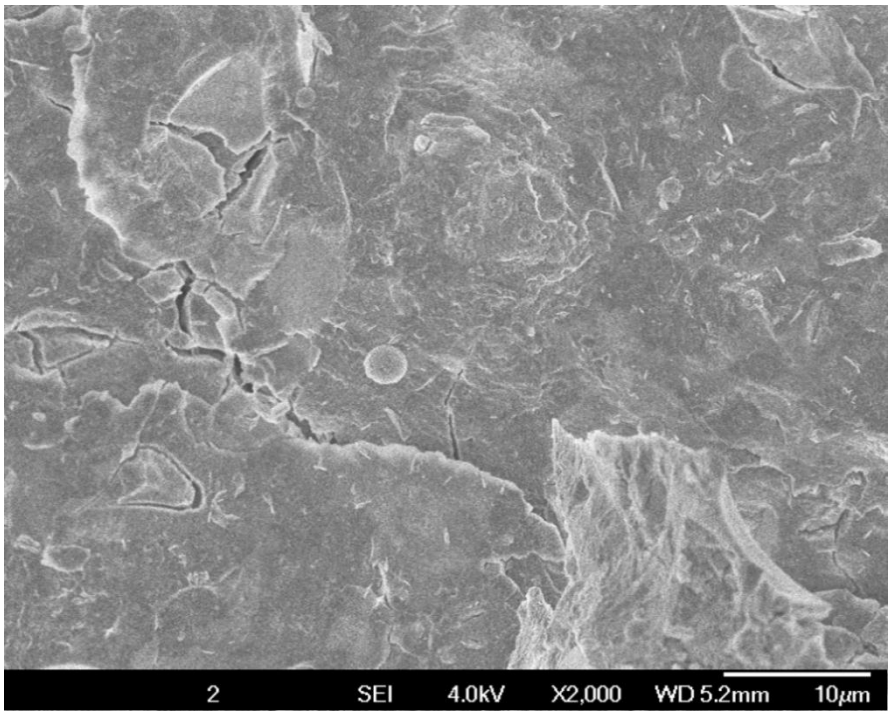

(b) SEM image at ×2,000 magnification

Figure 4.37: SEM images of G50F33P17 at 14 days

Denser and complex matrix formation in G50F33P17 can be observed in Figure 4.37. However, numbers of micro-cracks were found in the paste as shown in Figure 4.37(b). The number of unreacted fly ash particles has significantly decreased. The addition in GGBS replacement contributed in higher rate of geopolymerization. Upon hydration process, partially-dissolved PFA particle were found in the paste matrix as shown in Figure 4.38. Similar product was found in G70F20P10 as shown in Figure 4.40. The surface has been clung with micro-particles of reacted product.

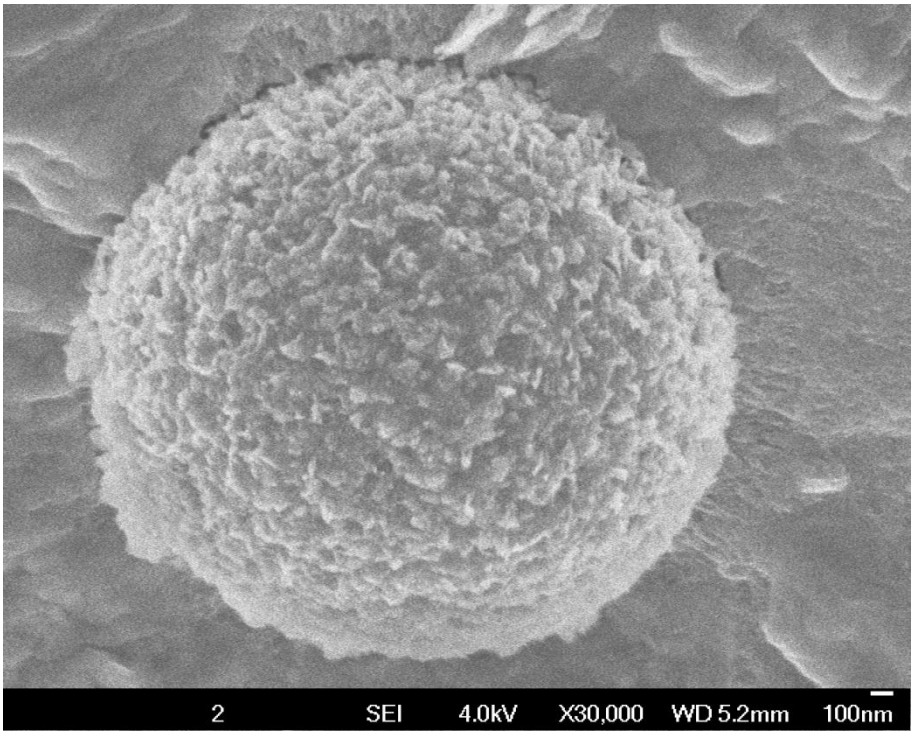

Figure 4.38: Partially-dissolved PFA particle found in G50F33P17

4.9.4 SEM images of G70F20P10

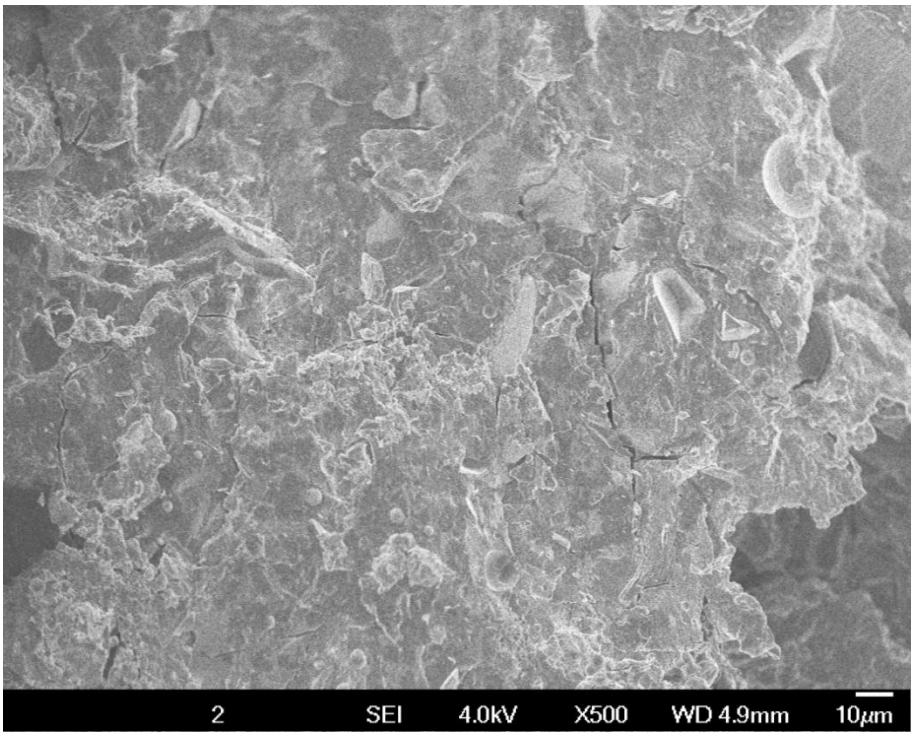

(a) SEM image at ×500 magnification

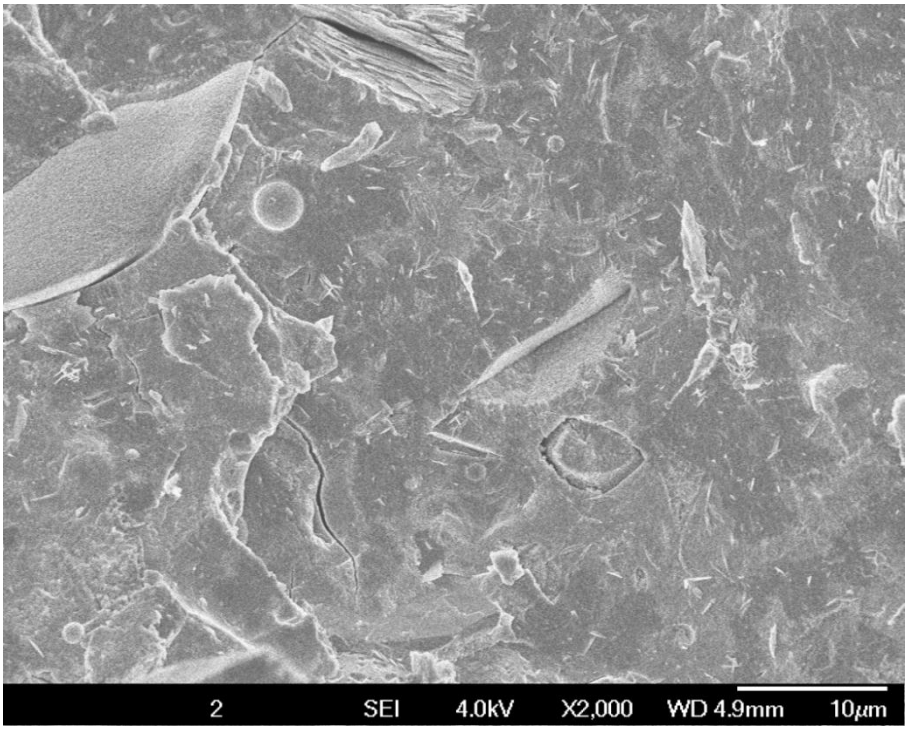

(b) SEM image at ×2,000 magnification

Figure 4.39: SEM images of G70F20P10 at 14 days

Homogenous and well-packed paste clustered with glassy particles had developed in G70F20P10. Exothermal process had happened during the reaction between GGBS and alkali activator, liberated heat enhanced the dissolution rate of PFA and POFA, thus improved the formation of geopolymeric pastes. However, micro-cracks were still spotted in the paste. Blended geopolymer mortar which comprises of GGBS and fly ash would lead to dual formation of calcium alumina-silicate hydrate C-(A)-S-H and sodium-alumina-silicate hydrate (N-A-S-H) gels. The rate of formation of aforementioned gel phases rely on the synthesis of binder. The reaction includes the disassociation of Ca ion in the alkaline medium as well as the participation of Si and Al ions in the geopolymerization reaction together with the leachates of fly ash to form a secondary gel of C-A-S-H in conjunction with N-A-S-H (Khan *et al.*, 2016). Hence, the formation of complex, integrated geopolymeric matrix contributed to high compressive strength, denser microstructure with satisfactorily UPV value and durable in terms of moisture absorption and porosity performance.

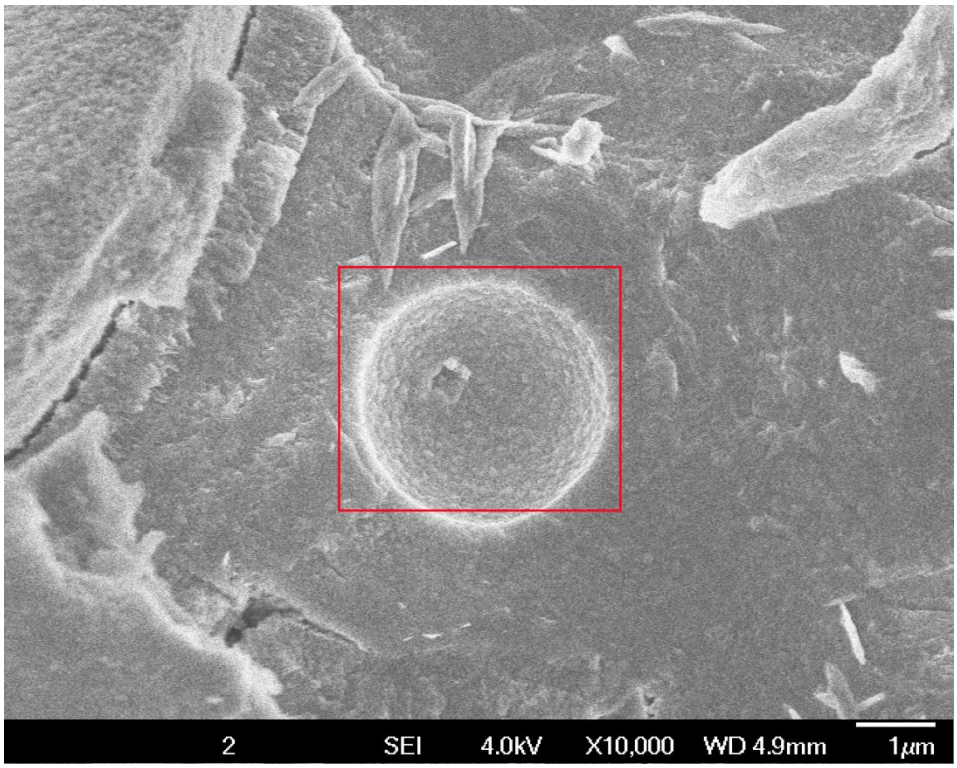

(a) Partial dissolution PFA particle

Figure 4.40: Partial-dissolved, broken PFA particle found in G70F20P10

Besides, similar to G50F33P17, a partial dissolution of PFA particle was found as shown in Figure 4.40 (a). The broken particle was filled with mico-particles of reacted products as shown in Figure 4.40 (b). As oppose to the unreacted fly ash particle shown in G10F60P30 (Figure 4.35), greater inclusion of GGBS improved the reactivity of fly ash particle. During the reaction between GGBS binder with activator, the released heat by hydration process of GGBS binder tends to accelerate the dissolution of fly ash particles, thus enhanced the reactivity of fly ash at ambient temperature (Cheah *et al.*, 2016).

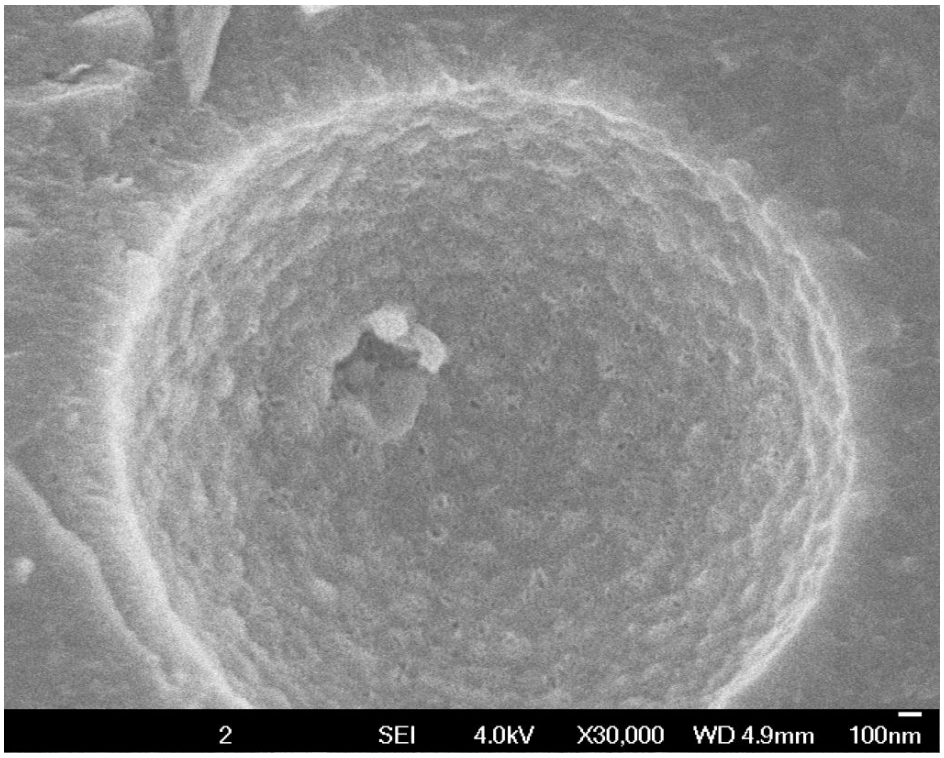

(b) Broken particle which filled with micro-particles reacted product

Figure 4.40: Partial-dissolved, broken PFA particle

4.9.5 SEM images of G90F7P3

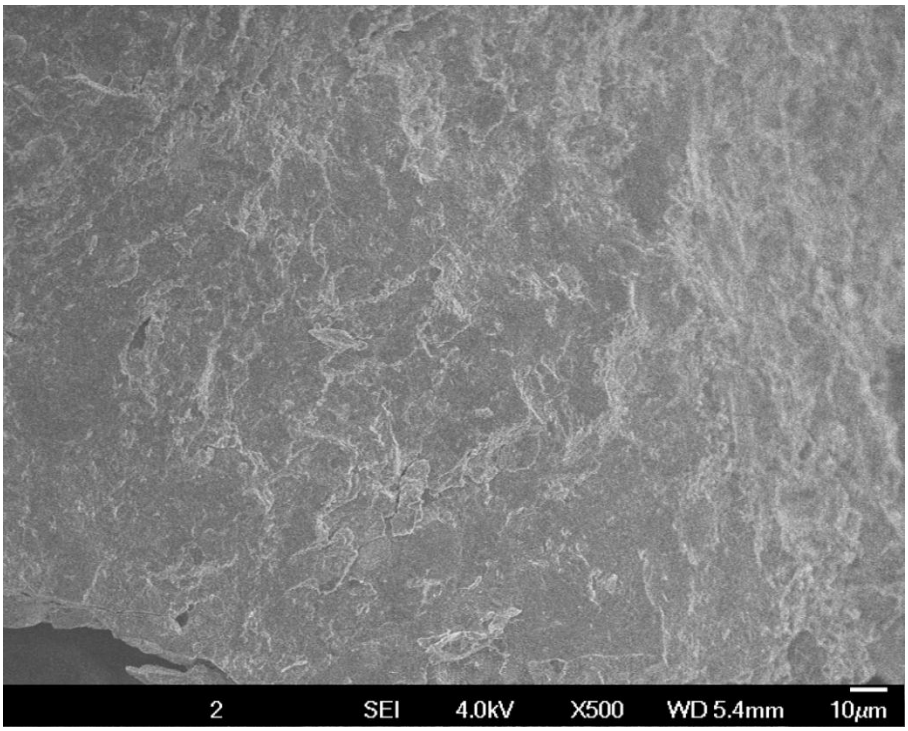

(a) SEM image at ×500 magnification

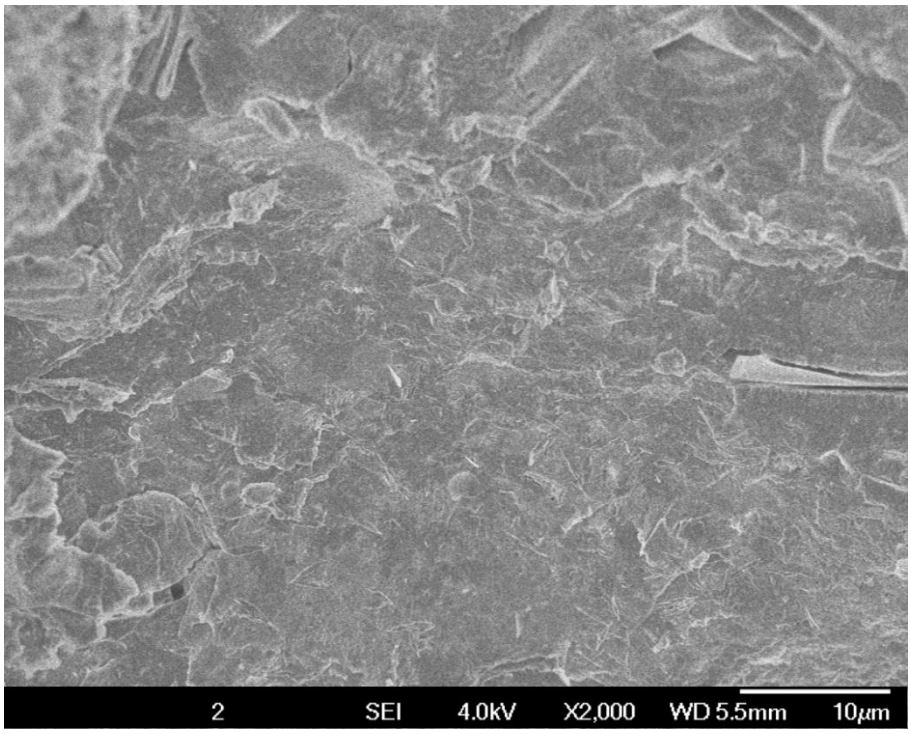

(b) SEM image at ×2,000 magnification

Figure 4.41: SEM images of G90F7P3 at 14 days

Minimum cracks with compacted and homogenous gels formation in G90F7P3. This can be explained by larger amount of GGBS contributed to sufficient dissolved of Ca^{2+} in the system for formation of calcium aluminate hydrate gels namely (C-A-H) gel and calcium aluminosilicate hydrate gel, known as (C-A-S-H) gel (Part et al., 2015). The compact microstructure development in G90F7P3 explained the optimum compressive strength of 53.54 MPa ±2.10 obtained in the experiment. Formation of sufficient reaction product with well-packed bonding has proven the overwhelming results of G90F7P3 in terms of UPV and density, of which 4.365 km/s ±0.16 and 2237 kg/m^3 ±4.16, respectively.

Inclusion of GGBS was found to increase the amorphousness of the reacted binder, increased the soluble Ca ion and resulted high amount of reactive Al to the matrix, thus caused the variations in the characteristics of calcium-silicate-hydrate (C-S-H) gel and enhanced the density of the geopolymer mortar through pore filling effect (Yusuf *et al.*, 2014b). Furthermore, fly ash has slow dissolution rate in nature with the absence of thermal activation, yet incorporation of GGBS enhances the reactivity of fly ash, thus accelerate the geopolymerization process at ambient temperature (Bilim and Ati, 2012).

4.10 SUMMARY AND DISCUSSION ON EXPERIMENTAL RESULTS

In summary, inclusion of ground granulated blast-furnace slag (GGBS) contributed enhance the overall engineering properties as well as durability performance of geopolymer mortar at ambient temperature. Throughout the research, the author found that the specimens with maximum replacement level of GGBS demonstrated overwhelming engineering properties including compressive strength, density and ultrasonic pulse velocity values. This can be explained by high reactivity of GGBS particle as well as the contribution of Ca^{+} into geopolymeric system by substituted into (N-A-S-H) gel, thus forming (C-(N)-A-S-H) gel. Paradoxically, adverse effect on the workability and flow ability of geopolymer is observed attributed to the quick reaction of GGBS particles to sodium alkali activator accelerate the geopolymerization process, thus shorten the setting times. Geopolymer product with inferior workability would weaken the paste-aggregate bonding, thus drastically reduced its strength as well as vast increment in water absorption and porosity rates.

On the other hand, pulverized fly ash (PFA) with low reactivity at ambient temperature tends to prolong both initial and final setting times of geopolymer mortar, as well as improved the flow ability of fresh mortar. Hence, the author concluded that hybrid geopolymer product able to take the advantages of GGBS in order to preserve the high compressive strength at ambient temperature without compromise its workability, thus enhance the bonding of geopolymer product with the presence of Ca ion into the matrix. Moreover, palm oil fuel ash (POFA) contributed to develop larger amount of reacted products as well as extended the geopolymerization process by consecutively supply of Si into the system. However, the high sorptivity of POFA in nature tends to increase the water absorption and porosity of geopolymer mortar by created micro-voids which initially filled with water. Therefore, the author suggested the POFA to be treated prior to be blended into geopolymer binder, for instance ultrafine treatment and thermal incineration.

CHAPTER 5

CONCLUSION AND RECOMMENDATION

5.1 GENERAL CONCLUSION

In the past decade, geopolymer technology has been proven that elevated curing is required in order to develop comparable strength and durability performances to ordinary Portland cement product. The dissolution mechanism of pozzolanic binder was differed from ordinary Portland cement which can be dissolved and reacted with solely H_2O at ambient temperature. On the contrary, geopolymer needs of thermal activation incorporate with high pH alkali activator such as potassium or sodium alkali to ensure sufficient dissolution of pozzolanic particles, following by reaction and condensation among the Ca, Si and Al ions. Nevertheless, throughout the research, the author found that inclusion of GGBS with high amorphousness particles able to develop geopolymer product with comparable engineering properties and durability performances to typical heat-cured geopolymer at ambient temperature. Hence, this finding allows geopolymer technology to be adopted in Malaysia construction industry, whereby previously this technology was been limited to off-site manufacture production such as precast building component.

5.2 Engineering Properties of Alkali-activated Ternary Hybrid Geopolymer Mortar

This research is to study the engineering properties of sodium alkali-activated POFA-GGBS-PFA ternary blended geopolymer mortar at ambient temperature. Throughout the study, the following conclusion can be drawn:

I. High compressive strength (>50 MPa) geopolymer mortar can be achieved with above 70 % GGBS at 56 days.
II. Upward trend is observed in density with increase in GGBS replacement.
III. All the specimens are categorized as 'Good' ultrasonic pulse velocity (UPV) values at 14 days onwards, while higher UPV values can be achieved with increase in replacement of GGBS.
IV. Inclusion of GGBS contributes to high compressive strength at ambient temperature, yet accelerates the setting times and adverse effect on workability.
V. Denser and homogenous geopolymeric microstructure development with high replacement of GGBS; while looser and presence of unreacted fly ash particle in the microstructure with lower GGBS.
VI. GGBS contributes Ca ion with high reactivity, enhances the amorphousness in the system, thus improve both the initial and final strength of geopolymer mortar at ambient temperature yet compromising the workability.
VII. PFA contributes lower SiO_2/Al_2O_3 ratio in the system, thus improve the initial strength of geopolymer mortar.
VIII. POFA contributes large number of SiO_2 which prolong the strength development resulted in high final strength yet the compromise on low initial strength.

5.3 Durability Performance of Alkali-activated Ternary Hybrid Geopolymer Mortar

The durability performances of sodium alkali-activated POFA-GGBS-PFA ternary hybrid geopolymer mortar cured at ambient temperature have been studied in this research including water absorption ability, porosity rate and capillary absorption coefficient of geopolymer mortar. Throughout the research, the following finding can be made:

I. Downturn movement in water absorption with the increase in GGBS content. The optimum water absorption of 3.57 % was achieved by geopolymer specimen with 90 % replacement level of GGBS at 56 days.
II. Similar trending is observed in porosity, minimum porosity of 20.02 % to be found in geopolymer mortar with 90 % replacement level of GGBS at 56 days.
III. Capillary absorption of geopolymer mortar is determined by the presence of continuous-path of voids, meanwhile geopolymer product with high porosity does not guarantee similar in capillary absorption. Nevertheless, addition in replacement of GGBS would conduce in minimize the capillary absorption coefficient of geopolymer mortar.

5.4 Recommendation for Future Research

In light with the challenges in low adoption of geopolymer technology in Malaysia construction industry, following strategies are proposed to future study in order to develop reliable quantified data to eliminate doubtful against geopolymer technology as well as to facilitate the implementation of geopolymer concrete in the industry application:

I. Innovation of new curing and activation methods which may facilitate the application of geopolymer technology in Malaysia industry as well as minimize the cost for commercial alkaline activator, subject to acceptable error allowance for poor workmanship on site.
II. Establishment of standard specification and testing methods with high accuracy specially designed for geopolymer. This able to improve the formality of geopolymer technology application in construction industry.
III. Compatibility studies between N-A-S-H and C-A-S-H gels developed in binary or ternary blended geopolymer as well as the reaction of exposure to chemical attack.
IV. Conduct case study of life cycle assessment (LCA) on current constructed project which used of geopolymer concrete component, such as the University of Queensland's Global Change Institute (GCI), Australia.

REFERENCES

Al-Majidi, M. H., Lampropoulos, A., Cundy, A. and Meikle, S. (2016) 'Development of geopolymer mortar under ambient temperature for in situ applications', *Construction and Building Materials*. Elsevier Ltd, 120, pp. 198–211. doi: 10.1016/j.conbuildmat.2016.05.085.

Aliabdo, A. A., Abd Elmoaty, A. E. M. and Salem, H. A. (2016) 'Effect of water addition, plasticizer and alkaline solution constitution on fly ash based geopolymer concrete performance', *Construction and Building Materials*. Elsevier Ltd, 121, pp. 694–703. doi: 10.1016/j.conbuildmat.2016.06.062.

Assi, L., Ghahari, S. A., Deaver, E. E., Leaphart, D. and Ziehl, P. (2016) 'Improvement of the early and final compressive strength of fly ash-based geopolymer concrete at ambient conditions', *Construction and Building Materials*. Elsevier Ltd, 123, pp. 806–813. doi: 10.1016/j.conbuildmat.2016.07.069.

Atiş, C. D., Görür, E. B., Karahan, O., Bilim, C., İlkentapar, S. and Luga, E. (2015) 'Very high strength (120MPa) class F fly ash geopolymer mortar activated at different NaOH amount, heat curing temperature and heat curing duration', *Construction and Building Materials*, 96, pp. 673–678. doi: 10.1016/j.conbuildmat.2015.08.089.

Bilim, C. and Ati, C. D. (2012) 'Alkali activation of mortars containing different replacement levels of ground granulated blast furnace slag', *Construction and Building Materials*, 28(1), pp. 708–712. doi: 10.1016/j.conbuildmat.2011.10.018.

Chandara, C., Mohd Azizli, K. A., Ahmad, Z. A., Saiyid Hashim, S. F. and Sakai, E. (2012) 'Heat of hydration of blended cement containing treated ground palm oil fuel ash', *Construction and Building Materials*. Elsevier Ltd, 27(1), pp. 78–81. doi: 10.1016/j.conbuildmat.2011.08.011.

Chandara, C., Sakai, E., Azizli, K. A. M., Ahmad, Z. A. and Hashim, S. F. S. (2010) 'The effect of unburned carbon in palm oil fuel ash on fluidity of cement pastes containing superplasticizer', *Construction and Building Materials*. Elsevier Ltd, 24(9), pp. 1590–1593. doi: 10.1016/j.conbuildmat.2010.02.036.

Cheah, chee ban, Part, W. K. and Ramli, M. (2017) 'Mechanical and Durability Performance of Novel Self-activating Geopolymer Mortars', *Procedia Engineering*, 171, pp. 564–571. doi: 10.1016/j.proeng.2017.01.374.

Cheah, C. B., Chung, K. Y., Ramli, M. and Lim, G. K. (2016) 'The engineering properties and microstructure development of cement mortar containing high volume of inter-grinded GGBS and PFA cured at ambient temperature', *Construction and Building Materials*. Elsevier Ltd, 122, pp. 683–693. doi: 10.1016/j.conbuildmat.2016.06.105.

Collins, F. and Sanjayan, J. (2008) 'Unsaturated capillary flow within alkali activated slag concrete', *Journal of Materials in Civil Engineering*, 20(9), pp. 565–570. doi: 10.1061/(ASCE)0899-1561(2008)20:9(565).

Deb, P. S., Nath, P. and Sarker, P. K. (2014) 'The effects of ground granulated blast-furnace slag blending with fly ash and activator content on the workability and strength properties of geopolymer concrete cured at ambient temperature', *Materials and Design*. Elsevier Ltd, 62, pp. 32–39. doi: 10.1016/j.matdes.2014.05.001.

Deb, P. S., Nath, P. and Sarker, P. K. (2015) 'Drying shrinkage of slag blended fly ash geopolymer concrete cured at room temperature', *Procedia Engineering*. Elsevier B.V., 125, pp. 594–600. doi: 10.1016/j.proeng.2015.11.066.

Gao, X., Yu, Q. L. and Brouwers, H. J. H. (2015) 'Characterization of alkali activated slag–fly ash blends containing nano-silica', *Construction and Building Materials*, 98, pp. 397–406. doi: 10.1016/j.conbuildmat.2015.08.086.

Gao, X., Yu, Q. L. and Brouwers, H. J. H. (2016) 'Assessing the porosity and shrinkage of alkali activated slag-fly ash composites designed applying a packing model', *Construction and Building Materials*, 119, pp. 175–184. doi: 10.1016/j.conbuildmat.2016.05.026.

Garcia-Lodeiro, I., Palomo, A., Fernandez-Jimenez, A. and MacPhee, D. E. (2011) 'Compatibility studies between N-A-S-H and C-A-S-H gels. Study in the ternary diagram Na2O-CaO-Al2O3-SiO 2-H2O', *Cement and Concrete Research*, 41(9), pp. 923–931. doi: 10.1016/j.cemconres.2011.05.006.

Görhan, G. and Kürklü, G. (2014) 'The influence of the NaOH solution on the properties of the fly ash-based geopolymer mortar cured at different temperatures', *Composites Part B: Engineering*, 58, pp. 371–377. doi: 10.1016/j.compositesb.2013.10.082.

Islam, A., Alengaram, U. J., Jumaat, M. Z. and Bashar, I. I. (2014) 'The development of compressive strength of ground granulated blast furnace slag-palm oil fuel ash-fly ash based geopolymer mortar', *Materials and Design*. Elsevier Ltd, 56, pp. 833–841. doi: 10.1016/j.matdes.2013.11.080.

Islam, A., Alengaram, U. J., Jumaat, M. Z., Bashar, I. I. and Kabir, S. M. A. (2015) 'Engineering properties and carbon footprint of ground granulated blast-furnace slag-palm oil fuel ash-based structural geopolymer concrete', *Construction and Building Materials*. Elsevier Ltd, 101, pp. 503–521. doi: 10.1016/j.conbuildmat.2015.10.026.

Kazemian, A., Gholizadeh Vayghan, A. and Rajabipour, F. (2015) 'Quantitative assessment of parameters that affect strength development in alkali activated fly ash binders', *Construction and Building Materials*. Elsevier Ltd, 93, pp. 869–876. doi: 10.1016/j.conbuildmat.2015.05.078.

Khan, M. Z. N., Shaikh, F. uddin A., Hao, Y. and Hao, H. (2016) 'Synthesis of high strength ambient cured geopolymer composite by using low calcium fly ash', *Construction and Building Materials*. Elsevier Ltd, 125, pp. 809–820. doi: 10.1016/j.conbuildmat.2016.08.097.

Komljenovic, M., Bascarevic, Z. and Bradic, V. (2010) 'Mechanical and microstructural properties of alkali-activated fly ash geopolymers', *Journal of Hazardous Materials*, 181(1–3), pp. 35–42. doi: 10.1016/j.jhazmat.2010.04.064.

Lee, N. K. and Lee, H. K. (2013) 'Setting and mechanical properties of alkali-activated fly ash/slag concrete manufactured at room temperature', *Construction and Building Materials*. Elsevier Ltd, 47, pp. 1201–1209. doi: 10.1016/j.conbuildmat.2013.05.107.

Mackenzie, K. J. D. and Welter, M. (2014) 'Geopolymer (aluminosilicate) composites: synthesis, properties and applications', *Advances in Ceramic Matrix Composites*. Woodhead Publishing Limited. doi: 10.1533/9780857098825.3.445.

McLellan, B. C., Williams, R. P., Lay, J., Van Riessen, A. and Corder, G. D. (2011) 'Costs and carbon emissions for geopolymer pastes in comparison to ordinary portland cement', *Journal of Cleaner Production*. Elsevier Ltd, 19(9–10), pp. 1080–1090. doi: 10.1016/j.jclepro.2011.02.010.

Mijarsh, M. J. A., Megat Johari, M. A. and Ahmad, Z. A. (2014) 'Synthesis of geopolymer from large amounts of treated palm oil fuel ash: Application of the Taguchi method in investigating the main parameters affecting compressive strength', *Construction and Building Materials*. Elsevier Ltd, 52, pp. 473–481. doi: 10.1016/j.conbuildmat.2013.11.039.

Mijarsh, M. J. A., Megat Johari, M. A. and Ahmad, Z. A. (2015) 'Effect of delay time and Na2SiO3 concentrations on compressive strength development of geopolymer mortar synthesized from TPOFA', *Construction and Building Materials*. Elsevier Ltd, 86, pp. 64–74. doi: 10.1016/j.conbuildmat.2015.03.078.

Nath, P. and Sarker, P. K. (2014) 'Effect of GGBFS on setting, workability and early strength properties of fly ash geopolymer concrete cured in ambient condition', *Construction and Building Materials*, 66. doi: 10.1016/j.conbuildmat.2014.05.080.

Nath, P., Sarker, P. K. and Rangan, V. B. (2015) 'Early age properties of low-calcium fly ash geopolymer concrete suitable for ambient curing', in *Procedia Engineering*. doi: 10.1016/j.proeng.2015.11.077.

Nath, S. K. and Kumar, S. (2013) 'Influence of iron making slags on strength and microstructure of fly ash geopolymer', *Construction and Building Materials*. Elsevier Ltd, 38, pp. 924–930. doi: 10.1016/j.conbuildmat.2012.09.070.

Nath, S. K., Maitra, S., Mukherjee, S. and Kumar, S. (2016) 'Microstructural and morphological evolution of fly ash based geopolymers', *Construction and Building Materials*, 111. doi: 10.1016/j.conbuildmat.2016.02.106.

Okoye, F. N., Prakash, S. and Singh, N. B. (2017) 'Durability of fly ash based geopolymer concrete in the presence of silica fume', *Journal of Cleaner Production*. Elsevier Ltd, 149, pp. 1062–1067. doi: 10.1016/j.jclepro.2017.02.176.

Omer, S. A., Demirboga, R. and Khushefati, W. H. (2015) 'Relationship between compressive strength and UPV of GGBFS based geopolymer mortars exposed to elevated temperatures', *Construction and Building Materials*. Elsevier Ltd, 94, pp. 189–195. doi: 10.1016/j.conbuildmat.2015.07.006.

Part, W. K., Ramli, M. and Cheah, C. B. (2015) 'An overview on the influence of various factors on the properties of geopolymer concrete derived from industrial by-products', *Construction and Building Materials*. Elsevier Ltd, 77, pp. 370–395. doi: 10.1016/j.conbuildmat.2014.12.065.

Phoo-Ngernkham, T., Maegawa, A., Mishima, N., Hatanaka, S. and Chindaprasirt, P. (2015) 'Effects of sodium hydroxide and sodium silicate solutions on compressive and shear bond strengths of FA-GBFS geopolymer', *Construction and Building Materials*. Elsevier Ltd, 91, pp. 1–8. doi: 10.1016/j.conbuildmat.2015.05.001.

Civil Engineering Portal. (1992) *Ultrasonic Pulse Velocity Method*. [Online] Available from http://www.engineeringcivil.com/ultrasonic-pulse-velocity-method.html/ [Accessed 1st April 2017].

Puligilla, S. and Mondal, P. (2013) 'Role of slag in microstructural development and hardening of fly ash-slag geopolymer', *Cement and Concrete Research*. Elsevier Ltd, 43(1), pp. 70–80. doi: 10.1016/j.cemconres.2012.10.004.

Ranjbar, N., Mehrali, M., Alengaram, U. J., Metselaar, H. S. C. and Jumaat, M. Z. (2014) 'Compressive strength and microstructural analysis of fly ash/palm oil fuel ash based geopolymer mortar under elevated temperatures', *Construction and Building Materials*. Elsevier Ltd, 65, pp. 114–121. doi: 10.1016/j.conbuildmat.2014.04.064.

Ranjbar, N., Mehrali, M., Behnia, A., Alengaram, U. J. and Jumaat, M. Z. (2014) 'Compressive strength and microstructural analysis of fly ash/palm oil fuel ash based geopolymer mortar', *Materials & Design*, 59, pp. 532–539. doi: 10.1016/j.matdes.2014.03.037.

Salami, B. A., Megat Johari, M. A., Ahmad, Z. A. and Maslehuddin, M. (2016) 'Impact of added water and superplasticizer on early compressive strength of selected mixtures of palm oil fuel ash-based engineered geopolymer composites', *Construction and Building Materials*. Elsevier Ltd, 109, pp. 198–206. doi: 10.1016/j.conbuildmat.2016.01.033.

Salih, M. A., Abang Ali, A. A. and Farzadnia, N. (2014) 'Characterization of mechanical and microstructural properties of palm oil fuel ash geopolymer cement paste', *Construction and Building Materials*. Elsevier Ltd, 65, pp. 592–603. doi: 10.1016/j.conbuildmat.2014.05.031.

Salih, M. A., Farzadnia, N., Abang Ali, A. A. and Demirboga, R. (2015) 'Development of high strength alkali activated binder using palm oil fuel ash and GGBS at ambient temperature', *Construction and Building Materials*. Elsevier Ltd, 93, pp. 289–300. doi: 10.1016/j.conbuildmat.2015.05.119.

Shaikh, F. U. A. (2016) 'Mechanical and durability properties of fly ash geopolymer concrete containing recycled coarse aggregates', *International Journal of Sustainable Built Environment*. The Gulf Organisation for Research and Development, 5(2), pp. 277–287. doi: 10.1016/j.ijsbe.2016.05.009.

Singh, B., Ishwarya, G., Gupta, M. and Bhattacharyya, S. K. (2015) 'Geopolymer concrete: A review of some recent developments', *Construction and Building Materials*. Elsevier Ltd, 85, pp. 78–90. doi: 10.1016/j.conbuildmat.2015.03.036.

Singh, B., Rahman, M. R., Paswan, R. and Bhattacharyya, S. K. (2016) 'Effect of activator concentration on the strength, ITZ and drying shrinkage of fly ash/slag geopolymer concrete', *Construction and Building Materials*. Elsevier Ltd, 118, pp. 171–179. doi: 10.1016/j.conbuildmat.2016.05.008.

Soutsos, M., Boyle, A. P., Vinai, R., Hadjierakleous, A. and Barnett, S. J. (2016) 'Factors influencing the compressive strength of fly ash based geopolymers', *Construction and Building Materials*. Elsevier Ltd, 110, pp. 355–368. doi: 10.1016/j.conbuildmat.2015.11.045.

Sukmak, P., S. Horpibulsuk, and S.-L. S. (2013) 'Strength development in clay–fly ash geopolymer' *Construction and Building Materials*. Elsevier Ltd, 40, pp. 566–574. doi: 10.1016/j.conbuildmat.2012.11.015.

Turner, L. K. and Collins, F. G. (2013) 'Carbon dioxide equivalent (CO2-e) emissions: A comparison between geopolymer and OPC cement concrete', *Construction and Building Materials*. Elsevier Ltd, 43, pp. 125–130. doi: 10.1016/j.conbuildmat.2013.01.023.

Voltaggio, M., Spadoni, M., Sacchi, E., Sanam, R., Pujari, P. R. and Labhasetwar, P. K. (2015) 'Assessment of groundwater pollution from ash ponds using stable and unstable isotopes around the Koradi and Khaperkheda thermal power plants (Maharashtra, India)', *Science of the Total Environment*. Elsevier B.V., 518–519, pp. 616–625. doi: 10.1016/j.scitotenv.2015.02.083.

Wang, W. C., Wang, H. Y. and Lo, M. H. (2015) 'The fresh and engineering properties of alkali activated slag as a function of fly ash replacement and alkali concentration', *Construction and Building Materials*. Elsevier Ltd, 84, pp. 224–229. doi: 10.1016/j.conbuildmat.2014.09.059.

Wardhono, A., Law, D. W. and Strano, A. (2015) 'The strength of alkali-activated slag/fly ash mortar blends at ambient temperature', *Procedia Engineering*. Elsevier B.V., 125, pp. 650–656. doi: 10.1016/j.proeng.2015.11.095.

Williamson, T. and Juenger, M. C. G. (2016) 'The role of activating solution concentration on alkali-silica reaction in alkali-activated fly ash concrete', *Cement and Concrete Research*. Elsevier Ltd, 83, pp. 124–130. doi: 10.1016/j.cemconres.2016.02.008.

Xie, J. and Kayali, O. (2014) 'Effect of initial water content and curing moisture conditions on the development of fly ash-based geopolymers in heat and ambient temperature', *Construction and Building Materials*. Elsevier Ltd, 67, pp. 20–28. doi: 10.1016/j.conbuildmat.2013.10.047.

Yang, K. H., Song, J. K., Ashour, A. F. and Lee, E. T. (2008) 'Properties of cementless mortars activated by sodium silicate', *Construction and Building Materials*, 22(9), pp. 1981–1989. doi: 10.1016/j.conbuildmat.2007.07.003.

Yap, S. and Foong, K. (2013) 'Waste Materials in Malaysia for Development of Sustainable Concrete: A Review', *Electronic Journal of Structural Engineering*, 13(1), pp. 60–64.

Yong, M., Liu, J., Alengaram, U. J., Santhanam, M., Zamin, M. and Hung, K. (2016) 'Microstructural investigations of palm oil fuel ash and fly ash based binders in lightweight aggregate foamed geopolymer concrete', *Construction and Building Materials*. Elsevier Ltd, 120, pp. 112–122. doi: 10.1016/j.conbuildmat.2016.05.076.

Yusuf, M. O., Megat Johari, M. A., Ahmad, Z. A. and Maslehuddin, M. (2014a) 'Effects of H2O/Na2O molar ratio on the strength of alkaline activated ground blast furnace slag-ultrafine palm oil fuel ash based concrete', *Materials and Design*. Elsevier Ltd, 56, pp. 158–164. doi: 10.1016/j.matdes.2013.09.078.

Yusuf, M. O., Megat Johari, M. A., Ahmad, Z. A. and Maslehuddin, M. (2014b) 'Strength and microstructure of alkali-activated binary blended binder containing palm oil fuel ash and ground blast-furnace slag', *Construction and Building Materials*. Elsevier Ltd, 52, pp. 504–510. doi: 10.1016/j.conbuildmat.2013.11.012.

Zhang, Z., Provis, J. L., Reid, A. and Wang, H. (2014) 'Geopolymer foam concrete: An emerging material for sustainable construction', *Construction and Building Materials*. Elsevier Ltd, 56, pp. 113–127. doi: 10.1016/j.conbuildmat.2014.01.081.

Zhou, W., Yan, C., Duan, P., Liu, Y., Zhang, Z., Qiu, X. and Li, D. (2016) 'A comparative study of high- and low-Al2O3 fly ash based-geopolymers: The role of mix proportion factors and curing temperature', *Materials and Design*. Elsevier Ltd, 95, pp. 63–74. doi: 10.1016/j.matdes.2016.01.084.

LIST OF STANDARDS

British Standard Institution (1999). *Methods of test for mortar for masonry. Determination of consistence of fresh mortar (by flow table)*. London, BS EN 1015-3:1999.

British Standard Institution (2009). *Testing hardened concrete. Compressive strength of test specimens.* London, BS EN 12390-3:2009

British Standard Institution (2004). *Testing Concrete. Determination of ultrasonic pulse velocity.* London, BS EN 12504-4:2004.

British Standard Institution (2011). *Testing concrete. Method for determination of water absorption.* London, BS 1881-122:2011.

British Standard Institution (2002). *Methods for determination of water absorption coefficient due to capillary action of hardened mortar*. London, BS EN 1015-18:2002.

British Standard Institution (2009). *Testing hardened concrte. Density of hardened concrete*. London, BS EN 12390-7:2009.